2013-07-30

Vertical Connectivity in Mesophotic Coral Ecosystems

Daniel M. Holstein
University of Miami, dan.holstein@gmail.com

UNIVERSITY OF MIAMI

VERTICAL CONNECTIVITY IN MESOPHOTIC CORAL ECOSYSTEMS

By

Daniel M. Holstein

A DISSERTATION

Submitted to the Faculty
of the University of Miami
in partial fulfillment of the requirements for
the degree of Doctor of Philosophy

Coral Gables, Florida

August 2013

UNIVERSITY OF MIAMI

A dissertation submitted in partial fulfillment of
the requirements for the degree of
Doctor of Philosophy

VERTICAL CONNECTIVITY IN MESOPHOTIC CORAL ECOSYSTEMS

Daniel M. Holstein

Approved:

_____ Claire B. Paris, Ph.D. Professor of Applied Marine Physics	_____ M. Brian Blake, Ph.D. Dean of the Graduate School
_____ John W. McManus, Ph.D. Professor of Marine Biology	_____ Andrew Bakun, Ph.D. Professor of Marine Biology
_____ Margaret W. Miller, Ph.D. Ecologist NOAA National Marine Fisheries Service	_____ Tyler B. Smith, Ph.D. Professor of Marine Biology University of the Virgin Islands

HOLSTEIN, DANIEL M. (Ph.D., Marine Biology and Fisheries)

Vertical Connectivity in Mesophotic Coral Ecosystems. (August 2013)

Abstract of a dissertation at the University of Miami.

Dissertation supervised by Professor Claire B. Paris.
No. of pages in text. (204)

Mesophotic coral ecosystems (MCE) are defined as phototrophic coral habitats found deeper than 30 m. Despite being aware of these ecosystems for over 200 years, surprisingly little information is available on their ecology and biology. Recently, MCE have received renewed interest, as it appears that depth and distance from shore have the potential to buffer coral organisms from the detrimental effects of coastal development and climate change. The "deep reef refugia hypothesis" (DRRH) is an umbrella term for a collection of hypotheses concerning the role of MCE in the uncertain future of coral reefs, yet our predictions are limited by shortcomings in our understanding of some very basic effects of depth on corals and associated communities. In order to investigate the effects of depth on coral reproductive biology, sampling of *Montastraea faveolata* and *Porites astreoides* coral tissues was conducted along a depth gradient from 5 to 40 m during coral reproductive seasons in the Northern United States Virgin Islands (USVI), and observations of coral spawning and planulation were made. Samples were histologically analyzed for gamete development, reproductive activity and fecundity. Mesophotic populations of both *M. faveolata* and *P. astreoides* were reproductively active in MCE with similar gametogenic cycles to nearby shallow coral populations. There was evidence of *M. faveolata* split spawning in August and September at all

depths, and oocyte development was delayed but more rapid in mesophotic corals. *M. faveolata* fecundities were significantly higher in MCE (35-40 m) than in shallow (5-10 m) sites, but the differences were not significant between mid-depth (15-22 m) and either shallow or mesophotic sites. There was no difference found in *P. astreoides* fecundity between mesophotic, mid-depth and shallow sites, however planulation appeared to be delayed in mesophotic colonies by 1-2 weeks. Differences in fecundity per area and coral cover between depths determine the number of propagules a unit reef will produce at different depths. In the case of *M. faveolata*, ova production is likely an order of magnitude greater at 35 m than at 10 m. The Connectivity Modeling System, an individual-based stochastic biophysical model of larval dispersal, parameterized with depth-specific productivity estimates and species-specific reproductive seasons and larval traits, was used to evaluate the vertical connectivity of *M. faveolata* and *P. astreoides* larvae between MCE and shallow coral habitats in the Northern USVI. Sensitivity analyses were performed to test the sensitivity of mesophotic larval subsidy into shallow habitats to depth-specific productivity, pelagic larval mortality, depth-specific fertilization rates and depth-specific post-settlement survivorship. Simulated mesophotic subsidies to shallow recruitment were found to be considerably robust, and mesophotic subsidy to shallow recruitment accounted for a greater proportion of total recruitment as shallow productivity was reduced. Even when modeled mesophotic fertilization rates and larval post-settlement survivorship were dramatically reduced, the model predicted what would likely be demographically significant mesophotic larval subsidy into shallow habitat. Mesophotic *M. faveolata* skeletal density, extension and calcification were estimated using micro-computed tomography. Results suggest that rates of linear

extension of *M. faveolata* in USVI MCE may be quite fast compared to other Caribbean MCE, and that total calcification in MCE may rival shallow coral calcification. Lastly, consistencies and inconsistencies in the population connectivity of two coral and three fish constituent species in Caribbean coral reef assemblages were investigated using a nested biophysical model. Connectivity networks of coral species were more fragmented than fish, and the networks of corals and fish showed different patterns of betweenness centrality. This suggests that populations of corals and fish will likely be affected by habitat fragmentation in different ways, and that they require specific management consideration. This dissertation suggests that MCE are integral to the population connectivity of corals in the USVI and likely to wider Caribbean metapopulation connectivity as well. Further study of these highly productive ecosystems is necessary to better understand the DRRH and the role of MCE in the past, present and future of coral reefs.

For my mother

Champion of the treasures of creativity, curiosity and silliness.

Acknowledgements

There are many people who supported this dissertation in body, spirit and finance. The guidance and leadership of Dr. Claire B. Paris ensured the quality of this dissertation and pushed me to pursue excellence in my work. My dissertation committee members, Dr. Andy Bakun, Dr. John W. McManus, Dr. Margaret W. Miller and Dr. Tyler B. Smith helped me to ask the important questions and to synthesize a cohesive exposition.

My family and particularly my nephew, Arthur, were a source of continued inspiration. Kristine Stump provided endless support and levity when it was most needed. Ian Enochs supplied both his boisterous friendship and his cogent advice. Viktor Brandtneris and a long list of enthusiastic students at the University of the Virgin Islands were indispensable to the success of my field work and to the preservation of my humor. Tyler Smith and Marilyn Brandt provided intellectual and field support, as well as their invaluable friendship.

I must thank my collaborators, including Dr. Peter J. Mumby, Dr. Ian C. Enochs, Dr. Derek Manzello, Dr. Ana Vaz, Xaymara Serrano, and Dr. Andrew Baker. None of this would have been possible without the members of the Paris Laboratory, including Andy Kough, Erica Staaterman, Matt Foretich, Dr. Ana Vaz, Dr. David Lindo and Cedric Guigand.

Lastly, thank you to the Rosenstiel School family, for being my friends and a part of my life.

Funding sources:

NSF-RAPID (to Claire B. Paris) 1048697, Natural Environmental Research Council and EU FORCE project (to Peter J. Mumby and Claire B. Paris), NSF Science Made Sensible Fellowship, RSMAS Fellowship, Rowland Fellowship

TABLE OF CONTENTS

LIST OF FIGURES

LIST OF TABLES

Chapter 1: Introduction

Over nearly the last two hundred years, the study of coral reef ecosystems has focused primarily on habitats shallower than 30 m. Deep-sea cold-water coral ecosystems have received increased attention in the last several decades, visited and studied through the use of submersibles and remote and automated underwater vehicles. Coral reef habitats in intermediate depths have been largely neglected in our investigations of the sea; a *mare incognitum* deeper than the physiological limits of traditional SCUBA technology, and shallow enough that the use of more advanced – and expensive – marine technologies has not often been applied.

Intermediate depth coral ecosystems require distinction from what are often termed "deep-sea reefs", which refer to cold water aphotic corals and associated organisms. The term "mesophotic" (Pomar 2001) is used to describe benthic habitats in the lower range of the photic zone, yet above the oligophotic zone. In practice, and in coral reef science, mesophotic coral ecosystems (MCE) are generally characterized as benthic habitats deeper than 30 m in which phototrophic corals are present. The shallow limit of MCE is not simply delineated by the limits of traditional SCUBA, but also the depth at which the physical environment precipitates marked changes in species composition (Liddell and Ohlhorst 1988; Kahng et al. 2010) (Figure 1.1).

The presence of corals growing at intermediate depths has been recognized for at least 120 years (Darwin 1889). Some of the first direct observations of intermediate depth coral reefs were made in the 1970s and 1980s (Loya 1972; Dustan 1975; Dunstan and Dustan 1979; James and Ginsburg 1980; Graus and Macintyre 1982; Done 1983; Liddell and Ohlhorst 1988). Loya (1972) observed increases in species richness at depths up to

30 m in the Red Sea, despite light intensity only 5% of surface intensity. However, after this initial wave of characterization, MCE were largely ignored again until the early 21st century.

More recent explorations of MCE have revealed environments with what might be considered remarkable living coral cover (Bak et al. 2005; Armstrong et al. 2006; Armstrong 2007; Menza et al. 2007, 2008; Smith et al. 2008; Bare et al. 2010; Bridge et al. 2010). This is likely the effect of a shifting baseline (Pauly 1995), where MCE have been less degraded than shallow reefs throughout the last 30 years of shallow coral reef decline (Gardner et al. 2003; Wilkinson 2008), and partly explains the renewed interest in these environments over the past decade. MCE appear to be buffered from many of the coastal and global stressors associated with coral reef degradation, including coral thermal bleaching (Glynn 1996; Riegl and Piller 2003; West and Salm 2003), surface waves and fragmentation (Goldberg 1983) and terrestrial sedimentation and pollution (Menza et al. 2008; Smith et al. 2008). This notion has prompted the development of a "deep reef refugia hypothesis" (DRRH) which stipulates that MCE may have the capacity to behave as refugia for coral organisms and associated species during periods of adverse conditions, including the present adversity caused by coastal development, overfishing and global climate change (Glynn 1996; Riegl and Piller 2003). A refugium need not be directly connected – for example, through larval exchange – to degraded populations in order to provide metapopulation resilience. However, the degree of population connectivity between degraded shallow reefs and MCE refugia has implications for shallow coral reef resilience, population dynamics and management, and study of this

connectivity has become integral to the DRRH (Hughes and Tanner 2000; Lesser et al. 2009; Bongaerts et al. 2010a)

Lesser et al. (2009) and Bongaerts et al. (2010a) provide comprehensive reviews of the present scientific understanding of MCE, particularly in the Caribbean, and general assessments of the DRRH. Both sets of authors highlight gaps in our knowledge of MCE that afford considerable caveat to the potential that mesophotic reefs may be a source of larvae to degraded shallow habitat. The present work included in this dissertation endeavors to address several of these knowledge gaps, and includes an in-depth evaluation of the refugia potential of MCE in the US Virgin Islands (USVI).

Goals, objectives and chapter overview

The intention of this dissertation was to directly address knowledge gaps in both the DRRH and in the study of marine metapopulations: (1) Are mesophotic corals reproducing? If so, (2) how does depth affect reproductive output of corals in MCE compared to the reproductive output of shallow corals? (3) How do the confluence of coral biology and the physical environment affect the migration of larvae from mesophotic habitats into shallow habitats? (4) Are MCE in the USVI potential refugia for coral species? (5) Can biophysical modeling and graph theory provide tools with which to identify habitat critical to the persistence of marine populations? The dissertation chapters are arranged as follows:

Chapter 2: Mesophotic reproductive refugia for two depth-generalist species
An evaluation of the reproductive capacities of two Caribbean corals over a depth gradient extending into the mesophotic zone, and the reproductive output expected from habitats of varying depth.

Chapter 3: Micro-computed tomography of small mesophotic coral samples for the estimation of annual growth and calcification

An investigation of a novel application of micro-computed tomography to the study of mesophotic coral sclerochronology.

Chapter 4: Modeling of vertical connectivity and mesophotic coral refugia in the US Virgin Islands

A high-resolution dispersal modeling study of the magnitude and direction of larval exchange between mesophotic and shallow habitats in the northern USVI.

Chapter 5: Consistency and inconsistency in multispecies population network dynamics of coral reef ecosystems

The development of a framework of analyses with which to evaluate larval connectivity in complex multi-species habitat networks, and a discussion regarding management implications.

Chapter 2 examined coral fecundity, gametogenesis and spawning/planulation through histological analysis of reproductive tissues in *Montastraea faveolata*, a broadcast spawning species, and *Porites astreoides*, a brooder. Estimations of reproductive effort and output in habitats of different depths were made based on polyp fecundity, polyp spacing and coral cover. Additional coral gamete and larval characteristics with implications for dispersal potential such as specific gravity were estimated in the laboratory. Hypotheses tested included (1) equal egg/larval production in corals from depths of 5-40 m, and (2) equal rates of development and gamete size (*M. faveolata only*) in corals from depths of 5-40 m. Kojis and Quinn (1984) and Richmond (1987) investigated the effects of depth on coral fecundity in the Pacific, and Rinkevich and Loya (1987) in the Red Sea. In each case only brooding species were studied (Table 1.1). Villinski (2003) addressed the fecundity of the Caribbean broadcast spawning coral *M. faveolata* along a depth gradient of 3-18 m (Table 1.1). The study described in Chapter 2 also focuses on *M. faveolata*, and more than doubles the depth range studied by

Villinski (2003), with maximum depths approaching 40 m, while simultaneously addressing the effects of depth on the reproduction of a brooder, *P. astreoides.* This is the first known such study to these depths for both of these species, and potentially also the first study of coral fecundity in MCE in the Caribbean.

Chapter 3 investigated the novel application of an advanced technology – micro-computed tomography (micro-CT) – in measuring the growth, density and calcification of mesophotic coral fragments collected for the soft tissue analysis in Chapter 2. Density (growth) banding is notoriously difficult to discern in mesophotic *M. faveolata* (Baker and Weber 1975), and micro-CT may provide a novel tool for making necessary assessments of coral health and growth in mesophotic habitats. Understanding mesophotic coral growth and calcification rates enhances the ability to make predictions regarding the response of MCE to climate change and perturbation. This chapter also stresses that growth may vary considerably between MCE, and that it is possible that total calcification in MCE exceeds calcification in degraded shallow habitats.

In Chapter 4 the refugia potential of MCE in the northern USVI was assessed through the development of a biophysical model of coral larval dispersal parameterized with species specific coral reproductive and larval traits (Chapter 2), and three-dimensional settlement habitat based on shallow and mesophotic coral habitat in the USVI. It was hypothesized that depth-specific coral productivity (discussed in Chapter 2) would affect the model's predictions of mesophotic larval settlement in shallow habitats. Because the effects of depth on coral gamete fertilization and post-settlement survivorship of mesophotic coral planulae larvae are unknown, the sensitivity of the model's predictions of vertical larval connectivity to these factors was examined. This

study has specific implications for the study of DRRH and the use of biophysical modeling in the prediction of coral reef persistence and health. Biophysical modeling of marine larvae has become an important tool in evaluating population connectivity and barriers to dispersal (Cowen 2000; Paris et al. 2005, 2013, 2002; Cowen et al. 2003, 2006; Baums et al. 2006; Steneck 2006; Botsford et al. 2009; Cowen and Sponaugle 2009; Pelc et al. 2010; Mumby et al. 2011a; Sponaugle et al. 2012; Staaterman et al. 2012; Foster et al. 2012; Kough et al. 2013). To date, the study described in Chapter 4 may be the first to address vertical habitat connectivity using a biophysical model, and the first known use of a biophysical model in the evaluation of the DRRH.

Chapter 5 provides a framework and suggests novel indices for describing habitat connectivity in complex, large-scale multi-species networks. Those particularly interested in the methods and results of Chapter 4 may benefit from reading Chapter 5 for additional context. Chapter 5 investigates inherent differences in the management of different marine species imposed by species-specific larval traits and dispersal. Also, this chapter explores methods to identify regions or habitats that would be ideal for protection due to natural resilience to larval supply failure and importance in population connectivity for one or multiple species.

Context and outlook

This dissertation presents major findings in the understanding of the effects of depth on the reproductive capacity of depth-generalist coral species in the Caribbean. The novel application of micro-CT in Chapter 3 renews interest in the sclerochronology of intermediate-depth corals during a time when understanding the rates of coral deposition

of $CaCO_3$ may be becoming critical for their conservation due to the acidification of shallow oceans. The incorporation of vertical migration into the biophysical modeling of marine larval dispersal represents a significant contribution to the study of population connectivity, and the results from the biophysical model described in Chapter 4 have the potential to change how we address the DRRH.

The work described here is complementary to studies of population genetics, and results from concurrent studies in the USVI support the findings of this dissertation. Additionally, Chapters 2 and 3 complement ongoing studies of energetics and heterotrophic feeding in mesophotic corals. Potentially the greatest contribution of this work to our understanding of coral reefs is that MCE are not merely "fringe" habitats in which corals and associated organisms live perilously close to the extremes of their capabilities. These vibrant ecosystems are more than simply refugia, but are vital parts of larger coral reef metapopulations. Intermediate depth habitat has likely been critical to the persistence of coral reefs throughout their existence, and our recently renewed interest in mesophotic coral ecosystems may be a reflection of how little we really know.

Table 1.1. Studies investigating the effects of depth on coral fecundity.

Species	Reproductive mode	Depth range	Location	Source
Acropora palifera	Brooder	0-20	Pacific	Kojis and Quinn (1984)
Pocillopora damicornis	Brooder	5-33	Pacific	Richond (1987)
Stylophora pistillata	Brooder	5-45	Red Sea	Rinkevich and Loya (1987)
Montastraea faveolata	Broadcast	3-18	Caribbean	Villinksi (2003)

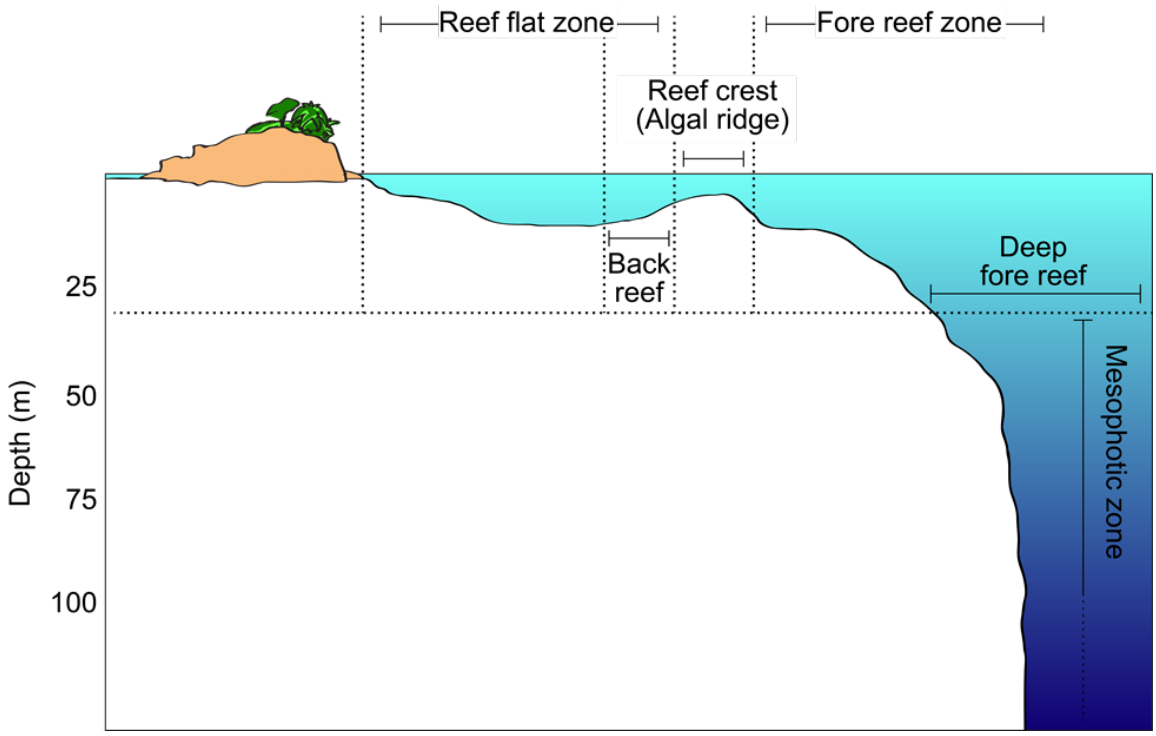

Figure 1.1. Coral reef zonation demonstrating the deep fore reef as a part of the mesophotic zone. Illustration adapted from Lesser et al. (2009).

Chapter 2: Mesophotic reproductive refugia for two depth-generalist coral species

Background

Globally, shallow water coral reefs are at risk of severe degradation due to escalating and interacting stressors that occur at local and global scales (Glynn 1996; Wellington et al. 2001; Hughes et al. 2003a; Carpenter et al. 2008; Wilkinson 2008; Wilkinson and Souter 2008). The drastic decline in living coral on shallow reefs over the past 30 years, particularly in the Caribbean, may compromise the ability of these reefs and associated species to persist in a changing climate (Gardner et al. 2003; Hughes et al. 2003b; Carpenter et al. 2008).

Mesophotic coral ecosystems (MCE) existing between 30 and 150 meters depth are largely uncharacterized, and it has been shown that MCE may be buffered from some of the stressors associated with habitat degradation in shallower reefs (Bak et al. 2005; Armstrong et al. 2006; Armstrong 2007; Nemeth et al. 2008; Smith et al. 2010), such as coral thermal bleaching (Glynn 1996; Riegl and Piller 2003; West and Salm 2003), surface waves and fragmentation (Goldberg 1983) and terrestrial sedimentation and pollution (Smith et al. 2008). Overlap of scleractinian coral species has been shown to be high between shallow and mesophotic habitat in the US Caribbean and Puerto Rico (Armstrong et al. 2006; Armstrong 2007; Bongaerts et al. 2010a; Smith et al. 2010), and US Virgin Island (USVI) MCE have been shown to often have higher coral cover than adjacent shallow reefs (Menza et al. 2008; Smith et al. 2008), suggesting that Caribbean reefs with the highest modern coral cover may also be the least studied. The role of these

deeper light-dependent coral populations in the stability, resilience and connectivity of coral reefs in the greater Caribbean is largely unknown.

The hypothesis that MCE could represent a refuge for shallow coral species threatened by a changing climate and coastal development has been termed the "deep reef refugia hypothesis" (DRRH), and has been increasingly discussed in the literature in recent years (Hughes and Tanner 2000; Riegl and Piller 2003; West and Salm 2003; Armstrong et al. 2006; Venn et al. 2008; Lesser et al. 2009; Bongaerts et al. 2010a). In an assessment of the to-date understanding of the DRRH, Bongaerts et al. (2010) recognized that a major knowledge gap in the DRRH includes estimating the potential for mesophotic coral propagules to colonize shallow habitats. In order to fill this knowledge gap (1) the reproductive capacities and behaviors of mesophotic corals must be investigated and (2) the potential for larval exchange between mesophotic and shallow habitat to occur must be estimated, likely utilizing a number of techniques including genetic and physical models of connectivity. The current paper focuses on the first goal, estimating the reproductive capacity and behaviors of two depth-generalist species of coral in the USVI.

Coral recruitment can be highly variable in space and time. Most adult corals are completely sedentary, and thus reproductive success depends on the successful fertilization and development of free-swimming planulae larvae. Variability in gamete viability, adult conspecific density and fecundity, timing of reproductive activities, and the physical conditions of both dispersal and settlement habitat are just some of the factors affecting the reproductive success of corals. Corals have evolved a number of reproductive strategies to maximize reproductive success. Most corals release gametes in

synchronous mass spawning events (broadcast spawning), which maximizes fertilization potential (Harrison and Wallace 1990) and may be timed with favorable oceanographic conditions(van Woesik 2009). These externally fertilized gametes develop into larvae in the water column and disperse. In contrast, the brooding reproductive strategy includes the internal fertilization of conspecific sperm. Brooded larvae develop internally and are competent to settle very quickly after release, which minimizes the time larvae need to spend in the water column and increases settlement success (Szmant 1986). Additionally, many corals have evolved hermaphroditism, which increases the probability that any local conspecific is a potential mate (Harrison and Wallace 1990 and citations therein).

Little is known about the effects of depth on the reproductive capacity and behavior of phototrophic scleractinian corals, and only a handful of previous studies have been published. Kojis and Quinn (1984) found a negative correlation with depth and fecundity in the Pacific brooding coral *Acropora palifera* from 3 to 40 m. Rinkevich and Loya (1987) found a similar correlation for the brooding coral *Stylophora pistillata* in the Red Sea (5-45 m), and a truncated reproductive season for deeper-living colonies. In contrast, Richmond (1987) found no correlation of fecundity with depth in another Pacific brooding species, *Pocillopora damicornis*. The only known study focusing on a broadcast coral (Villinski 2003) found no correlation between depth and fecundity of *M. faveolata* polyps, but did find differences in gametic characteristics and a decrease in colony fecundity related to polyp spacing (which is depth dependent [Graus and Macintyre 1982]). However, the maximum sampling depth in the Villinski study was 18 meters, which does not approach mesophotic depths, and may not have been deep enough to observe heterogeneity in egg production related to increasing depth. In regards to

mesophotic coral spawning observations, previous to this study the only known observations were made by Vize (2006), who observed spawning of *M. cavernosa, M. franksi* and *Diploria strigosa* at 33 to 45 m at Flower Garden Banks, all within the same spawning temporal windows as shallower conspecifics, however observations were limited to only a few coral colonies.

The relationships between depth and coral fecundity require further investigation, and these are likely species-specific. Because MCE can be remarkable in total area (Riegl and Piller 2003; Locker et al. 2010; Smith et al. 2010) and coral cover, even dramatically reduced fecundity with increasing depth may still imply a large larval load due to the number of reproducing colonies. The current study investigated gamete development, fecundity and reproductive synchronization of two scleractinian corals, *M. faveolata* and *P. astreoides* from shallow, mid-depth and mesophotic reef sites. This study will inform further research into the potential for larval exchange between MCE and shallow reefs, and provides insight into the DRRH.

Methods

Sampling for coral reproductive characteristics was performed off the south side of St. Thomas, USVI in 2010, 2011 and 2012. St. Thomas and St. John make up the northern USVI, and are joined together and to the British Virgin Islands and Puerto Rico by the shallow Puerto Rican Shelf platform. The insular shelf south of St. Thomas is a gradual slope, and extensive linear MCE can be found on submerged banks along the shelf edge (Figure 2.1).

M. faveolata – the broadcast species chosen for study – belongs to the *M. annularis* species complex (Knowlton et al. 1992; Weil and Knowlton 1994) which is comprised of the principal structural reef-building scleractinian corals in the Caribbean (Goreau 1959). Its morphology ranges from encrusting to plating to massive, and it grows in thick plates at depth (Graus and Macintyre 1976, 1982; Pandolfi and Budd 2008). It can be distinguished in the field by its shape, tissue color, polyp size and spacing, and corallite structure (Knowlton et al. 1992). The species is simultaneously hermaphroditic, with each polyp producing egg and sperm simultaneously. Each colony typically spawns once a year, about one week after full moon in either August or September (Szmant 1986, 1991; Szmant et al. 1997). Spawning usually lasts for under an hour, during which egg and sperm bundles are extruded from the oral cavity of the polyp and float to the ocean surface where eventually they break apart and potentially cross-fertilize (Szmant et al. 1997). *M. faveolata* is a depth-generalist that can be abundant in shallow habitats and has been shown to be dominant and extremely abundant in MCE in the USVI (Armstrong et al. 2006; Armstrong 2007; Smith et al. 2008 [represented in the *M. annularis* species complex]).

Porites astreoides is a small to medium sized encrusting/mounding brooding coral with a similar depth range to *M. faveolata*. *P. astreoides* is common both in shallow habitats and in USVI MCE (Armstrong et al. 2006; Armstrong 2007; Smith et al. 2008). In contrast to *M. faveolata*, *P. astreoides* releases fully developed planula larvae from April until as late in the year as September, with peak larval release focused around new moons in April and May (Szmant 1986; Chornesky and Peters 1987; Mcguire 1998).

Sample collection

M. faveolata tissue samples (~20cm^2) were taken from central high-points on colonies larger than 400cm^2 in order to target reproductively mature colonies (Szmant 1985b). Samples were collected in late summer in 2010 and 2011 using a hammer and cold chisel (Figure 2.2). In 2010, samples were taken from five reef sites on August 26-28, several days prior to the date of expected spawning in August. Sites ranged in depth from 5-45m (n >= 10*site^{-1}, N = 79) (Figure 2.1, Table 2.1). All sampling was performed using open-circuit SCUBA, at times utilizing enriched air (nitrox) or mixed gas (heliox). In all cases, samples were taken pseudo-randomly utilizing a random compass heading and a minimum of 15 fin kicks in order to reduce the potential of sampling clones.

In July and August 2011 *M. faveolata* was sampled at three sites over five weeks (n >= 5 site^{-1} week^{-1}, N = 77). The three sites included a shallow inshore site (Black Point, 5-8m), a mid-depth off-shore island site (Flat Cay, 16-21m), and a mesophotic site (Grammanik Bank, 37-40m). All tissues were fixed in zinc-buffered formalin (Z-Fix) for 24 hours, and rinsed in fresh water for another 24 hours before being stored in 70% EtOH until processing.

In 2011, *P. astreoides* tissue samples (~20cm^2) were taken from central high-points on colonies at least 100cm^2 using a hammer and cold chisel at the same three reef sites weekly for five consecutive weeks in April and May (n >= 5 site^{-1} week^{-1}, N = 79). Colonies sampled from Grammanik Bank were slightly shallower than *M. faveolata* sampled at the same site (34-37m). All tissues were fixed in zinc-buffered formalin (Z-Fix) for 24 hours, and rinsed in fresh water for another 24 hours before being stored in

70% EtOH until processing. Full *P. astreoides* colonies from each site were brought to the lab for planulation observations.

The longest diameter, perpendicular diameter and height were recorded for each sampled coral colony. Colony surface area is often estimated using an equation for a two dimensional ellipse (Crabbe et al. 2002; Crabbe and Smith 2003; Villinski 2003), calculated from the largest diameter of the coral head and the perpendicular diameter. An alternative method for mounding corals uses the equation for a hemisphere in order to account for colony height (a single average diameter is used, Naumann et al. [2009]), however this method assumes all radii (length/2, width/2, height) are equal. Both these estimators may fail to describe surface area in corals such as *M. faveolata* because the morphology of *M. faveolata* changes dramatically from shallow to mesophotic environments (Graus and Macintyre 1982). Elliptical surface area potentially underestimates mounding coral surface area, and hemispherical surface area potentially over estimates the surface area of plating morphologies (Figure 2.3). Colony surface area was instead estimated as half the surface area of a three-dimensional scalene ellipsoid using the longest diameter, perpendicular diameter and the height of the colony (from the Thomsen approximation)[1]:

$$Surface\ Area \approx 4\pi \left(\frac{1}{3} * \left(\left(\frac{a}{2}\right)^p \left(\frac{b}{2}\right)^p + \left(\frac{a}{2}\right)^p (c)^p + \left(\frac{b}{2}\right)^p (c)^p \right) \right)^{\frac{1}{p}} \Big/ 2 \qquad (1)$$

Where a is the longest diameter of the colony, b is the diameter of the colony perpendicular to a, and c is the height of the colony. p is a constant equal to 1.6075. This

[1] This approximation has been discussed by Sigma Xi mathematician David W. Cantrell and Gerard P. Michon (http://www.numericana.com/answer/ellipsoid.htm#thomsen). See also Xu et al. 2009 for use in primary literature.

method should theoretically be a better estimator of coral surface area than a two-dimensional ellipse or an average hemisphere, particularly when making comparisons between shallow and mesophotic coral colonies.

In 2012, ten partial colonies of *M. faveolata* were collected several days before predicted spawning in both August and September from a deep site (35-40m) and a shallow site (5-10m). These samples were kept in temperature-controlled (27°C +/-1°C) flow-through seawater Tables in the laboratory and were exposed to near-natural light cycles. In the evenings throughout the potential spawning window, these partial colonies were observed for spawning behavior in isolated glass jars. Additionally, video systems were deployed in August and September 6-9 days after full moon in an effort to capture video of spawning at mesophotic and shallow reef sites. Video systems were built using two GoPro HD cameras and external lights mounted on a PVC or milk-crate frame. One camera was directed downward to capture video of the coral colony surface, while the other was directed outward to survey nearby coral colonies. The systems were deployed from a boat in tandem with a drop camera.

Egg bundle/planulae specific gravity and cross-transplantation

Egg bundle rising rates were estimated from video of *M. faveolata* colonies spawning in the lab on the evening of September 7th, 2012. From these rates the average specific gravity of an egg-bundle was estimated using a derivation of the Navier-Stokes equations (Okubo 1980):

$$w_{buoyant} = \frac{2(\rho_w - \rho_b)gR^2}{9k} \quad (2)$$

thus:

$$\rho_b = \rho_w - \frac{9kw_{buoyant}}{2gR^2} \quad (3)$$

Where $w_{buoyant}$ is the average buoyant velocity (rising rate) of an egg bundle, ρ_w is the specific gravity of seawater (1.0221 at 29°C and 35ppt), ρ_b is the specific gravity of the egg bundle, g is the gravitational force, R is the radius of the egg bundle and k is the kinematic viscosity of seawater ($0.8613*10^{-6}$ m^2s^{-1} at 29°C and 35ppt).

On the evenings of May 2nd and 3rd, 2011, whole colonies of *P. astreoides* from each sampling site were observed for planulation. Estimates of the specific gravity of larvae were obtained by depositing sub-sampled larvae in one of a series of plastic buckets containing sea water of ranging known density, and observing the larvae for positive, negative or neutral buoyancy.

Additional sub-samples of larvae were prepared for field transplantation experiments. Coral larvae have been shown to be sensitive to ultraviolet radiation (Gleason and Wellington 1995; Wellington and Fitt 2003; Gleason et al. 2005), and larvae brooded in deeper habitats may be more sensitive than larvae from shallow habitats (Gleason and Wellington 1995; Gleason et al. 2005). Transplant experiments were conducted in order to estimate survivorship of mesophotic *P. astreoides* larvae in shallower habitats. Because sufficient numbers of larvae were obtained only from Grammanik Bank colonies, only larvae from this site were used in transplantation experiments. 10 larvae were placed in 5 UVA and UVB transparent acrylic tubes with nylon mesh caps per site and tubes were fastened to the substrate on their long edge using zipties (150 larvae total). Tubes were revisited over the course of 12 days in order to estimate percent survival.

Histological preparations

Samples were decalcified using a solution of 10% HCl and 0.5g EDTA l^{-1}. The decalcification solution was replaced every 24 hours until all calcium carbonate had been dissolved. After decalcification, tissue was stored in 70% EtOH until further processing. A tissue processor (Sakura Tissue-Tek II) was used to dehydrate and parafinize tissues. Parafinized tissue was arranged for cross and longitudinal sectioning and embedded in paraffin blocks using a tissue embedding station (Sakura Tissue-Tek TEC). Blocks were then sectioned on a Leica RM2235 microtome with 4 micron thickness at three depths, beginning just below the oral opening, with subsequent sections occurring every 100 microns. Sections were arranged on microscope slides and prepared for staining. Tissue was stained using a modified Heidenhain's aniline blue stain. Because the initial set of sections for *M. faveolata* were not quite deep enough for accurate analyses of fecundity, these samples were resectioned, two sections per sample, with sections extending at least 600 microns deeper into the tissue.

Reproductive characteristics

M. faveolata histological sections were analyzed for (1) presence/absence of male and female gonads and gametes of each reproductive stage (Szmant 1985a, 1985b, 1986, 1991), (2) the fecundity, or number of oocytes or ova per gonad, and the number of gonads per polyp (Szmant 1985b, 1991; Van Veghel 1994; Villinski 2003) as well as (3) the size and condition of gametes. *P. astreoides* histological sections were evaluated for (1) presence/absence of male and female gonads and planulae larvae, and (2) the density

of larvae in the tissue over area. Slides were analyzed using both standard light microscopy as well as an Olympus VS120-S5 digital slide scanner, and measurements were made using the Fiji software package (Schindelin et al. 2012).

The number of polyps per surface area was estimated by utilizing a white light 3D scanner to digitize samples (3D3 Solutions HDI Advance). Polyps were enumerated on the 3D scans in Leios 3D scan data processing software, and then those digital surfaces were smoothed to find the basal surface area (Figure 2.4).

Fecundity per cm^2 was estimated as the product of:

$$Fecundity_M = eggs * gonad^{-1} * gonads * polyp^{-1} * polyps * cm^{-2} \quad (4)$$

or

$$Fecundity_P = planulae * cm^{-2} \quad (5)$$

Where $Fecundity_M$ represents *M. faveolata* fecundities cm^{-2} and $Fecundity_P$ represents *P. astreoides* fecundities cm^{-2}. Fecundity per *M. faveolata* polyp was estimated as the product of the average number of gonads per polyp in cross-section and the average number of oocytes or ova per gonad in longitudinal section for at least 3 polyps per sample (when possible). In order to derive depth-specific unit reef egg production, estimates of percent coral cover were calculated from diver transects performed at each site by University of the Virgin Islands researchers from 2001-2012. The products of equations 4 and 5 were then multiplied by coral cover to estimate the number of eggs per $1km^2$ unit reef as a function of depth.

Results

Montastraea faveolata

Video observations in the field in August and September 2012 revealed evidence of mesophotic spawning in the *M. annularis* species complex. On August 11th, nine nights after full moon, spawning was observed in an *M. faveolata* colony between 35 and 40m at ~21:00. In addition, gamete bundles were observed in the water column. On the evening of September 7th (seven nights after full moon), a full-colony spawn of *M. franksi* was captured on video at ~38m at 20:49 (Figure 2.5a).

Spawning behavior was also observed in *M. faveolata* colony fragments kept in the laboratory (Figure 2.5b). Corals were kept in flow-through seawater Tables with a controlled temperature of 27°C (+/- 1°C) and salinity of 35 ppt. On the evening of August 10th (8 nights after full moon) one mesophotic colony of ten (10% of total) released gamete bundles at ~21:00, and one shallow colony of ten (10%) released gamete bundles about two hours later at ~23:00. These were not whole-fragment spawns. On September 7th (seven nights after full moon) four of ten mesophotic colonies (40%) and three shallow colonies (30%) released gamete egg bundles in whole-fragment spawns. Mesophotic colonies released gametes between 20:00 and 20:45, whereas shallow colonies released gametes between 21:45 and 22:30, with some gamete bundles still being released as late as 23:20.

From video and photos taken in the laboratory, the mean rising rate of gamete bundles from a mesophotic coral was found to be .006279 $m*s^{-1}$ (SD +/- 0.001907). Mean gamete bundle diameter was estimated to be 0.00182 m (SD +/- .000376). Using equations 2 and 3 and the conditions of the seawater in the laboratory, the mean specific

gravity of *M. faveolata* gamete bundles was estimated to be 1.0213, with a range of 1.0193-1.0221 based on calculations made using one standard deviation in both rising rate and gamete bundle diameter.

After 00:45-01:00 post spawning, individual gamete bundles were still relatively intact when experiencing little to no water motion, however bundles had begun to show signs of breaking down. By 01:10, most gamete bundles had broken down considerably but were still easy to differentiate visually. By 01:45-02:00, bundles were almost completely broken down into individual eggs and not differentiable. Preliminary cross-fertilization (within depth bins only) trials did result in successful fertilization of both shallow and mesophotic gametes as shown by the development of swimming planulae larvae; however, no larvae survived past a couple of days, possibly due to poor laboratory conditions.

Reproductive histology

When stained with Heidenhain's aniline blue, *M. faveolata* oocytes stained gold to orange, and spermaries (spermatozoa) stained deep red. The mesoglea stained blue (Figures 2.6, 2.7 and 2.8). *M. faveolata* colonies from all sites were found to contain both male and female gametes in 2010 and 2011. Due to variation in sampling and histological processing, samples from 2010 are most useful as indicators of the percentage of colonies that were reproductively active during the sampling period. 54.5-80% of colonies were reproductive in August 2010 at each site (Table 2.2).

In 2011 *M. faveolata* histological analysis revealed presence of spermaries of stages II-V and oocytes/ova of stages II-IV (Szmant 1985a) in corals from all sites

(Figure 2.6). Stage I spermaries and oocytes were also identified at all sites, however they are not included in this analysis due to difficulty in identification of these early stage gametes. Analysis of spermatogenesis suggested development from earlier stage spermaries in late July and early August to late stage mature spermaries prior to spawning at all sites (Figure 2.9). Late stage spermaries were absent (lost) from coral tissues at all sites approximately one week after full moon, indicative of spawning. In some cases, stage V spermaries remained, however the presence of free spermatozoa in the mesentery suggested that these spermaries were residual after spawning occurred (Figure 2.7). At Grammanik Bank (GB) 60% of colonies contained stage V spermaries on the 19th of August, and by the 25th of August no colonies contained intact stage V spermaries. Both Flat Cay (FL) and Black Point (BP) experience similar losses of stage V spermaries from 40% of colonies. Additional evidence of spawning was present in tissues from all sites in the last week of sampling, including wasted mesenteries and the aforementioned residual spermatozoa in the mesentery (Figure 2.7). The presence of early stage spermaries increased in colonies at all sites late in August (Figure 2.9).

Oogenesis is a longer process than spermatogenesis, and by the first week of sampling in 2011 over 75% of colonies from each site contained stage II oocytes (Figure 2.9). Colonies rapidly lost stage II oocytes as they developed into stage III and IV oocytes/ova throughout the sampling period. This development was delayed but more rapid in mesophotic colonies. Histological evidence of spawning characterized by the loss of stage IV ova from coral tissue was seen in colonies from Grammanik Bank, of which 100% contained stage IV ova just prior to the time of expected spawning, and 60% contained stage IV ova one week later. A loss of stage IV ova was also observed in

colonies from Black Point. There was also evidence of ova retention and development beyond the date of August 2011 spawning at all sites.

Oocyte/ovum diameters were measured from three oocytes/ova in each of three polyps per colony. Oocyte diameters increased during the first three weeks of sampling at all sites. During these three weeks, oocytes measured from Grammanik Bank corals were significantly smaller than those from Flat Cay and Black Point (weekly Kruskal-Wallis ANOVA/Bonferroni method: $p < 0.01$ in week one, post-hoc comparison GB < FL, $p = 0.01$; $p < 0.001$ in week 2, post-hoc comparison GB<FL and GB<BP, $p < 0.001$ and $p = 0.041$, respectively; $p < 0.01$ in week 3, post-hoc comparison GB<FL and GB<BP, $p = 0.049$ and $p = 0.005$, respectively) (Figure 2.10). However, by week four, oocytes from Grammanik Bank had increased in diameter to the point that there were no significant differences in oocyte/ovum diameter between sites, and the same was true for week five, post any spawning that may have occurred. At week four, average oocyte/ova diameters (SD) for Black Point, Flat Cay and Grammanik Bank were 283.36µm (61.93), 265.77µm (59.22), and 275.01µm (45.60) respectively.

M. faveolata fecundity estimates, expressed as the number of gonads per polyp, the number of oocytes/ova per gonad and the product of these two estimates, were pooled between weeks 1 through 4 (pre-spawning samples). The pooled results were non-normal, even after log-transformation. Levene Tests for all estimates resulted in p-values greater than 0.05, suggesting that Kruskal-Wallis ANOVA tests would be appropriate in all cases. The number of gonads per polyp tended towards 12 (one gonad per septa), however colonies from Grammanik bank had significantly more gonads per polyp than either Black Point or Flat Cay corals (Kruskal-Wallis ANOVA/Bonferroni method, p =

0.0028; post-hoc comparison, GB>FL and GB>BP, p = 0.001 and 0.033, respectively) (Table 2.3, Figure 2.11a). Polyps from all sites were sometimes found to have as many as 24 gonads (two gonads per septa); however polyps containing more than 12 gonads were more common in corals from Grammanik Bank. The number of oocytes/ova per gonad generally ranged from 8-12 (maximum recorded was 19), however polyps in corals from Grammanik Bank had significantly more oocytes/ova per gonad than corals from Black Point (Kruskal-Wallis ANOVA/Bonferroni method, p = 0.046; post-hoc comparison, p = 0.028) (Table 2.3, Figure 2.11b and examples in Figure 2.8). There was no difference found in oocytes/ova per gonad between Grammanik Bank and Flat Cay, or between Flat Cay and Black Point. The product of these two estimates is the fecundity per polyp, which was found to be heterogeneous across sites, with Grammanik Bank corals having significantly higher oocyte/ovum production per polyp than Black Point corals (Kruskal-Wallis ANOVA/Bonferroni method, p=0.021; post-hoc comparison, p= 0.009) (Table 2.3, Figure 2.11c). Again, no difference was found between Grammanik Bank and Flat Cay, or Flat Cay and Black Point.

No significant relationship was found between oocyte/ovum production per polyp and the surface area of sampled colonies. A significant increasing linear relationship ($p < 0.001$, $R^2 = 0.381$) was found between oocyte/ovum production per polyp and depth (Table 2.4, Figure 2.12).

Reproductive capability

Due to variability in the accurate identification of *M. faveolata* in long-term (2001-2012) coral reef monitoring datasets collected and compiled by researchers at the

University of the Virgin Islands, *M. annularis* species complex coral cover was pooled and plotted against depth (square root-transformed) and a third-order polynomial was fitted to the data ($p < 0.0001$, $R^2 = 0.51$, Figure 2.13). In this model coral cover of *M. annularis* species complex corals increases with depth nonlinearly until ~30m where it stabilizes at ~28% until a depth of ~40m where coral cover begins to decline dramatically. By 50m depth *M. annularis* species complex coral cover drops to zero.

The number of polyps*cm^{-2} of coral surface decreases with depth. Black Point corals had significantly higher numbers of polyps*cm^{-2} (on average, nearly twice) compared to both Flat Cay and Grammanik Bank corals, which were not significantly different from each other (one-way ANOVA, $p = 0.012$, Figure 2.14). The same data was log-transformed and plotted over depth, and a linear regression was performed ($p = 0.014$, $R^2 = 0.381$, Figure 2.15).

The resulting regression lines from the previous three analyses (oocyte/ovum production per polyp, coral cover and the number of polyps*cm^{-2}) were used to estimate the number of ova produced in a $1km^2$ reef area at each depth from 10-50m (equation 4, Figure 2.16 scenario I). Additionally, three hypothetical ova production scenarios were calculated in order to evaluate which factors drive depth-specific differences in whole-reef ova production. These included (II) equal fecundity at all depths (Villinski 2003, ovum production per polyp = 96 [median literature value, Szmant et al. 1997]), (III) equal fecundity to 20m (Villinski 2003), and linearly decreasing fecundity from 20m-45m, and (IV) linearly decreasing fecundity from 10m to 45m.

Scenario I, which was derived from this study's productivity estimates, predicts ~300% greater ova production (1.1 trillion more ova) per km^2 at 35 m than at 10m. When

polyp fecundity is equal at all depths and productivity is driven only by coral cover and polyp spacing (scenario II), ova production is 163.5% greater (~700 billion more ova) per km^2 at 35m than at 10m. Thus, changes in polyp fecundity with depth results in an additional 41% (443 billion) greater ova production per square kilometer at 35m than a scenario of equal fecundity (scenario I vs. scenario II). In scenarios of reduced fecundity with depth, reproductive output per km^2 at 35m still exceeds that at 10m by nearly 10%.

Porites astreoides

Whole colonies of *P. astreoides* were observed in the laboratory for planulation over the nights of May 2nd and 3rd of 2011. Due to inhospitable conditions in flow-through Tables, by the time of observation colonies from Black Point and Flat Cay were showing obvious signs of stress, including paling and shedding mucous. Because they were collected several days later, mesophotic colonies from Grammanik Bank were not yet showing signs of stress. One colony from Flat Cay planulated during observations, and released between 50-100 larvae on the evening of May 3rd. No planulation was observed from Black Point colonies. All Grammanik Bank colonies planulated in the laboratory over the two evenings of observation. These colonies released 1000s of larvae over the two nights of observation.

Larvae from Grammanik Bank colonies immediately began actively swimming at the surface of isolation buckets. These larvae were subsampled in order to estimate their specific gravity, with ~5 larvae per each of 6 seawater treatments (specific gravity 1.013:1.018, 0.001). Estimated specific gravity of these larvae was 1.015-1.017.

High mortality was observed at all sites during larval transplantation (Figure 2.17). Transplants were visited at 4-5 and 11-12 days after planulation, with a lag of one day at Grammanik Bank. The percent of larvae surviving at 4 days post planulation was not significantly different between Flat Cay and Black Point (Figure 2.17). After 11 days no larvae survived at either Flat Cay or Black Point. At Grammanik Bank after 12 days, an average of 6% (+/- 3.58%, SE) of larvae (3 of 50) survived, and appeared to have settled in the acrylic tubing. Acrylic tubes at Grammanik Bank had visibly lower levels of fouling on their surfaces than tubes at the two shallower sites.

Reproductive histology

Histological analysis of *P. astreoides* tissues from all sites revealed the presence of oocytes/ova, spermaries and planulae (Figure 2.18). The presence of oocytes in tissues was nearly ubiquitous across the five week sampling period at all sites, and remained present in 80-100% of colonies (Figure 2.19). The presence of spermaries increased at all sites over the first 2-3 weeks of sampling. Spermaries began to disappear from the tissues of corals from both Flat Cay and Grammanik Bank after the third week of sampling, which corresponded generally with new moon. After week 3 spermaries were present in 40% of colonies from Black Point for the remainder of the sampling period.

The presence of planulae in coral tissues increased over the first two weeks of sampling at all sites, with 100% and 80% of Black Point and Flat Cay colonies containing planulae by week 2, respectively (Figure 2.20). Week 2 also corresponded with peak planulae density per cm^2 in both Black Point and Flat Cay colonies. Peak in % colonies containing planulae in Grammanik Bank corals did not occur until week 4, however peak

planulae density per cm^2 occurred a week earlier at week 3. Peak mean planulae density (SE) was 13.29*cm^{-2} (3.32), 14.95*cm^{-2} (4.70) and 17.49*cm^{-2} (5.37) at Black Point, Flat Cay and Grammanik Bank respectively, and were not significantly different despite an increasing trend with depth (Tukey's-HSD). The overall average peak planulae density pooled from all sites was found to be 15.24*cm^{-2} (2.66).

There was a significant difference in planulae density between sites at weeks 4. Grammanik Bank corals had significantly higher average planulae per cm^2 than Black Point or Flat Cay, which were both near zero (one-way ANOVA, Tukey's-HSD, $p = 0.009$). At week 5 planulae density had begun to increase in Black Point corals, and not in Flat Cay or Grammanik Bank corals, however this difference was not significant.

Reproductive capability

P. astreoides coral cover estimates were pooled from coral reef monitoring surveys (2001-2012), plotted against depth, and a third-order polynomial was fitted to the data ($p < 0.0001$, $R^2 = 0.20$) (Figure 2.21). In this model coral cover of *P. astreoides* is relatively consistent with depth, with means ranging from ~0.5-1.5%, and an apparent slight dip in % cover between 15 and 25m. By 50m depth *P. astreoides* coral cover drops to near zero. The resulting regression line was used input into equation 5 to estimate *P. astreoides* planulae production over a $1km^2$ reef from 10-50m depth, based on equal planulae production per cm^2 of 15.24 (Figure 2.22). Because fecundity was equal at all depths, estimates of depth-specific planulae production were entirely dependent on coral cover. Higher coral cover shallower than 15m results in nearly 1.5 billion (300%) higher production of planulae at 10m versus at 20m. A deep peak in coral cover between 30 and

35m suggests nearly doubled planulae production at these depths compared to 20m, however production at 10m is still likely nearly 40% higher than at 35m.

Discussion

In the cases of both *M. faveolata*, a broadcast spawning species, and *P. astreoides*, a brooding species, colonies sampled from mesophotic reefs in the US Virgin Islands were found to be reproductive at the times and in magnitudes that suggest that depth may provide a reproductive refuge for depth-generalist species of coral in this region by providing habitat removed from shallow and coastal coral stressors, and yet conducive to coral reproduction. Although not directly addressed here, evidence provided in this study adds credit to the argument that MCE could serve as refugia habitat for these species as well, by providing stable habitat over evolutionary time scales from which populations could expand following climatic change (Bongaerts et al. 2010a; Keppel et al. 2012). This study directly addresses information gaps regarding the reproductive capabilities of MCE outline by Bongaerts et al. (2010) in their assessment of the DRRH, and may in fact suggest that USVI MCE produce far more reproductive product than nearby shallow reefs.

Reproductive timing

Video collected in the field and laboratory in 2012 suggests synchronous spawning on the order of hours and days of *M. faveolata* at sites separated by ~11km horizontally and ~30m vertically. Mesophotic *M. faveolata* colonies spawned earlier (~1 hr) than shallow colonies when observed in the laboratory. Although laboratory

conditions can skew spawning synchrony due to altered light cycles and separation from conspecifics, earlier spawning in deeper-living corals is not necessarily surprising, and may be due to truncated daylight hours at depth and an earlier sunset cue.

Histological analysis of the gametogenesis of *M. faveolata* supports the assertion that spawning at shallow, mid-depth and mesophotic sites is synchronous within days. Video, laboratory and histological observations also suggest that all depths experience split spawning, where some individuals spawn in August and others in September. In fact, the 2011 histological evidence suggests that different polyps within the same colony, and even different gonads within the same polyp, may experience split spawning. Many colonies retained late stage ova after a portion of the population spawned in August, which was indicated by the absence of late stage spermaries. This fact combined with the development of early stage spermaries and oocytes throughout August likely implies that many colonies spawned in September of 2011 (Figure 2.7).

Laboratory observations of mesophotic *P. astreoides* planulation suggest that these deeper-living corals reproduce in a similar gametogenic cycle to their shallow counterparts as well. Although we did not observe shallow *P. astreoides* planulation in the laboratory, mesophotic colonies (and one mid-depth colony) planulated on evenings predicted for shallow colonies in the Caribbean (Szmant 1986; Chornesky and Peters 1987; Mcguire 1998). Histological evidence suggests that the date at which peak larval density in colony tissues occurs may be delayed by as much as a week in mesophotic colonies as compared to shallow and mid-depth colonies (Figure 2.20), and a similar delay was seen in mesophotic colony planulation, as indicated by a loss of planulae from coral tissues (Figure 2.19). However, there is high variability in the date of planulation in

this species, with a range in planulation of more than 20 days straddling the new moon (Mcguire 1998). Thus, the differences seen between mesophotic *P. astreoides* and their shallower counterparts may be artificial. However, it is possible that these differences indicate distinct breeding populations, or that mesophotic *P. astreoides* experience environmental conditions that alter reproductive physiology or cues.

It is unlikely that direct hybridization occurs between mesophotic and shallow colonies of either *M. faveolata* or *P. astreoides* in the USVI, despite the potential for synchronous gametogenesis and spawning behavior. This is because these habitats are separated by considerable horizontal distances in most cases (Figure 2.1). However, hybridization could be likely on wall or seamount habitats, where buoyant or swimming gametes may have a greater potential of fertilization with conspecifics from a wide range of depths.

Reproductive magnitude

In 2010, the percentage of *M. faveolata* colonies that were reproductively active was between 70% and 80% for all sites visited but one (Table 2.2). For the most part, mesophotic sites appeared just as, if not more reproductively active than shallow and mid-depth sites. Over half of colonies at the deepest site visited (43m) were reproductive, but the site was nearly 20% less reproductive than any other, with fewer colonies containing gametes. This difference could have been due to a deep low-light threshold at which low light intensity limited metabolic energy available for reproduction; low-light thresholds have been implicated in reduced linear extension of coral skeletons over depth gradients (Bosscher and Meesters 1992; Bosscher 1993). That being said, more than half

of the population at the deepest mesophotic site was found to be putting some portion of metabolic energy into reproduction.

It was surprising to find that mesophotic *M. faveolata* coral polyps were more fecund than shallower corals, and that there seemed to be a continuum of fecundity from shallow to deep (Figures 2.11 and 2.12). Generally *M. faveolata* fecundity estimates fell within the ranges recorded by previous studies (Szmant et al. 1997; Villinski 2003), however the highest estimated fecundities in this study, particularly from the mesophotic samples, nearly doubled literature maximums. Because no relationship was found between colony size and fecundity in this study, it is assumed that differences seen between sites are not due to colony size, and all colonies were of minimum reproductive size. Villinski (2003) seems to be the only previous study that has addressed *M. faveolata* reproductive characteristics in relation to depth, and no significant differences in polyp fecundity were found to a depth of 18m. Indeed, the current study found no differences in the number of gonads per polyp or the number of oocytes per gonad between shallow (5-10m) and mid-depth (15-22m) sites, echoing the findings of Villinski (2003). However, this study did find that polyp fecundity was significantly higher at mesophotic depths (35-40m) than shallow depths, suggesting that the previous study may have overlooked this relationship by not sampling the full extent of *M. faveolata*'s depth range. This relationship was not found to be significant for *P. astreoides*; however peak planulae density was highest for this species at the mesophotic site.

One potential explanation for increased fecundity at depth despite reduced solar radiation available for photosynthesis (Kinzie III 1973; Fleischmann 1989) is that challenging physical conditions in mesophotic ecosystems increase adaptive pressure on

reproductive success. For example, the delayed but rapid development of oocytes seen in *M. faveolata* histological sections may imply that colonies that have entered a reproductive stage are subject to tight energetic constraints that encourage diverting energy to reproduction. If this is the case, mesophotic *M. faveolata* may be particularly vulnerable to disease or physical damage during or directly after reproductive cycles due to energetic limitations akin to those experienced by corals post-bleaching stress (Miller et al. 2009).

An alternative, or potentially concurrent, hypothesis is that the environmental stability of MCE (Bak et al. 2005; Menza et al. 2008; Smith et al. 2008; Lesser et al. 2009; Slattery et al. 2011) allows corals to enter reproductive stages at the expense of growth and colony maintenance. The reproduction and growth of trees and other fruiting plants has been well studied with respect to environmental variability (Wolgast and Zeide 1983, and citations therein). Plants in stable environments are capable of separating periods of growth from periods of fruiting in order to maximize reproductive potential, with "seed years" in trees being a particularly good example. It is possible that low environmental variability in mesophotic environments (reduced storm damage, low thermal bleaching incidence, low predation, relatively consistent light levels and temperature, etc.) results in the temporary cessation of growth and near-maximum gamete production during *M. faveolata* reproductive periods. Additionally, because of their position below the thermocline, mesophotic corals may be able to subsidize their metabolisms through heterotrophic feeding on a consistent source of dissolved and particulate carbon. This reliable energy resource may contribute to the observed depth-specific differences in fecundity and gamete development seen in *M. faveolata*.

Implications

Coral cover in USVI MCE is considerably higher than on USVI shallow reefs, with that relationship driven by the *M. annularis* species complex (Figure 2.13; Armstrong et al. 2006; Armstrong 2007; Menza et al. 2008; Smith et al. 2008). The implication is that despite greater polyp spacing at depth, the number of reproductive *M. faveolata* polyps increases with depth over a unit reef. If *M. annularis* species complex coral are grouped together, this study estimates that a hypothetical $1km^2$ USVI reef at 35m depth produces an order of magnitude more *M. annularis* species complex ova than a $1km^2$ reef at 10m depth ($1.146*10^{12}$, or over 300% more ova*km^{-2}, Figure 2.16, I). Differences in coral cover alone are responsible for over 160% higher estimated ova production at 35m versus 10m ($6.677*10^{11}$ more ova*km^{-2}; Figure 2.16, II). Elevated mesophotic fecundity is thus responsible for the production of over 40% more ova, or 443 billion more ova per square kilometer, at 35m beyond the effects of increased coral surface area. Scenarios III and IV (Figure 2.16) suggest that ova production at 35m would be near equal to that at 10m even after a 62.5% reduction in polyp fecundity (or similarly, a 62.5% reduction in coral surface area).

Assuming equal habitat area, it appears that over 85% of *M. annularis* species complex (and *M. faveolata* specifically) ova in the northern USVI are produced below 20m, and over half are produced between 30m and 50m. Of course, it is likely this has not always been the case. Gardner et al. (2003) estimated that shallow reefs in the USVI and Puerto Rico experienced a nearly 10% loss of coral cover between 1975 and 2000, and Miller et al. (2009) estimated an additional 42.4-61.8% loss in coral cover in shallow reefs after the 2005 bleaching and disease event. Smith et al. (*in press*) found that *M.*

annularis species complex coral cover was reduced by about 50% in 2005. USVI MCE appear to have been spared this fate (Smith et al. 2008), and thus discrepancies in reef-wide *M. annularis* species complex ova production between shallow and mesophotic reefs may largely be an artifact of shallow reef degradation. Regardless, modern USVI MCE are likely crucial to the continued reproductive success and metapopulation connectivity for many depth-generalist coral species.

Knowledge gaps

The spatial extent of reef habitats in the USVI was not addressed in this study. Smith et al. (2008, 2009) have characterized a large MCE on the shelf-edge south of St. Thomas, where coral habitat extent is nearly half the total shallow coral reef extent in St. Thomas and St. John combined (mapped by the National Oceanic and Atmospheric Administration's Center of Coastal Monitoring and Assessment). The true extent of MCE in the USVI, and indeed in the Caribbean basin, is unknown. Studies focusing on characterizing mesophotic habitat are crucial to incorporating the full implications of the current study into our understanding of the future of Caribbean coral reefs (Bongaerts et al. 2010a; Locker et al. 2010).

Fertilization – a crucial step in the reproductive cycle – was also not addressed in this study. It is possible that the physical conditions of deep and shallow environments create disparate fertilization conditions for corals in a number of ways, the most obvious being for broadcast spawning species such as *M. faveolata*. Traditionally it is understood that *M. faveolata* gamete bundles rise to the sea-air boundary where fertilization occurs after they are concentrated and break apart. Depth, therefore, may limit the fertilization

success in this species, as gamete bundles may break apart or disperse before they reach the sea surface. In this study it was found that in the absence of water motion, gamete bundles could remain intact for over an hour. Using rising rates estimated from laboratory video it would take egg bundles over an hour and a half to travel 35m vertically in ocean conditions similar to those found in the laboratory. However, buoyant velocity is affected by the temperature and salinity of water, and the rate of ascent of gamete bundles from MCE is investigated further in later chapters. Understanding the effects of depth on fertilization rates of corals is important for accurately estimating larval load, and should be the focus of future research.

Similarly, larval survivorship and post-settlement mortality have implications for the refugia potential of MCE. Gleason and Wellington (1995) found differential survivorship of *Agaricia agaricites* larvae taken from different depths when exposed to UVB radiation. It is possible that larvae of mesophotic origin have different rates of pelagic and post-settlement mortality as compared to larvae from shallower habitats. The transplant experiment carried out in the current study suggests that indeed, larval survivorship may be lower on shallower reefs. However this work must be expanded.

Ultimately, headway on many these knowledge gaps can be made through the use of biophysical modeling. It is difficult to predict the future competitive dynamics for settling organisms on coral reefs, especially when those dynamics are changing due to shifts in coral-algal dominance and climate change. What are the probabilities that mesophotic and shallow habitats are connected, and on what spatial and temporal scales? How many immigrating recruits are necessary for the DRRH to be valid? We must evaluate the potential for these mesophotic reproductive refugia to provide larvae to

shallow habitat and simultaneously sustain themselves, and we must begin to estimate to what degree these deeper habitats are connected to larger Caribbean coral metapopulations. These research questions will be addressed in later chapters focusing on the dispersal capabilities of mesophotic larvae.

Table 2.1. 2010 and 2011 sampling sites.

	Depth (m)
2010 Sites	
Flat Cay	6
S. Capella	22
College Shoal	34
Hammerhead Shoal	39
Grammanik N. Bank	43
2011 Sites	
Black Point	8
Flat Cay	19
Grammanik Bank	39

Table 2.2. Percent colonies found to be reproductive at each site in 2010. Sampling occurred over three days, several days prior to expected spawning in August.

2010	Site				
	Flat Cay	S. Capella	College Shoal	Hammerhead Shoal	Grammanik N. Bank
Depth (m)	6	22	34	39	43
n	18	21	10	19	11
% colonies reproductive	72.22%	76.19%	80%	73.68%	54.55%

Table 2.3. Fecundity estimates for each site in 2011. Data was pooled from weeks 1 through 4 of sampling (prior to expected spawning). Significant differences between sites are noted by lowercase letters (Kruskal-Wallis ANOVA/Bonferroni method).

2011	Site		Mean (±SE)	
	Black Point	Flat Cay	Grammanik Bank	*P*
Depth (m)	8	19	39	
Colonies	20	20	19	
Gonads*polyp^{-1}	10.78 (±0.83)^{a}	10.58 (±0.48)^{a}	14.39 (±0.97)^{b}	< 0.01
Ova*gonad^{-1}	7.48 (±0.59)^{a}	9.19 (±0.72)^{ab}	9.91 (±0.60)^{b}	0.46
Polyp Fecundity	87.05 (±10.10)^{a}	99.72 (±10.15)^{ab}	144.43 (±15.91)^{b}	0.02

Table 2.4. ANOVA Table of Fecundity v. Depth linear model.

	df	MS	F	*P*
Polyp fecundity				
Depth	1	33397	12.091	<0.001
Error	55	151914		

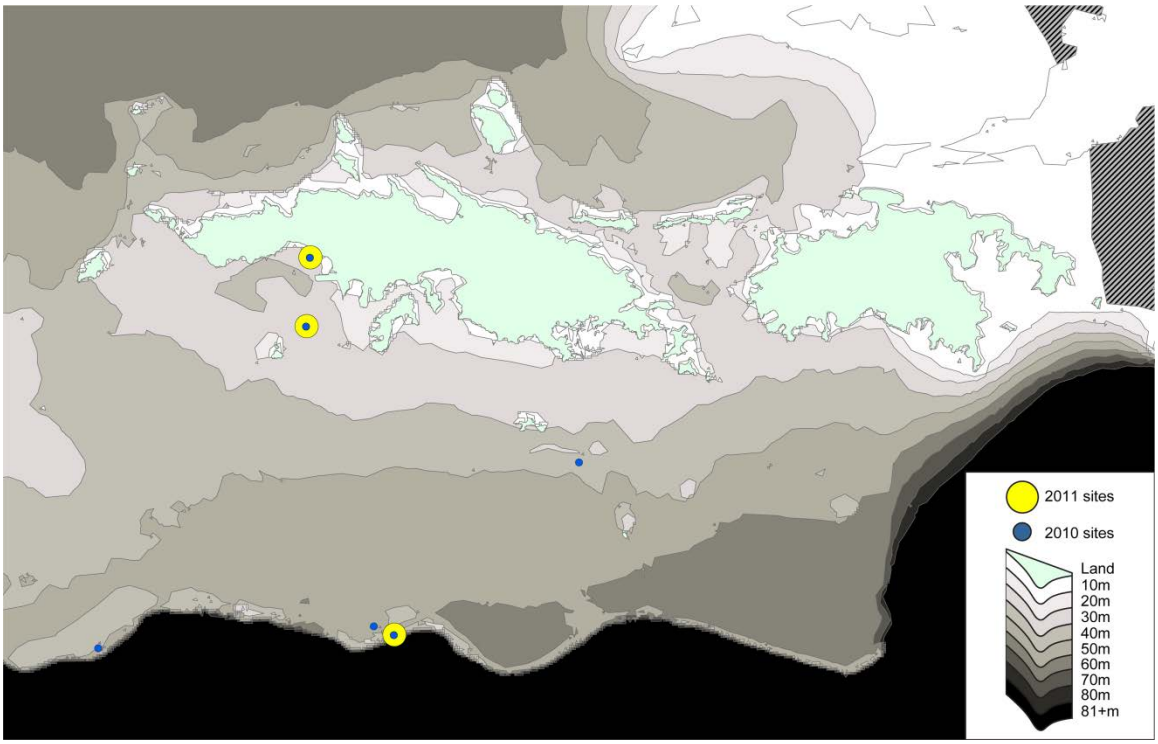

Figure 2.1. The northern US Virgin Islands of St. Thomas and St. John. Considerable mesophotic habitat (30-150m) exists on the broad insular platform, and well-mapped linear coral habitat exists on submerged banks near the shelf edge south of St. Thomas (Armstrong et al. 2006; Smith et al. 2008, 2010). Sample sites from 2010 (blue) ranged in depth from ~5-45m. In 2011 a subset of 2010 sites were visited weekly for five weeks in April-May (*P. astreoides*) and July-August (*M. faveolata*). Hatching denotes missing sounding data, and the British Virgin Islands of Tortola and Jost van Dyke are not shown.

Figure 2.2. Sample collection of an *M. faveolata* colony at Grammanik Bank (~38m).

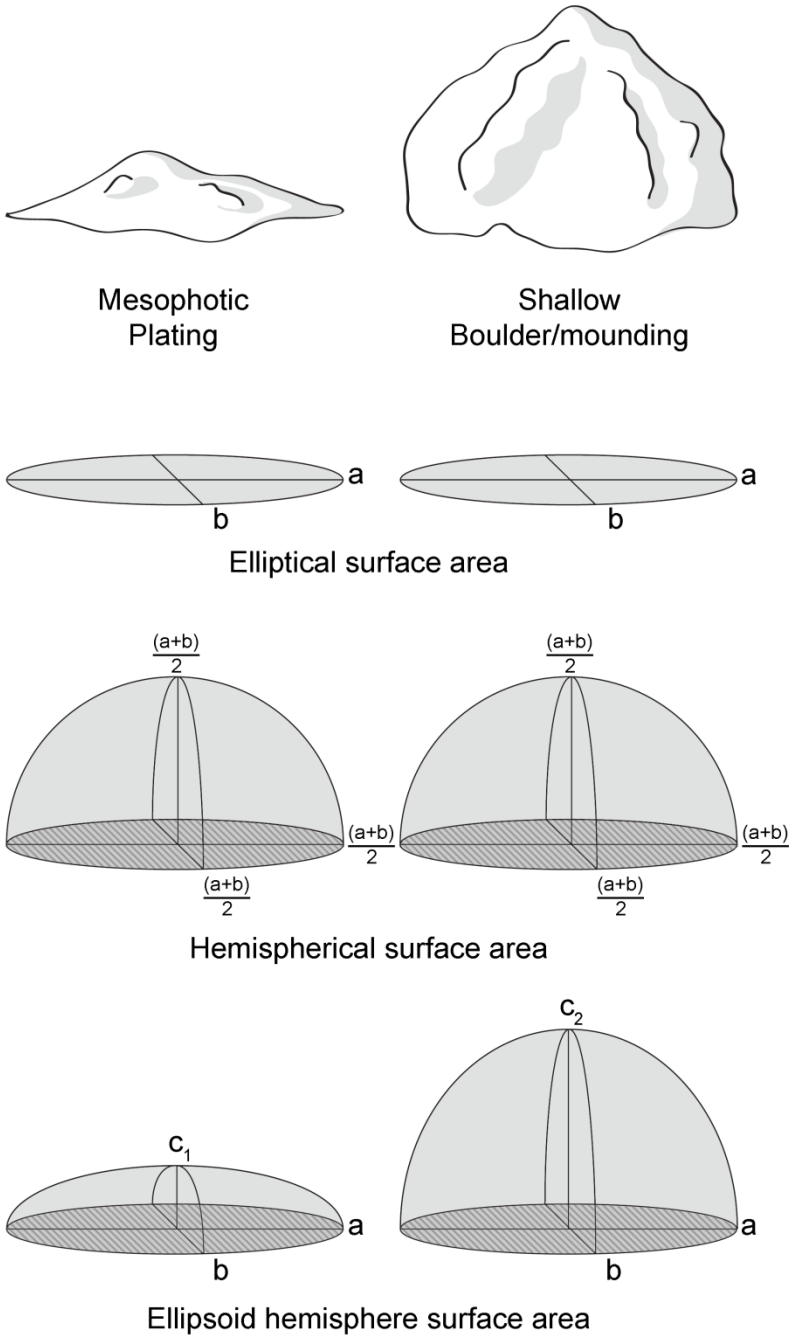

Figure 2.3. An illustration of the potential benefit of utilizing the surface area of a scalene ellipsoid when estimating coral colony surface area. This is preferable to the use of the hemispherical surface area, particularly when $a \neq b \neq 2c$ and in the case of *M. faveolata*, which has different morphologies in different habitats, and thus a ratio of width and height is not constant.

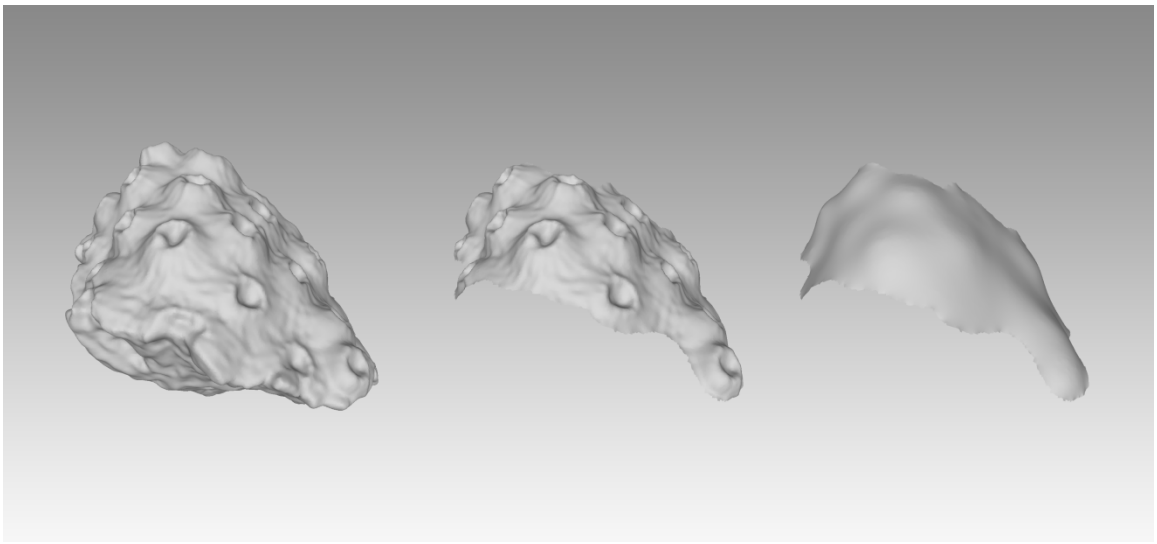

Figure 2.4. Three-dimensional surface reconstruction of an *M. faveolata* coral sample taken with a hammer and cold chisel. Five samples per site (N=15) were scanned and reconstructed, and the coral surface of the reconstruction was isolated and smoothed in order to estimate basal coral surface area. The polyps of each sample were enumerated and divided by this basal surface area, and the resulting polyp densities were compared between sites.

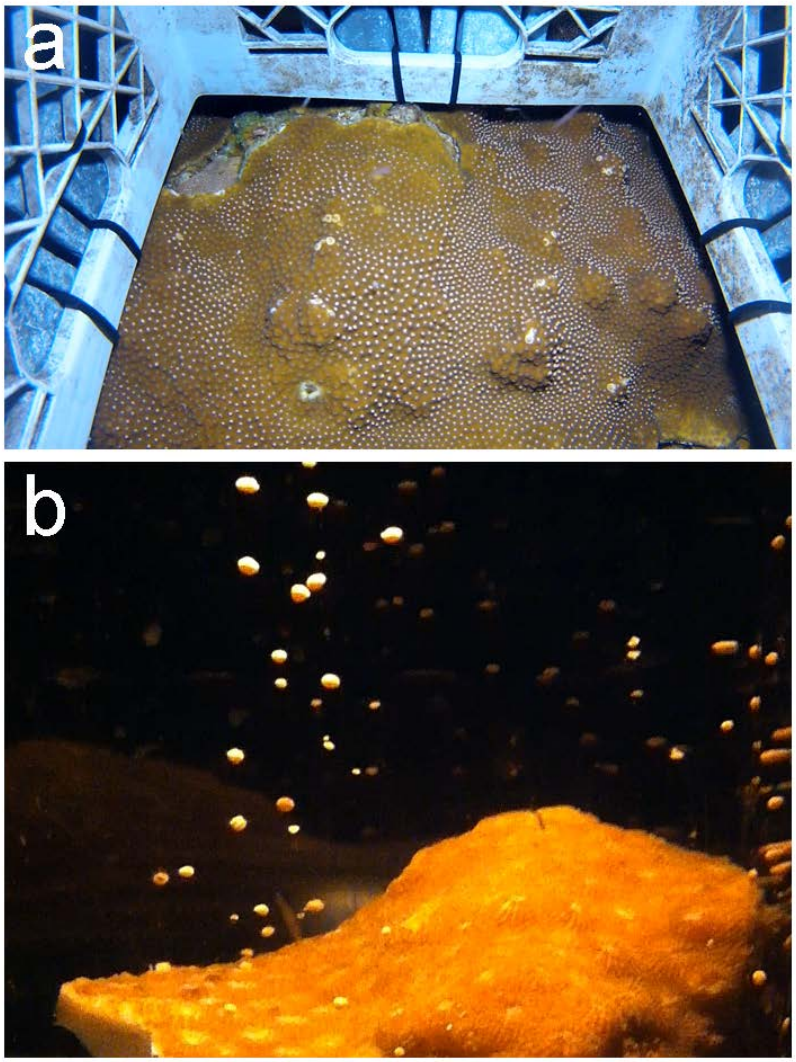

Figure 2.5. Coral spawning observations. (a) A large *M. franksi* colony setting at ~38m at 20:50 one week after full moon in September 2012. The colony underwent a whole-colony spawn. (b) Spawning of an *M. faveolata* coral fragment observed in the laboratory on the same evening, at 20:45.

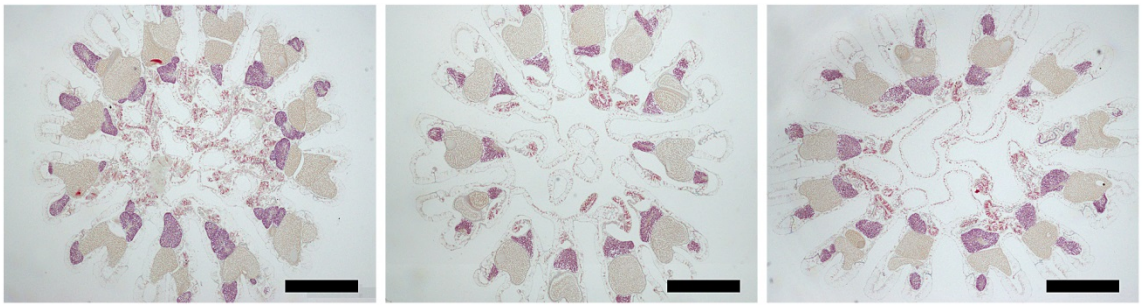

Figure 2.6. Histological cross-sections of fully fecund polyps just prior to spawning (week 4) from each site. From left to right, in order of descending depth, Black Point, Flat Cay and Grammanik Bank. In each example the polyp has at least 12 ripe gonads, all ova are stage IV (gold-tan), and spermaries are stage V (red). Bar = 500 µm. See Figures 2.7 and 2.8 for further reproductive structure identification.

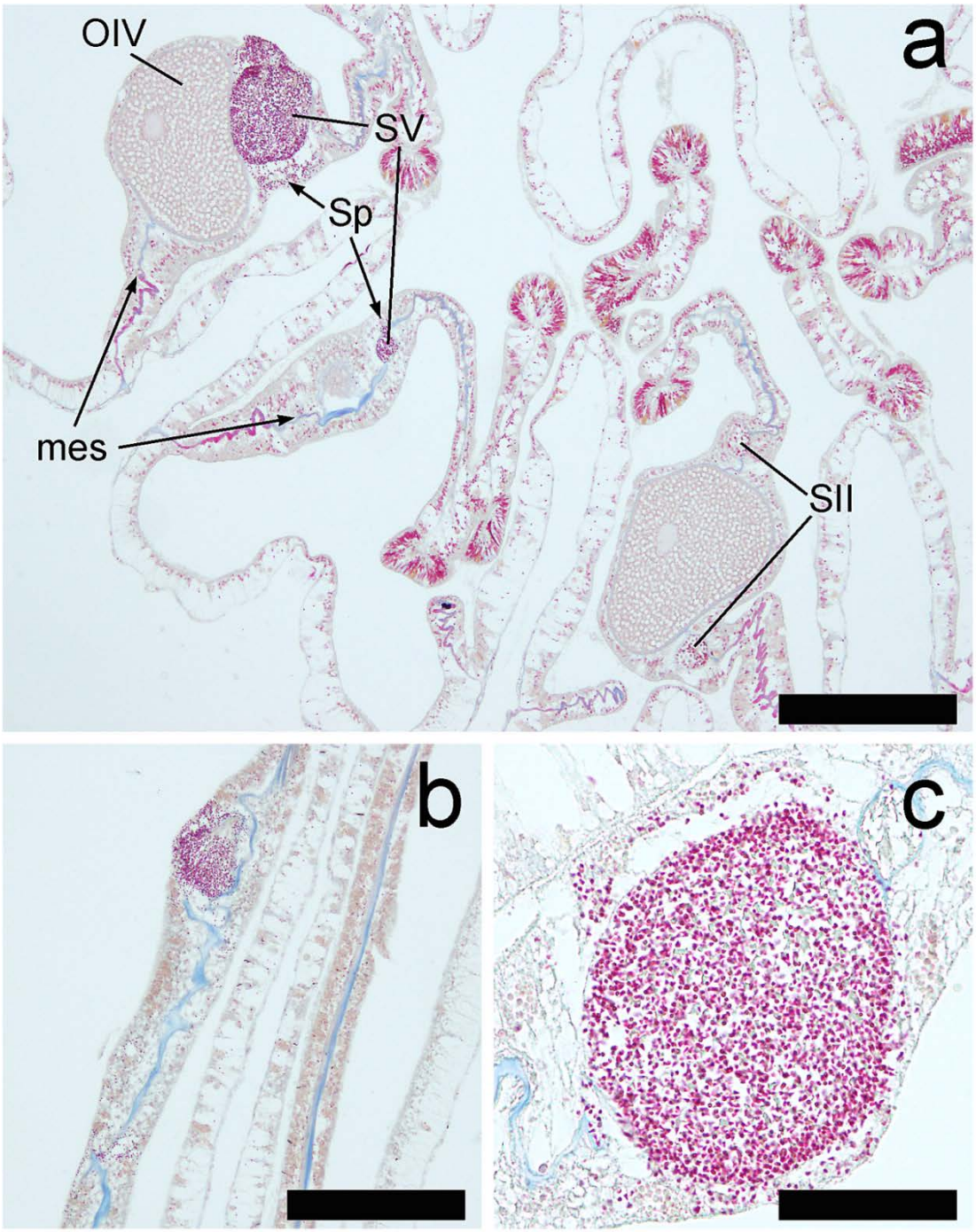

Figure 2.7. Histological evidence of spawning in *M. faveolata*. (a) "Wasted" or "loose" mesenteries (mes), remnant stage V spermaries (SV) and free spermatozoa in the mesentery (sp) are indicative that the polyp has undergone spawning. In this case, there are also remnant stage IV ova (OIV), and evidence of developing stage II spermaries. (b) Another example of wasted mesenteries, a remnant stage V spermary and free spermatozoa. (c) A close-up of a remnant stage V spermary and free spermatozoa not confined to the spermary (bar, a = 200 µm; b = 200 µm; c = 50 µm).

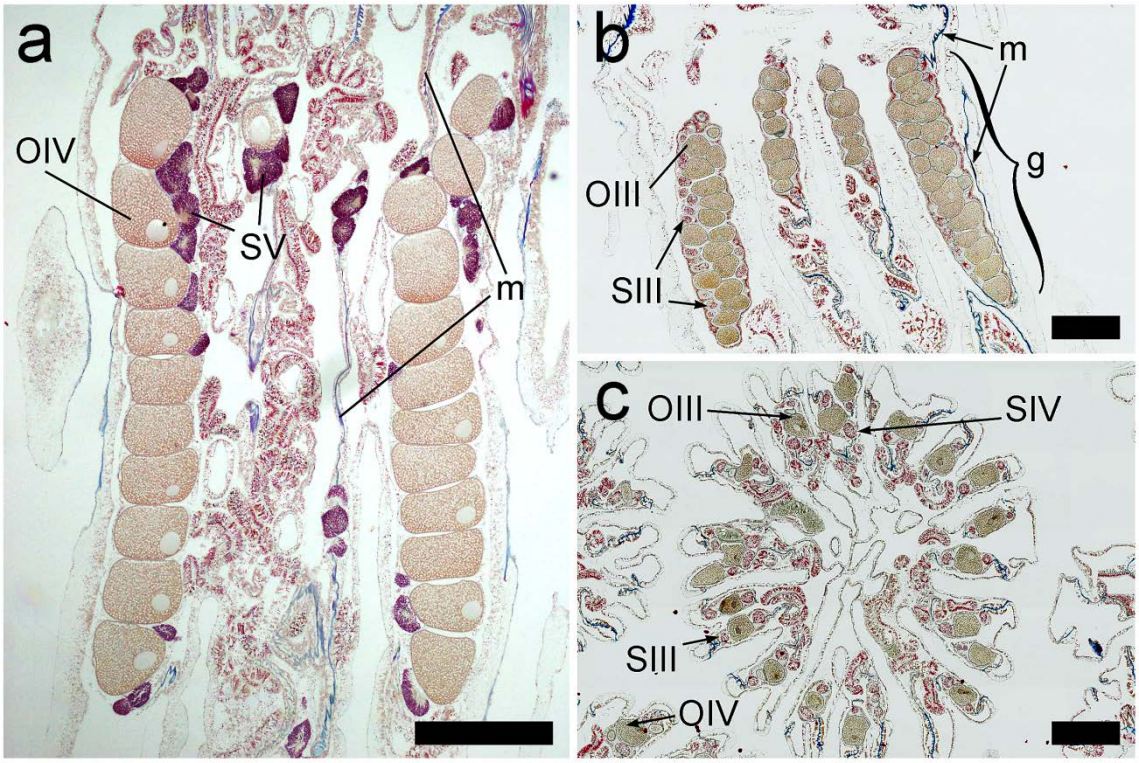

Figure 2.8. (a) A typical longitudinal section showing stage IV ova (OIV) and stage V spermaries (SV) arranged in gonads. The ova and spermaries are within the mesoglea, which is stained blue (m). (b) An example of highly fecund gonads (g) containing many more than 8-12 stage III oocytes (OIII) surrounded by stage III spermaries (SIII). In this example the gonad can be seen inside the mesoglea (m), attached to the mesenterial wall. (c) An example of a polyp containing many more than 12 gonads in cross-section, in this case at least 20. Gametocytes of different stages can be found within the same colony, the same polyp, and even the same gonad simultaneously. Bar is 500 µm.

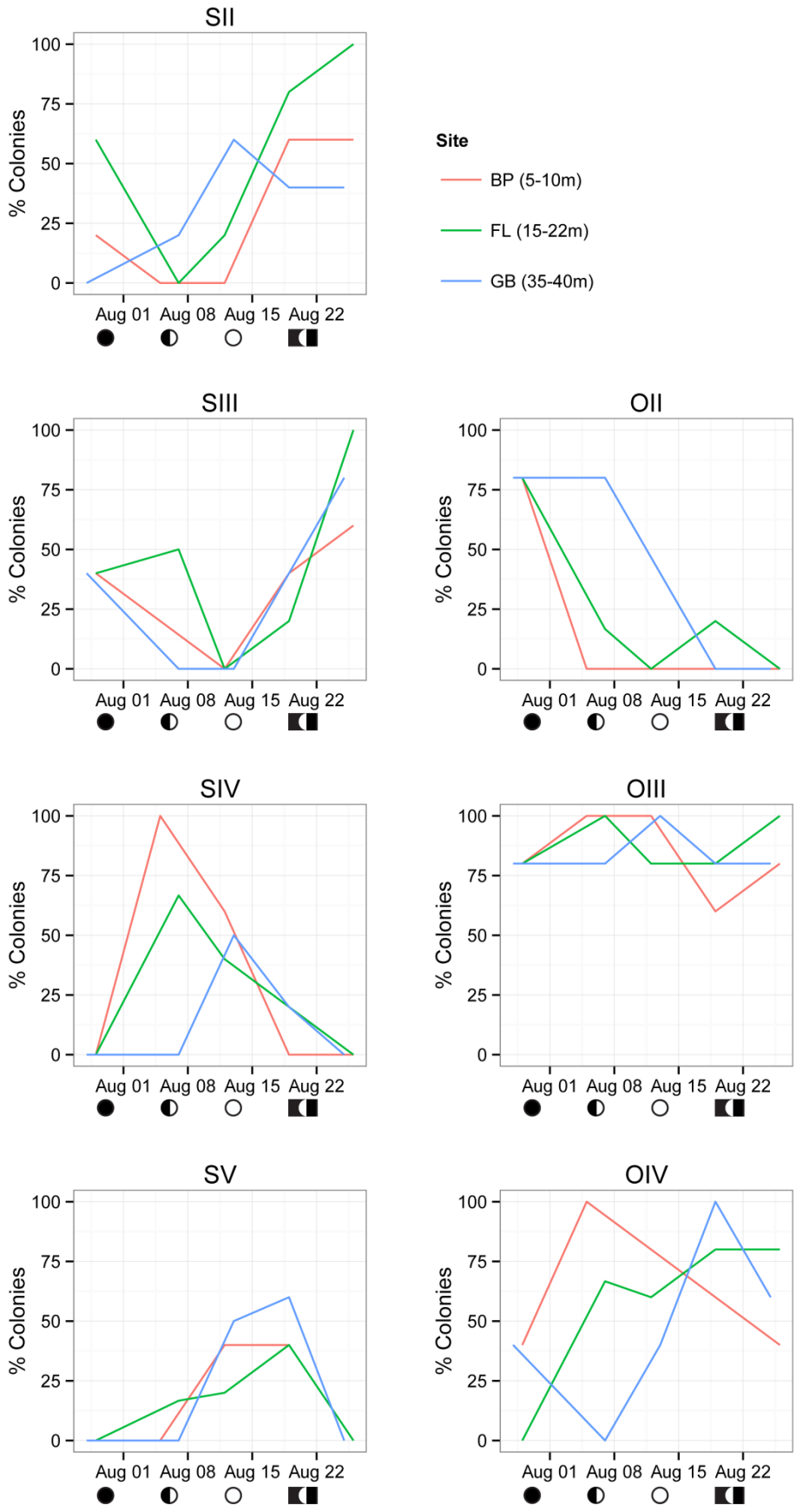
SII
SIII
OII
SIV
OIII
SV
OIV
% Colonies
100
75
50
25
0
Aug 01
Aug 08
Aug 15
Aug 22
Site
BP (5-10m)
FL (15-22m)
GB (35-40m)

Figure 2.9. *Montastraea faveolata* gametogenic stages of spermaries (left column) and oocytes (right column) observed in histological sections collected weekly (July 28th to August 26th 2011, 5 sampling times) from three sites: Black Point (BP, red), a shallow near-shore site; Flat Cay (FL, green), an offshore island mid-depth site; and Grammanik Bank (GB, blue), a mesophotic submerged bank site. Gametocytes were staged as I-V for spermaries and I-IV for oocytes (Szmant 1985a, 1991), however only stages II and later are shown. Plots represent the percentage of colonies that contained each stage. N = 5 or more for each date at each site. The lunar cycle is shown below the x-axis, as well as a black bar that represents expected spawning dates 6-9 days after full moon in August 2011.

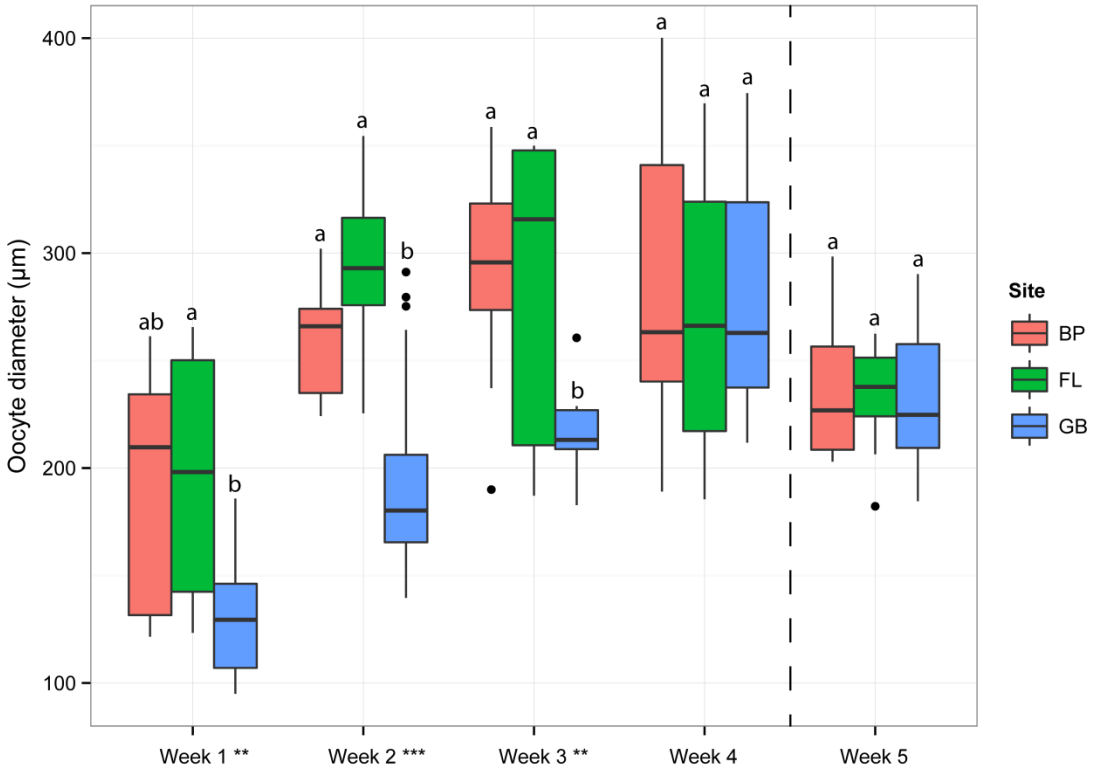

Figure 2.10. Boxplot of *M. faveolata* oocyte/ova diameters measured from histological sections from each site each sampling day. Upper and lower hinges correspond to the first and third quartiles, bars correspond to medians and whiskers extend to the highest and lowest values within 1.5 IQR (inter-quartile range). Data beyond whiskers are outliers represented as dots. Significant differences between sites were found in weeks 1, 2 and 3 (Kruskal-Wallis ANOVA, ** denotes $p < 0.01$, *** denotes $p < 0.001$; Bonferroni method post-hoc comparisons are noted by letters, adjusted $-p < 0.05$). No differences were found between sites in weeks 4 and 5. The dotted line denotes that spawning was expected between weeks 4 and 5.

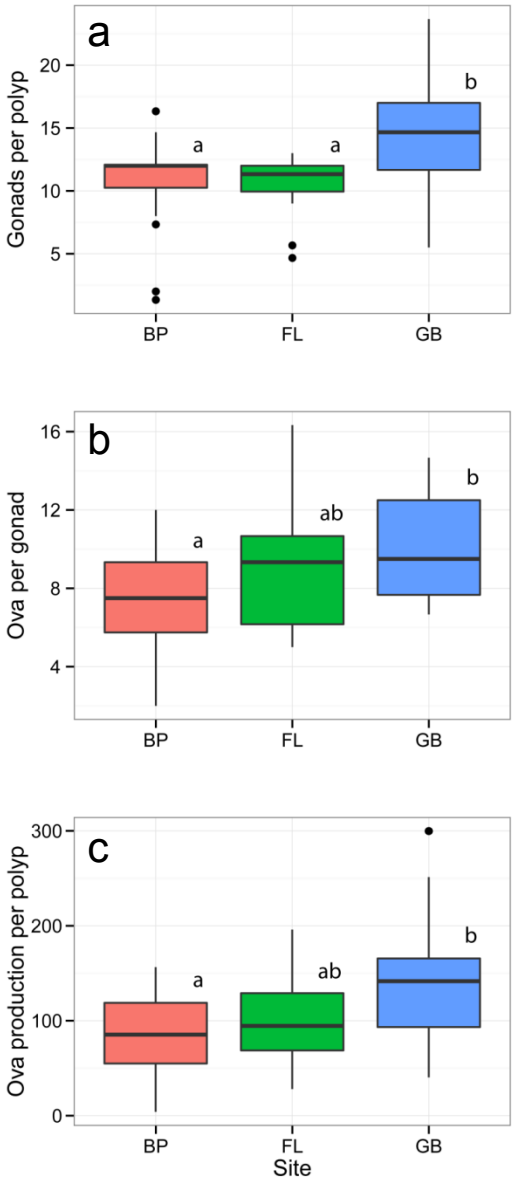

Figure 2.11. *M. faveolata* fecundity estimates and comparisons between 2011 study sites. The number of (a) ripe gonads and the number of (b) oocytes/ova per gonad were estimated for three polyps per sample. Ova production per polyp (c) is the product of the number of ripe gonads multiplied by the number of oocytes/ova per gonad. Data was pooled from sampling weeks 1 through 4. Comparisons were made with Kruskal-Wallis ANOVAs and the Bonferroni post-hoc method to arrive at adjusted p-values. Significant results are noted using letters in each boxplot ($p<0.05$). Sites are ordered from left to right by depth (BP, 5-10m; FL, 15-22m; GB, 35-40m). Upper and lower hinges correspond to the first and third quartiles, bars correspond to medians and whiskers extend to the highest and lowest values within 1.5 IQR (inter-quartile range). Data beyond whiskers are outliers represented as dots.

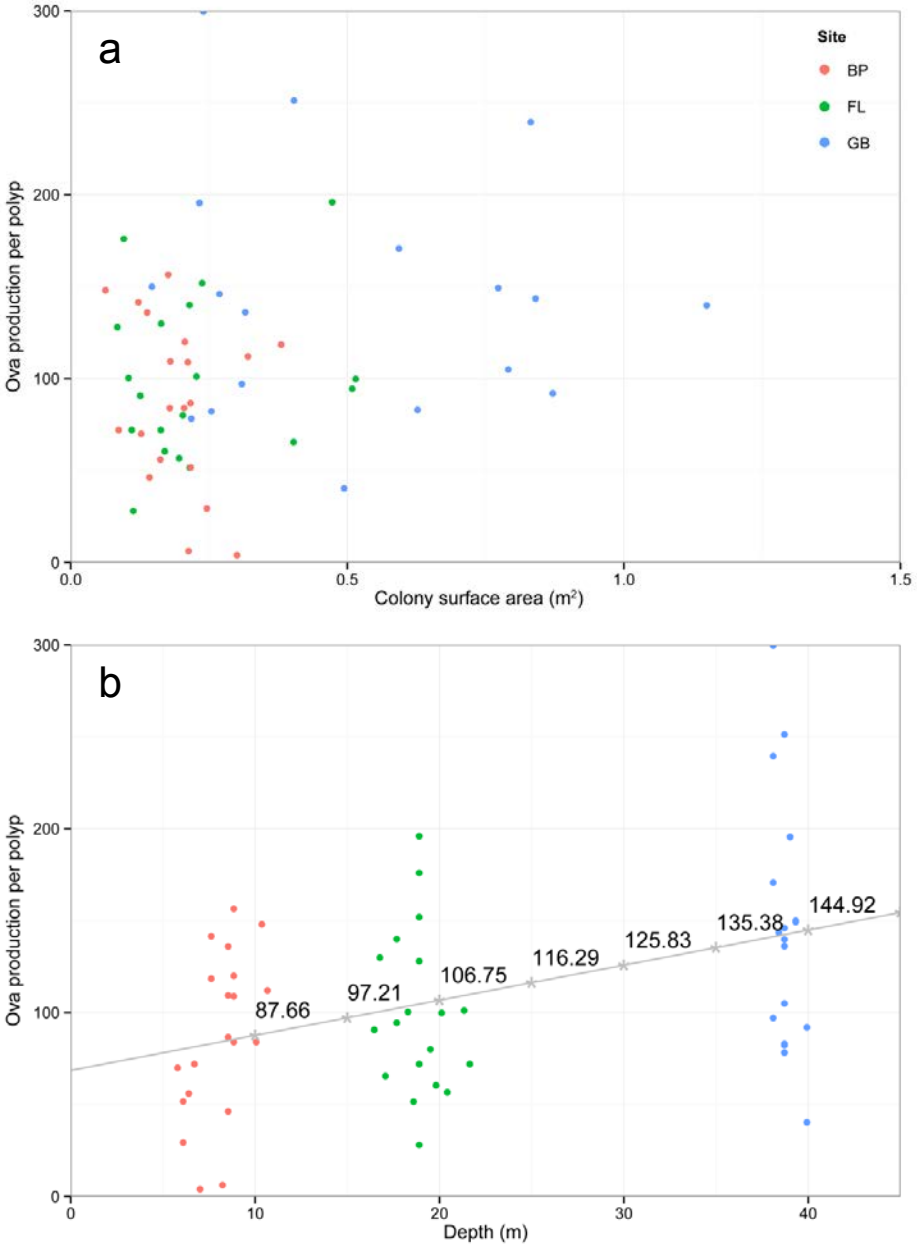

Figure 2.12. *M. faveolata* ova production versus (a) colony surface area and (b) depth in meters. No significant linear relationship was found between ova production per polyp and colony surface area, suggesting that the fact that colonies found at Grammanik Bank are larger does not affect per polyp fecundity. A significant positive linear relationship was found between ova production per polyp and depth ($p < 0.001$, $R^2 = 0.381$). Predicted values are shown for every 5m of increasing depth.

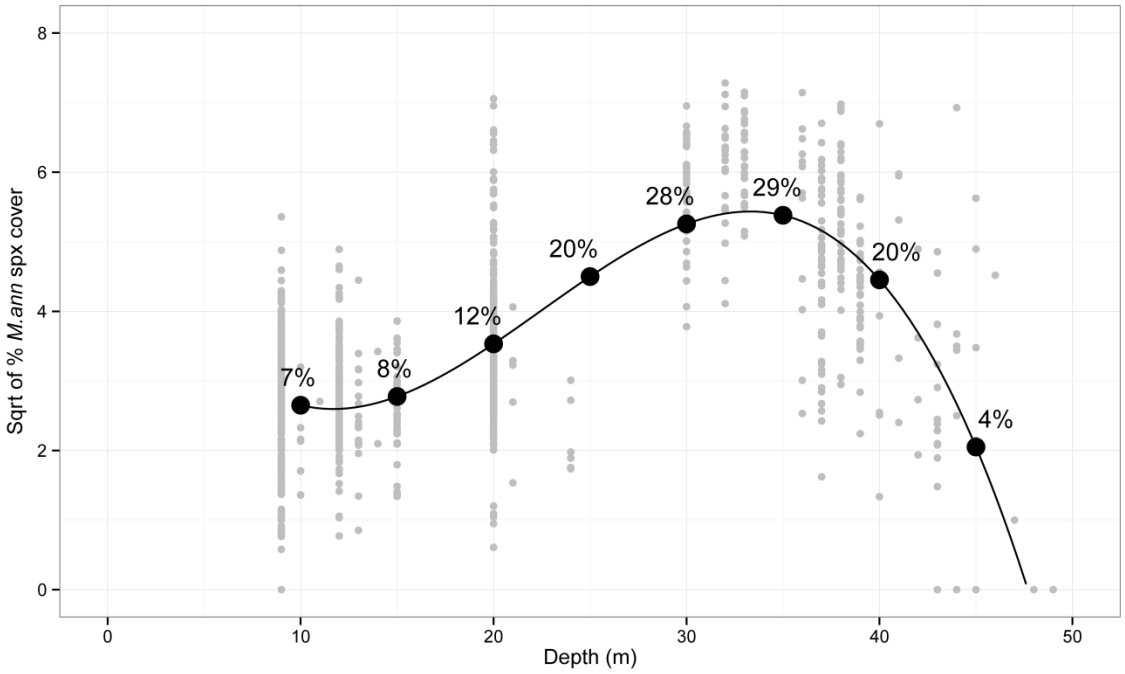

Figure 2.13. Third degree polynomial model of *M. annularis* species complex coral cover versus depth ($p < 0.0001$, $R^2 = 0.51$), derived from the Territorial Coral Reef Monitoring Program (Smith et al. 2011) from 2001-2012. Data was square-root transformed prior to fitting. Predicted values (squared from model to represent true coral cover estimates) are shown for every 5m of increasing depth.

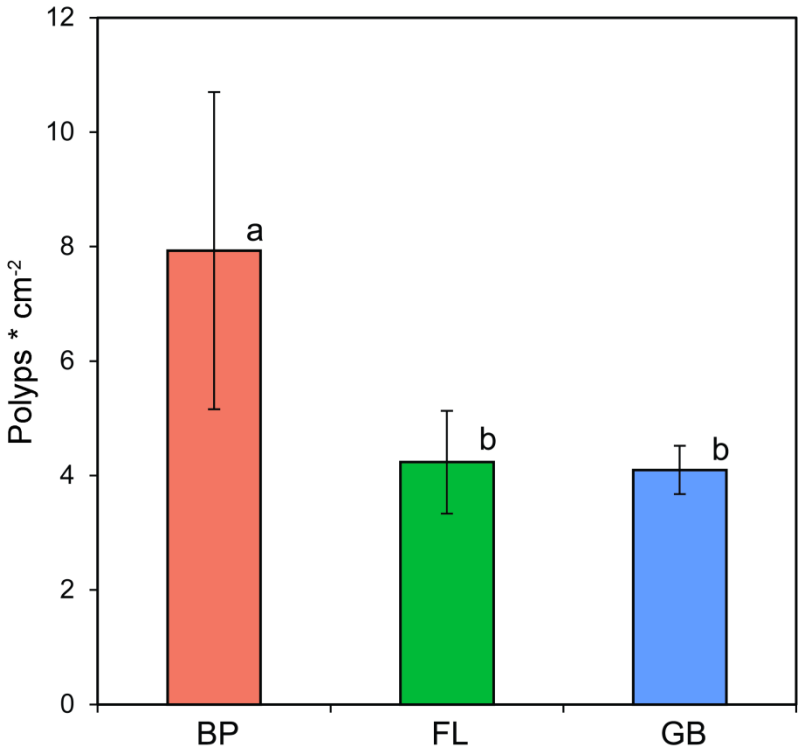

Figure 2.14. *M. faveolata* polyp densities by site. Polyps per cm^2 were estimated from three-dimensional reconstructions. Sites are ordered left to right by increasing depth. Mid-depth and mesophotic corals were found to have similar polyp-spacing, whereas shallow corals had significantly higher polyp densities (one-way ANOVA, $p = 0.012$, N=15).

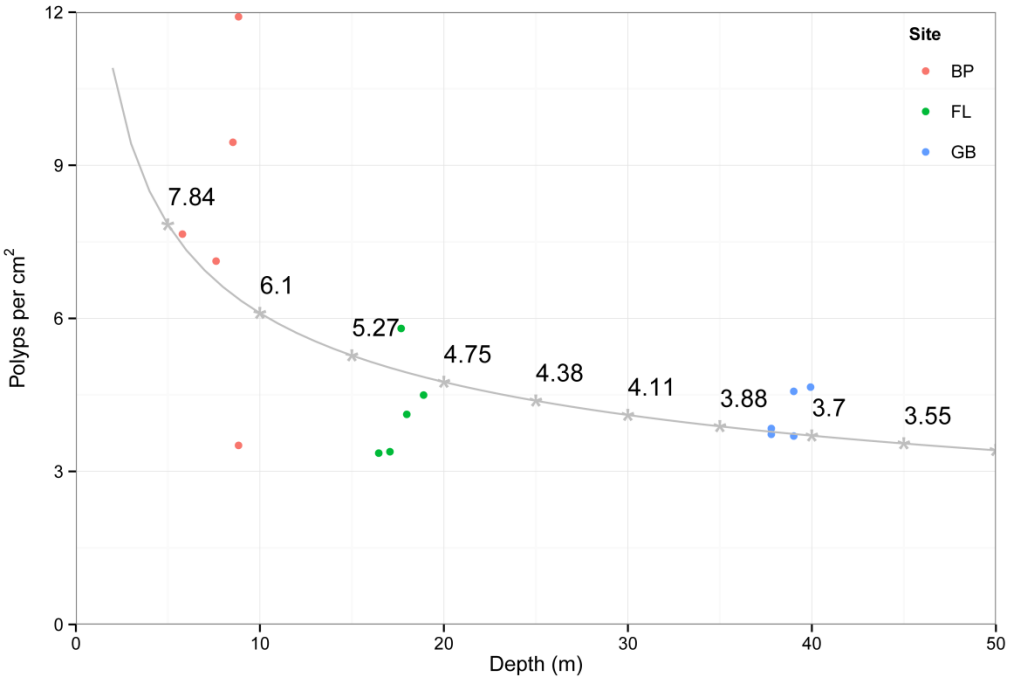

Figure 2.15. *M. faveolata* polyp densities versus depth in meters. Polyps per cm^2 were estimated from three-dimensional reconstructions. Data was log-transformed and a significant negative linear relationship was found ($p = 0.014$, $R^2 = 0.381$). Predicted values are shown for every 5m of increasing depth.

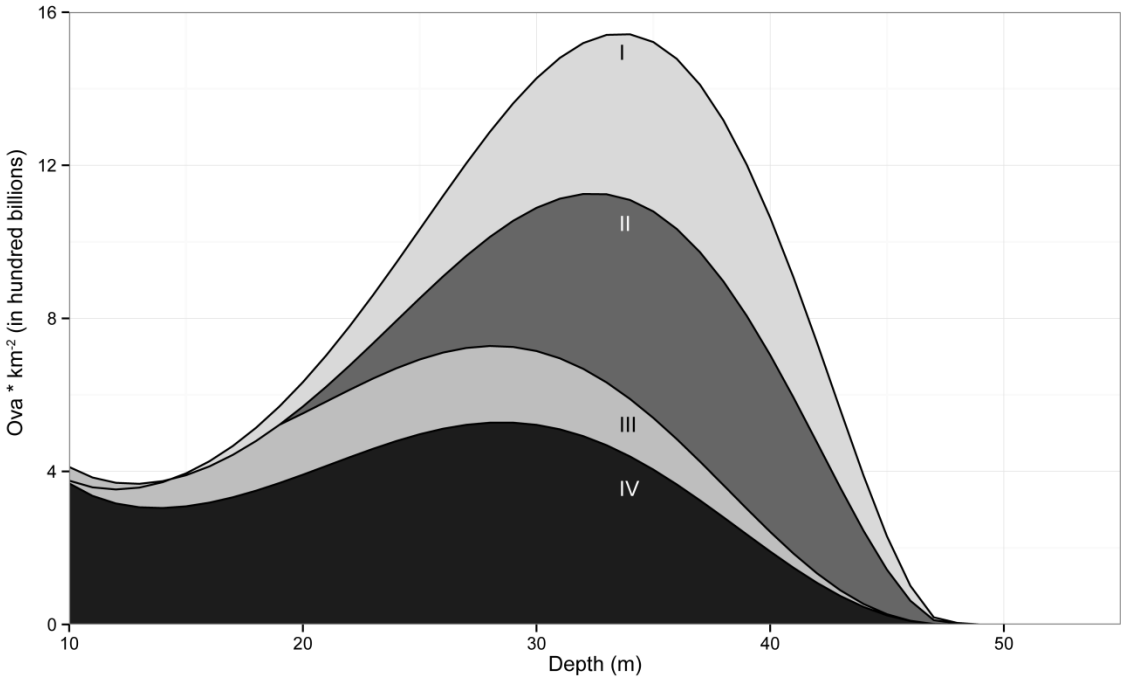

Figure 2.16. Reproductive capabilities for the *M. annularis* species complex – calculated as the products of fecundity per polyp, polyps per cm^2 and coral cover – on hypothetical $1km^2$ USVI reefs versus depth in four scenarios. (I) Empirically estimated depth-specific values for fecundity, polyp density and coral cover (these polyp density and coral cover estimates used for all following scenarios). (II) Equal fecundity with depth (Villinski 2003, median literature value of 96 eggs per polyp [Szmant et al. 1997]). (III) Equal fecundity to 20m depth (Villinski 2003, maximum depth in this study), and linearly decreasing fecundity from 20 to 45m. (IV) Linearly decreasing fecundity from 10m to 45m.

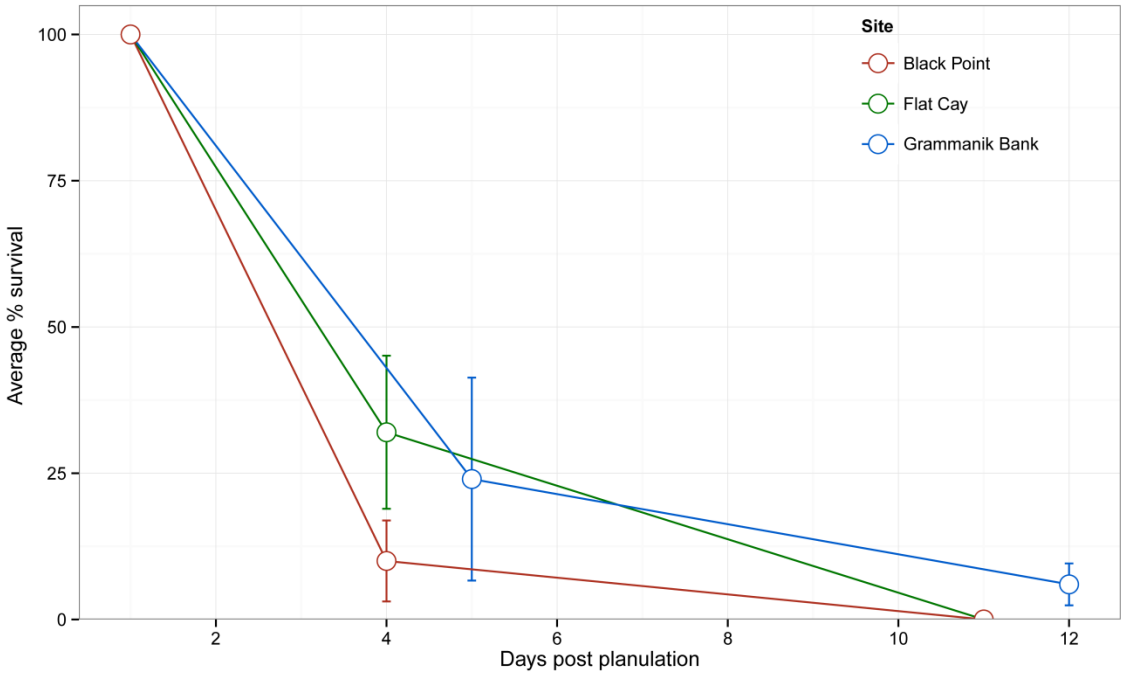

Figure 2.17. Mean survival of mesophotic *Porites astreoides* planulae larvae in transparent acrylic tubes transplanted to sites at 5-10m (Black Point), 15-22m (Flat Cay) and returned to the site of parent colonies at 37m (Grammanik bank). Mortality was high at all sites, with 50% mortality likely occurring between 2 and 4 days post planulation at all sites. By day 11 no larvae were surviving at Black Point or Flat Cay. By day 12, 3 of 50 larvae (6%) were surviving and Grammanik Bank. Error bars are standard error.

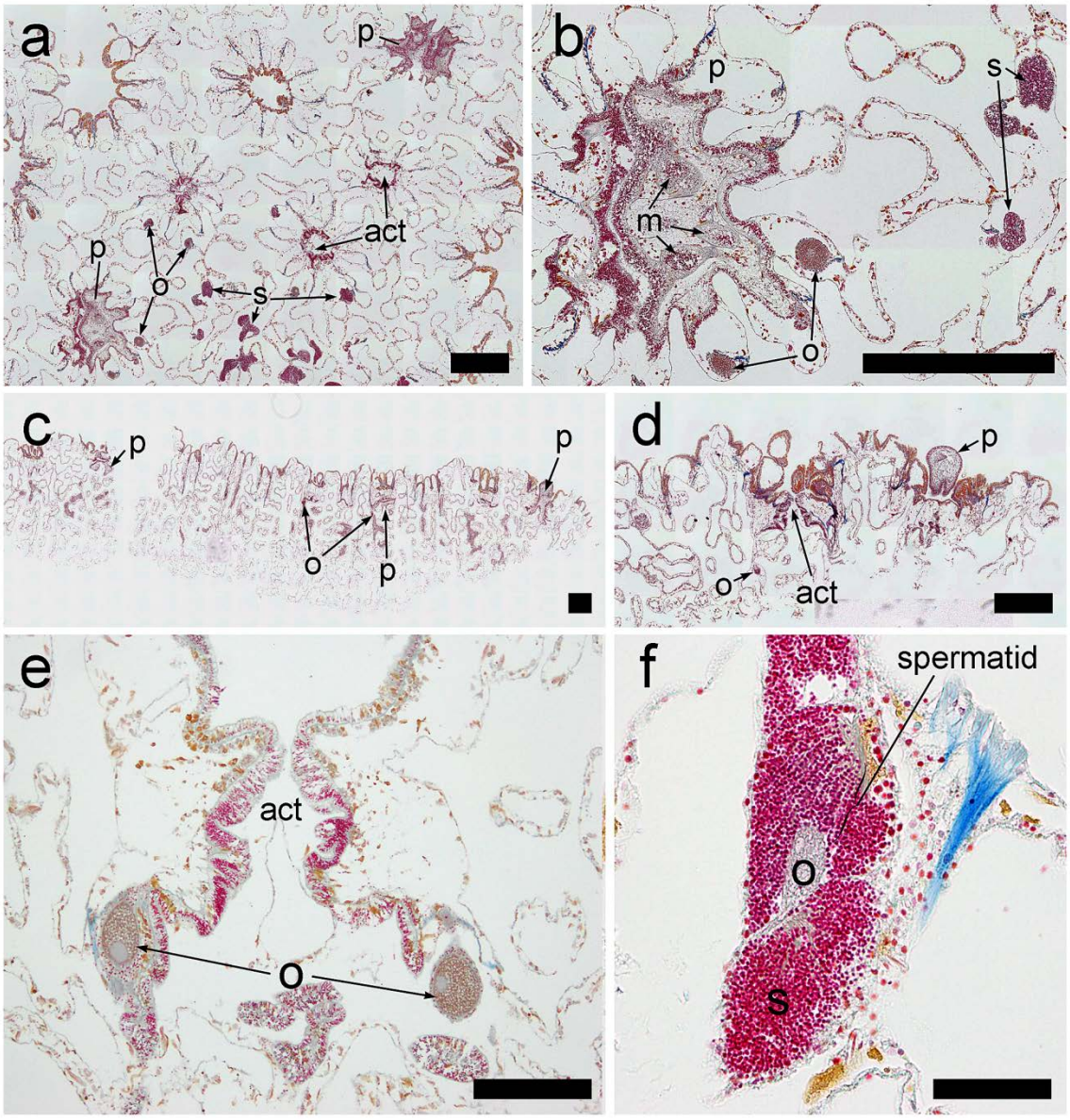

Figure 2.18. Selected views of reproductive structures of *P. astreoides*. (a) Cross-sectional view showing the simultaneous presence of oocytes, spermaries and planulae larvae. The actinopharynx of two polyps is also shown for reference. (b) A tighter view of (a), showing internal details of a larva, including mesenteries. (c) Longitudinal view showing the simultaneous presence of larvae and oocytes. (d) A tighter longitudinal view, showing a larva extruded from the oral opening of a polyp. (e) A longitudinal view of a single polyp, showing the actinopharynx and stage IV ova. (f) A 40x magnification of a stage V spermary and stage IV oocyte. Spermatozoa are arranged in spermatids within the spermary. (o = oocyte/ovum; s = spermary; p = planulae larva; act = actinopharynx; m = mesenteries; bar = 500 µm [a-d], 200 µm [e], and 50 µm [f]).

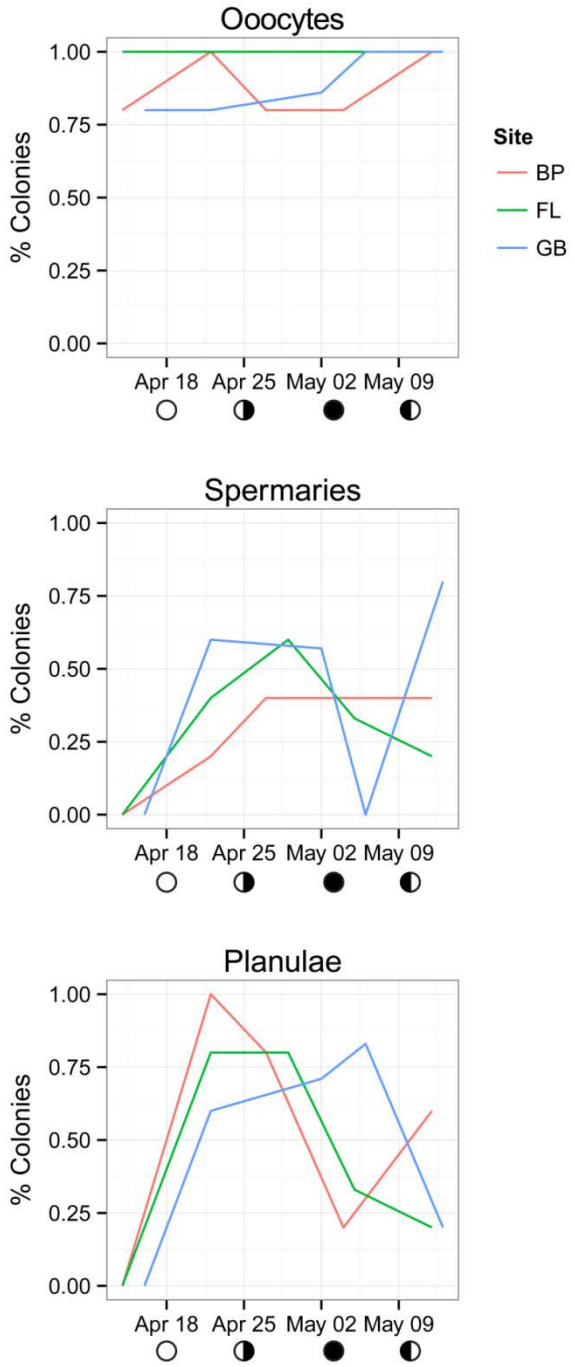

Figure 2.19. *P. astreoides* reproductive products found in histological analyses. Values plotted represent the percent of total colonies (3 sites, 5 sampling days, n >= 5, N = 79) containing oocytes/ova (top), spermaries (middle) and planulae (bottom) on each sampling day at each site. Sites include Black Point (BP, red), a shallow near-shore site; Flat Cay (FL, green), an offshore island mid-depth site; and Grammanik Bank (GB, blue), a mesophotic submerged bank site. The lunar cycle is shown below the x-axis.

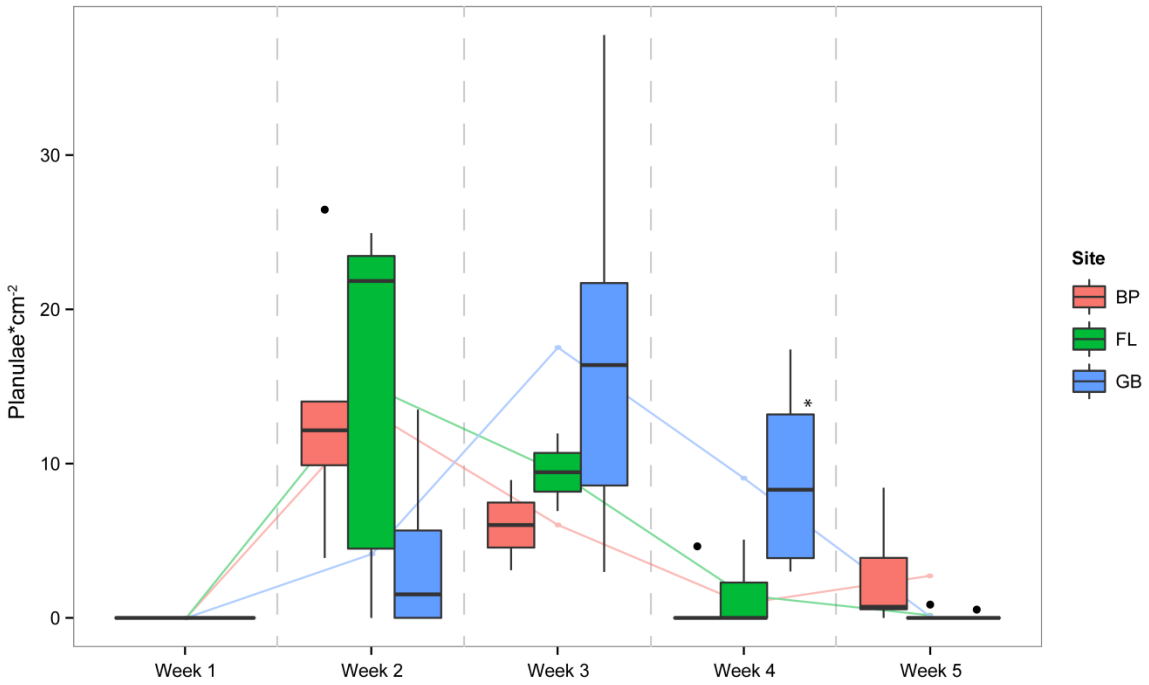

Figure 2.20. Planula densities in *P. astreoides* tissues for Black Point (5-10 m), Flat Cay (15-22 m) and Grammanik Bank (35-40 m) each week. Boxplot attributes as in Figure 2.10. Data beyond whiskers are outliers represented as dots. Lines plots connect mean values, and are included to illustrate the trend of increasing planulae density, and the loss of those planulae from the tissues, presumably due to planulation. Peak planulae densities occurred one week earlier (week 2) at mid-depth (FL) and shallow (BP) sites than at the mesophotic site (GB). At only one week (week 4) were planulae densities found to be significantly different between sites, with higher densities at Grammanik Bank (GB) than the other two sites (one-way ANOVA/Tukey's-HSD, $p = 0.009$).

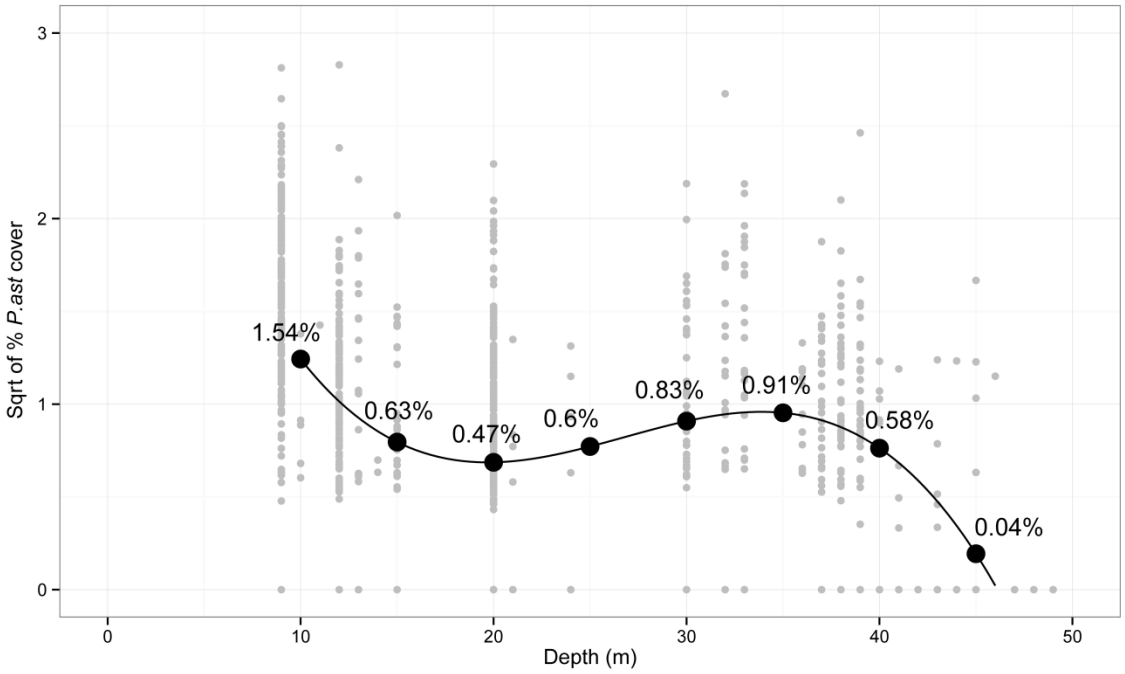

Figure 2.21. Third degree polynomial model of *P. astreoides* coral cover versus depth ($p < 0.0001$, $R^2 = 0.20$), derived from the Territorial Coral Reef Monitoring Program (Smith et al. 2011) from 2001-2012. Data was square-root transformed prior to fitting. Predicted values (squared from model to represent true coral cover estimates) are shown for every 5m of increasing depth.

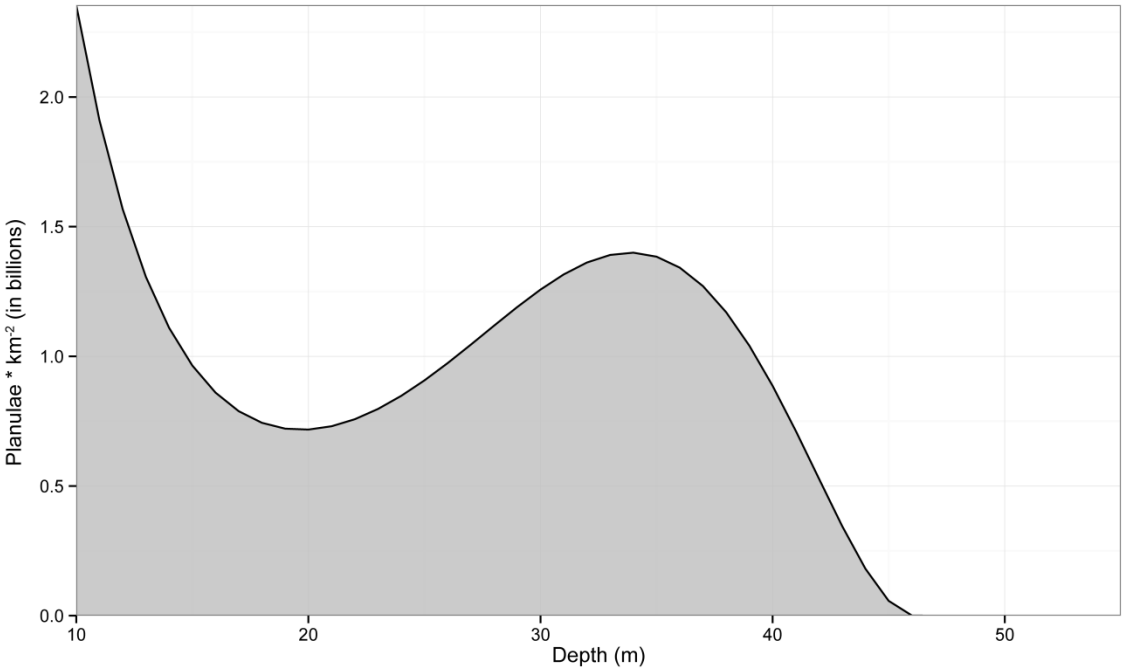

Figure 2.22. Reproductive capabilities for *P. astreoides* – calculated as the products of planulae per cm^2 and coral cover – on hypothetical $1km^2$ USVI reefs versus depth. Because peak planulae densities were not found to be significantly different between sites, a single value of 15.24 planulae*cm^{-2} was used for all depths.

Chapter 3: Micro-computed tomography of small mesophotic coral samples for the estimation of annual growth and calcification

Background

Darwin (1889) reported the presence of hermatypic corals growing deeper than 120 m over a century ago, yet despite the knowledge of their existence, our basic understanding of the physical and ecological processes that determine the distribution, growth and health of what are now termed mesophotic coral ecosystems (MCE) has been relatively lacking. This is mostly due to technical and financial challenges in exploring these environments, such as the physiological limitations of traditional SCUBA and the expense of using more advanced technologies such as submersibles and AUVs. We are now tasked with basic assessments of these ecosystems in a changing environment, while shallow coral reefs are experiencing unprecedented decline (Gardner et al. 2003; Wilkinson 2008).

Coral growth rates are often used as coral reef health indicators in environmental monitoring and assessment (Shinn 1966; Hudson 1981; Guzman et al. 1994, 2008; Edinger et al. 2000). Early in coral reef science, coral growth rates were ascertained through the repeated measurement of selected coral colonies over years or decades (Mayer 1915). Staining techniques were later developed, which involved staining a living coral's skeleton and harvesting that coral or a section thereof at a later date to estimate skeletal growth over time using the stained portion of skeleton as a temporal benchmark (Buddemeier and Kinzie III 1975; Dustan 1975). Nearly simultaneously the use of X-radiography to measure variation in annual density banding in coral skeletons, analogous to counting tree rings, also became a standard practice to estimate linear extension (Dodge et al. 1974; Baker and Weber 1975; Hudson et al. 1976; Hudson 1981).

X-ray micro-computed tomography (micro-CT) has been used to investigate coral skeletal morphology (Vago et al. 1994; Kruszyński et al. 2007) and porosity (Roche et al. 2010a, 2010b), and the response of coral skeleton growth and dissolution to the presence of boring organisms (Vago et al. 1994; Beuck et al. 2007). Micro-CT precision can be as fine as several microns, and the potential for applications to coral sclerochronology are many.

Goals and objectives

The objectives of this study were to explore and evaluate the application of micro-CT scanning to estimate the (1) density, (2) growth and (3) calcification rates of mesophotic *Montastraea faveolata* corals. Skeletal samples were small (1-2 cm in depth), and originally taken for soft tissue analysis. Thus the use of micro-CT represented an opportunity to apply this advanced technology to detecting annual density banding in small coral samples taken from environments with relatively low photosynthetically available light penetration. Baker and Weber (1975) note that *M. annularis* colonies growing deeper than 20 m often have insufficiently distinct density banding for the accurate detection of those bands using traditional X-radiography, and in this instance micro-CT may provide the resolution necessary to discern fine changes in density banding. Additionally, the collection of sufficiently large coral cores, or of entire coral colonies, can be expensive and destructive to MCE. The use of micro-CT to estimate recent coral growth from small samples may provide an ecologically and financially sustainable assessment and monitoring tool.

The scope of the larger study for which these samples were taken is in evaluating the refugia potential of mesophotic coral ecosystems (MCE) in the US Virgin Islands (USVI). Effective refugia are spatially removed from or resistant to adverse conditions, and the sclerochronology of mesophotic corals can give insight into historical rates of reef accretion, perturbation and stress (Shinn 1966; Hudson 1981; Edinger et al. 2000).

Methods

Samples were collected from sites south of St. Thomas in the US Virgin Islands (USVI). Sites ranged in depth from 0-10m, 15-25m and 30-40m. A hammer and cold chisel were used to remove small, ~20cm^{2}x~3cm coral samples from centrally located high points on *M. faveolata colonies*. Samples were fixed in buffered zinc formalin and stored in 70% EtOH. Mesophotic samples were taken from two sites, Hammerhead Shoal (2010) and Grammanik Bank (2011).

A subset of fragments were thoroughly dried in an oven, weighed, and scanned using a white light 3D scanner (3D3 Solutions HDI Advance, see Chapter 2) (Figure 3.1) in order to estimate coral fragment volume and density. Another subset of coral fragments were cut into rectangle cuboids along the growth axis, measuring ~1cm x ~1cm, with depth from surface into the coral skeleton depending on the depth of the coral sample. These fragments were then thoroughly dried before micro-CT scanning. Each sample was micro-CT scanned under the same scanning conditions, as was a reference BMD (Bone Mineral Density) sample from standardized coral fragments of known density. The BMD was used to calibrate micro-CT luminance data to known coral skeleton densities. Micro-CT digital density profiles were then arranged in three-

dimensional space and volume-of-interest (VOI) transects were drawn through the sample. The VOI was drawn through the coral fragment using two distinct methods. The first method was intended to include 3-5 polyps and the intercalical space between those polyps, from just below the surface of the fragment to the deepest portion of the fragment possible (herein referred to as "large" VOI, Figure 3.2a-b). The second method used a standard diameter cylinder-shaped VOI to track individual polyp calices from just below the fragment surface to the deepest point possible. "Polyp" VOIs were drawn for several polyps in each sample, and the results were averaged for each coral fragment.

The mean horizontal density was estimated every 64 μm along the VOI based on mean luminance. Mean density transects were imported into CoralXDS+ software for annual band delimitation, and annual extension and calcification rates were estimated for each sample. Because polyp-centric VOIs underestimate coral density because they ignore intercalical aragonite, mean extension rate from the polyp VOI datasets was multiplied by density estimates from the larger VOI dataset in order to estimate calcification rates. Mean density transects were also compared against historical temperature datasets.

Results and discussion

Coral density and depth

Graus and Macintyre (1982) suggest linear increases in *M. annularis* skeletal density with depth, based on data from Baker and Weber (1975). However, a non-linear relationship based on light-saturation (Chalker 1981; Bosscher and Schlager 1992) has become more widely accepted, where skeletal density increases most rapidly between 15

and 25 m. Coral fragment density was estimated using coral fragment mass and volume as determined using a white light 3D scanner, as well as using micro-CT mean luminance (Figure 3.3). Due to the use of coral fragments in soft tissue studies, different samples were used in each method. Results from both methods can be explained by non-linear relationships found by iterating values for the constants ρ_{max} (maximum density), ρ_{min} (minimum density) and the constant *r* through a non-linear least squares method (Figure 3.3):

$$Predicted\ Density = \rho_{max}/(1 + e^{(\rho_{min} + r * Depth)})$$

Differences between the two methods are likely negligible and due to samples size. Density profiles were very similar to literature profiles (Bosscher and Meesters 1992; Bosscher and Schlager 1992), and thus it was expected that growth rates of mesophotic corals would be similar to literature estimates, as density and growth are related linearly (Bosscher 1993).

Coral growth and calcification

Literature estimates of annual linear extension of *M. faveolata* shallower than 20 m is on the order of 5-15 mm yr^{-1} (Hudson 1981; Bosscher and Meesters 1992; Bosscher 1993), and in general, the samples collected from shallow sites were not large enough (deep enough in the coral skeleton) to resolve an entire year of growth, and so growth results for shallower corals are not shown. This technique would likely only be applicable to shallow colonies if sufficiently deeper (into the skeleton) coral cores were taken. In all, eleven mesophotic coral fragments underwent micro-CT; however growth results are only shown for four, all from 39-40 m. Results were very sensitive to the growth axis of

coral polyps, and seven of the eleven mesophotic coral fragments were not appropriate for growth analysis. This suggests that the reliable success of this method may be contingent on more methodically and systematically acquired coral skeletal samples than the fragments used in this study.

Density banding in digital 3-dimensional representations of micro-CT scans of mesophotic coral fragments were difficult to discern by eye (Figure 3.2). Banding patterns acquired using the two VOI methods were not consistent with each other (Table 3.1). A large VOI appeared to resolve fewer years, and higher growth rates were predicted using CoralXDS+ software to delineate peaks and valleys in density banding (Table 3.1). Density banding from large VOI appeared to mirror seasonal variation in water temperature (Figure 3.4). This would be appropriate, as high density bands coincide with maximum water temperatures in massive corals, and low density bands with minimum temperatures (Barnes and Lough 1993; Lough and Barnes 2000). Using a large VOI, maximum annual extension in mesophotic *M. faveolata* was more than 5 mm (Grammanik Bank, Figure 3.4) (Table 3.1).

Using the maxima and minima in large VOI coral density datasets, means (±SD) for annual extension and calcification were 3.63 mm yr^{-1} (±1.75 mm) and 0.54 g $CaCO_3$ cm^{-2} yr^{-1} (±0.29 g), respectively (n = 4, Table 3.1, 3.2). Polyp VOIs resulted in mean extension of 2.07 mm yr^{-1} (±0.39 mm) and mean calcification of 0.40 g $CaCO_3$ cm^{-2} yr^{-1} (±0.01 g) (Table 3.1, 3.2). Although the discrepancy in mean linear extension between large VOI and polyp VOI datasets is less than 2 mm, the differences require serious attention. The maximum annual linear extension in the large VOI dataset is 5.20 mm (Table 3.1). This annual growth was in a coral from Grammanik Bank (2011, Figure 3.4).

The other fragment from Grammanik Bank also showed high linear extension when analyzed with a large VOI (4.82 mm) (Figure 3.4). These estimates for linear extension are high for corals at this depth (39-40 m), based on literature values from Baker and Weber (1975), Bosscher and Meesters (1992) and Bosscher (1993).

When instead the coral fragments were analyzed with small polyp-centric VOI variation with temperature was not as obvious; however mean, minimum and maximum linear extension were closer to literature values (Table 3.1). In the literature the growth of *M. annularis* is shown to decrease non-linearly with depth, with sharp declines in annual extension generally occurring between 10 and 20 m, but growth rates decline more gradually to 35 m (Baker and Weber 1975; Bosscher and Meesters 1992; Bosscher 1993). Estimates for *M. annularis* growth rates deeper than 25 m generally range from 1-2 mm yr^{-1} (Baker and Weber 1975; Huston 1985; Bosscher and Meesters 1992) but have been as high as 4-5 mm yr^{-1} on reef areas with high light penetration (Graus and Macintyre 1982; Huston 1985; Bosscher and Meesters 1992). This suggests that the growth estimates acquired for mesophotic corals in this study through micro-CT are within the range of accepted literature values for this species, however growth rates determined using large VOI are at the high end of that range. Additionally, because density is averaged over only several polyps and intercalical space using large VOI, small changes in skeletal structure, such as extratentacular budding, could be erroneously interpreted as density banding.

It is difficult to ascertain which method (large or polyp VOI) is best for the estimation of linear extension in micro-CT, if either, without further study. Mesophotic corals are particularly dense, at times nearing the density of pure aragonite. The Skyscan

1174 micro-CT scanner used in this study had particular difficulty in resolving fine features in mesophotic corals for this reason. The combination of high density and fine density banding may have made it particularly difficult for micro-CT to be truly effective, and has certainly always been an issue when estimating the growth of dense deeper growing corals (Baker and Weber 1975). That being said, using polyp-centric VOIs has distinct disadvantages, namely that any banding that occurs in intercalical space is missed, and calcification rates cannot directly be calculated due to underestimation of density. The apparent response of coral density to annual temperature fluctuation in the large VOI dataset is satisfying (Figure 3.4); however it suggests high growth rates in at least two mesophotic corals from Grammanik Bank.

There is potential that high growth estimates for shelf-edge mesophotic corals are not an aberration, and that the growth estimates determined using a large VOI were accurate. Edinger et al. (2000) caution that the use of coral growth rate in the assessment of coral health can be misleading. In degraded coastal reef areas coral growth rates may be deceptively high due to nutrient stimulation of zooxanthellae growth and autotrophy (Atkinson et al. 1995) and/or to the stimulation of coral metabolism through heterotrophic feeding of dissolved and particulate organic matter (Lewis 1977; Risk et al. 1994; Edinger et al. 2000). This logic may also imply that the growth of light limited corals, such as those at mesophotic depths, may also be supplemented through nutrient enrichment or heterotrophic feeding. Indeed, Leichter and Genovese (2006) reported bimodal growth of the coral *Madracis mirabilis* with respect to depth, and suggested that high growth rates at light limited depths were likely due to episodic upwelling of nutrients and high availability of particulate organic matter due to the proximity of the

thermocline. The MCE sampled in this study are found on submerged banks near the insular shelf edge, and may experience and benefit from periodic upwelling of nutrient-rich water caused by breaking internal waves (Leichter et al. 1998, 2003, 2008; Leichter and Genovese 2006; Smith et al. 2010). This metabolic subsidy may explain the unexpectedly high growth rates found in *M. faveolata* corals from these sites; however isotopic analysis may be necessary to elucidate the degree of coral heterotrophic feeding occurring at these sites (Muscatine et al. 1989; Felis et al. 1998), and in-depth study of episodic upwelling to these MCE would be required to be certain that mesophotic coral growth is being subsidized by favorable environmental conditions.

Summary and conclusion

Density of *M. faveolata* samples from a gradient of depths calculated from micro-CT luminance agreed nicely with more traditional methods and with literature values (Graus and Macintyre 1982; Bosscher and Meesters 1992; Bosscher 1993). Density banding was evident using micro-CT; however the two methods described predicted different rates of linear extension. Ultimately the use of micro-CT in the estimation of growth rates in small samples of mesophotic *M. faveolata* is not without caveat, and requires further study. Should future study determine that the growth of *M. faveolata* at highly productive mesophotic sites is indeed greater than anticipated by most literature, it may be that micro-CT has provided observations that traditional methods may have missed by resolving difficult to discern density banding. Sampling using cores with standard diameter and depth would also likely yield more consistent results. However, the goal of this study was to determine if the opportunistic use of previously obtained coral

skeletal samples in micro-CT could provide a less-expensive and lower impact alternative to traditional coral growth assessment in mesophotic environments. The reality is that micro-CT has huge potential in sclerochronology applications, but that the process is sensitive to the condition of coral skeletal samples, and it appears that consistency between samples is important if comparisons are to be made.

It is important to note that the mesophotic sites sampled in this study have far higher coral cover than nearby shallow sites (Chapter 2). Because calcification occurs below living coral tissue, even if mesophotic corals grow more slowly than shallow corals, mesophotic reefs may accrete more net $CaCO_3$ per square kilometer than nearby degraded shallow reefs. Additionally, the possibility that the mesophotic corals sampled in this study may have high growth rates enforces the notion that basic assessments of the status of these reefs are necessary in order to make intelligent management decisions and realistic predictions about coral reefs in general.

Table 3.1. Estimated extension rates in four samples using micro-CT. Two different methods were used for selecting a VOI. The larger VOI resulted in larger growth rates.

n=4	mm yr-1				
	Mean extension	SD	min	max	# years resolved per sample
Large VOI	3.625	1.748	1.028	5.202	4,4,1,1
Polyp VOI	2.074	0.386	1.028	3.789	6,4,5,4

Table 3.2. Calcification rates estimated from micro-CT of four mesophotic samples. For the large ROI dataset, mean calcification was calculated my multiplying the linear extension and mean density of each growth band. For the small ROI dataset, mean density for each sample (obtained from large ROI datasets) was multiplied by mean linear extension.

n=4	g $CaCO_3$ cm^{-2} yr^{-1}	
	Mean calcification	SD
Large VOI	0.540	0.290
Polyp VOI	0.401	0.007

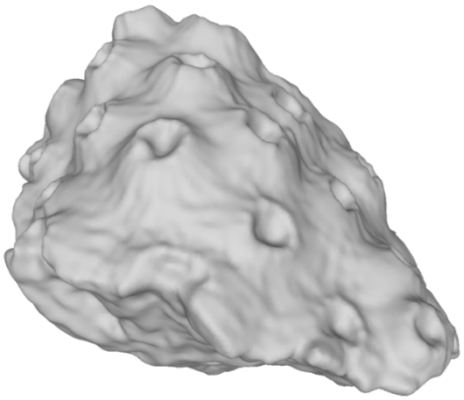

Figure 3.1. An example of a digitized coral fragment, scanned with the white light 3D3 Solutions HDI Advance. Scans such as these were used to estimate coral fragment volume. This fragment is about 30 mm across and 15 mm high.

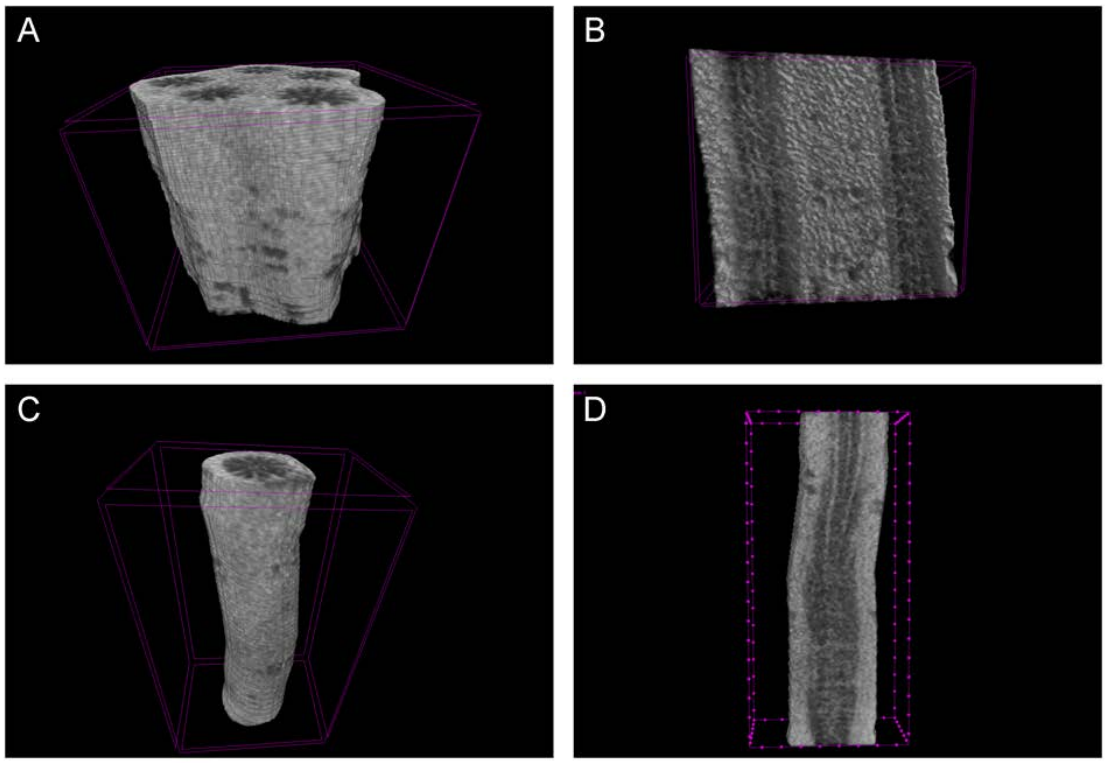

Figure 3.2. Examples of volumes of interest (VOI) used in density and growth analysis of M. faveolata. Brighter pizels denote higher luminance and density. A and B show a large VOI including five polyp calices and intercalical space (~15 mm diameter x ~15 mm height). B shows a cross-section. C and D show a polyp-centric VOI, including just one polyp calix. D is a cross-section (points on wireframe are 1 mm apart for reference, C and D are about 17 mm high and about 5 mm in diameter). There appears to be banding in the lower section of D, shown as brighter, denser horizontal bands.

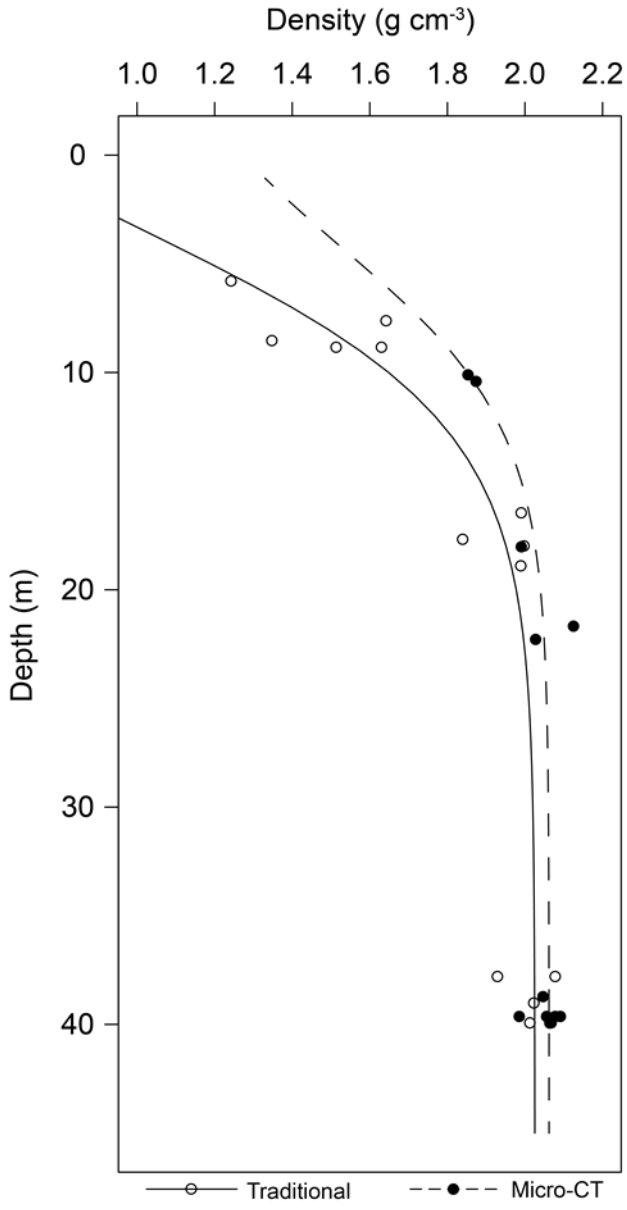

Figure 3.3. *M. faveolata* skeletal density profiles using a traditional method based on weight and volume of coral fragments (solid line), and using micro-CT luminance (dashed line). Both methods suggest similar density profiles. Note that density increases most rapidly between 10 m and 20 m, with little change between 20 m and 40 m.

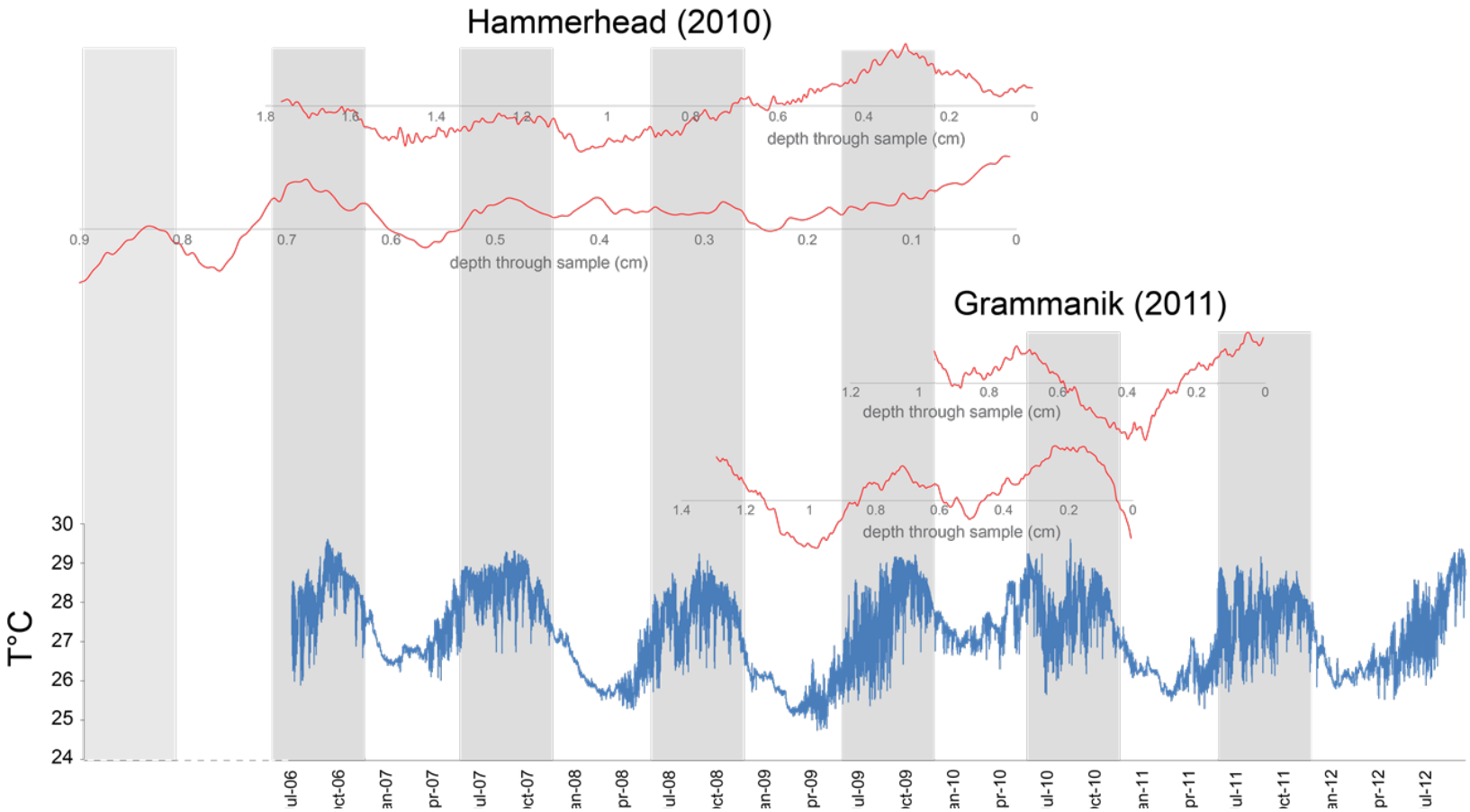

Figure 3.4. Comparisons of density banding in mesophotic *M. faveolata* coral fragments and water temperature at or near collection sites (Grammanik Bank and Hammerhead Shoal, 35-40 m). Fragments were analyzed using large ROI. Temperature data is shown from July 2006 to July 2012. Each of four density profiles has its own axis (grey numbers) which demark the distance through the coral sample in cm. Note that Grammanik Bank samples appear to have density bands that closely mirror changes in SST, and estimated growth rates are higher for these samples. Smaller peaks and valleys in density may show lunar banding

Chapter 4: Modeling of vertical connectivity and mesophotic coral refugia in the US Virgin Islands

Background

Coral reefs face a daunting set of challenges to their continued persistence in shallow tropical waters around the globe. Over-fishing of key functional groups and unsustainable coastal development have been attributed with the well-documented decline in coral reefs over the past 30 years (Jackson et al. 2001; Gardner et al. 2003; Pandolfi et al. 2003, 2005; Hughes et al. 2007). Global climate change presents coral organisms with another unique set of challenges, including increased incidence of thermal bleaching (Wellington et al. 2001; Baker et al. 2008), and decreased coral growth and calcification associated with ocean acidification (Hoegh-Guldberg et al. 2007; Pandolfi et al. 2011). Further, the effects of the consequential habitat fragmentation on coral population connectivity are poorly understood, and potentially severe (Tilman et al. 1994; Collingham and Huntley 2000; Hanski and Ovaskainen 2000). Although the environmental conditions that determine the abundance and distribution of coral reefs may be restricted, the extent and degree to which local and global coral reef stressors may disturb coral reefs is not uniform in space. Areas that provide natural resilience to local coral populations by reducing exposure to stress may have the potential to behave as refugia, and be particularly important to the persistence of corals reefs and the recovery of degraded reef areas.

The "deep reef refugia hypothesis" (DRRH) has been widely discussed due to observations that depth may reduce thermal and light stress on resident coral organisms (Glynn 1996; Riegl and Piller 2003; West and Salm 2003). Depth has also been shown to

mitigate the impacts of coastal sedimentation and pollution (Smith et al. 2008) and storm damage (Goldberg 1983). This suggests that depth could behave as refugia for corals and associated organisms and as a larval source to shallower habitats during or after periods of adverse conditions. In particular, recent attention has been paid to the refugia potential of what have been termed as "mesophotic" reefs, or mesophotic coral ecosystems (MCE), which are loosely defined as coral ecosystems found below 30m depth. In many areas of the Caribbean MCE have been found to be not only buffered from coastal and shallow coral stressors, but also in impressive condition compared to shallow Caribbean ecosystems (Bak et al. 2005; Armstrong et al. 2006; Menza et al. 2008; Smith et al. 2008).

Bongaerts et al. (2010a) highlight knowledge gaps in the DRRH, and mention specifically that larval exchange between deep and shallow habitat is integral to the validity of DRRH (Lesser et al. 2009). Despite this, very little evidence exists that supports or refutes that coral larval exchange actively occurs between deep and shallow habitats. Historical evidence of larval exchange, as shown by studies of coral population genetics, suggest that the exchange of migrants between deep and shallow habitats is both species- and location-specific. Bongaerts et al. (2010b) found genetic divergence of the brooding coral *Seriatopora hystrix* along a depth gradient in northeast Australia. Contrastingly, van Oppen et al. (2011) found genetic evidence of deep to shallow migration in the same coral in northwest Australia. Prada and Hellberg (2013) determined that populations of the octocoral *Eucinea flexuosa* in the Caribbean separated by depth are genetically divergent, however migration between populations likely occurs with some periodicity, and population genetic studies in the northern USVI suggest that

mesophotic and shallow populations are not genetically divergent (personal communications and manuscript *in prep* with Holstein, Serrano et al.).

Growing evidence suggests that coral larval connectivity occurs on shorter spatial scales than historically presumed (Cowen et al. 2002, 2006; Baums et al. 2003; Underwood et al. 2007; Foster et al. 2012), and that understanding habitat quality and productivity are crucial in developing realistic population models of coral reefs systems (Paris et al. 2005; Underwood et al. 2007; Botsford et al. 2009; Mumby et al. 2011a). In Chapter 2 evidence was provided that suggests that for some species larval production in MCE greatly exceeds shallow larval production, which has obvious implications for the potential for mesophotic larval subsidy to shallow reefs and the DRRH.

The goal of this study was to use a biophysical model of coral larval dispersal parameterized with three dimensional settlement habitat and species specific coral reproductive and larval traits to gauge the refugia potential of MCE in the US Virgin Islands (USVI). It was hypothesized that high mesophotic coral productivity would result in a higher mesophotic subsidy to shallow settlement. Because the effects of depth on coral gamete fertilization and the post-settlement survivorship of coral planulae larvae produced in deeper water and settling shallow reef areas are unknown, the sensitivity of local mesophotic larval subsidy to shallow areas to these factors was also examined. This study has the potential to inform local management of coral reef areas in the USVI, and has implications for the study of DRRH and the use of biophysical modeling in the prediction of coral reef persistence and health.

Methods

Numerical modeling

To investigate vertical coral connectivity in the US Virgin Islands, and in particular mesophotic to shallow larval exchange, a multi-scale biophysical model, the Connectivity Modeling System (CMS; Paris et al. 2013), was used to simulate larval transport of two depth-generalist coral species, the boulder star coral *Montastraea faveolata* and the mustard hill coral *Porites astreoides*. *M. faveolata* is a potentially endangered broadcast spawning species (IUCN, Aronson et al. 2008) and is a principle reef-building coral in the Caribbean. *P. astreoides* is a brooding coral predicted to have considerably different dispersal dynamics from *M. faveolata* and other broadcast spawning species, due to rapid larval competence. For a glossary of terms, see Table 4.1.

Hydrodynamic module

The CMS couples offline ocean current, GIS-based habitat and biological submodels. To maximize accuracy in larval dispersion calculations a hierarchy of oceanographic models was used, and those models were nested through the CMS Lagrangian scheme (Paris et al. 2013). The two larger oceanographic models were based in the community code of the HYbrid Coordinate Ocean Model (HYCOM, Bleck 2002), and included the HYCOM-Global 1/12 degree horizontal resolution (ca. 7km grid) model and the Gulf of Mexico GoM-HYCOM 1/25 degree horizontal resolution (ca. 4km grid) model. The smallest domain was centered directly over the northern USVI and was based in the Regional Ocean Modeling System framework (ROMS, Shchepetkin 2003; Moore et al. 2004; Shchepetkin and McWilliams 2005; Warner et al. 2005). This fine-scale

model had a horizontal resolution of 300m (Figure 4.1) (Cherubin et al. 2011). All three models included horizontal and vertical flow-velocities, temperature and salinity. The first 10 vertical layers (0-100m) were extracted from HYCOM models, whereas the ROMS model utilized 18 unequal vertical layers from depths of 0-150m in order to maximize the resolution of shallow hydrology.

Habitat module

Coral reef habitat was parameterized spatially explicitly in three dimensions. $1km^2$ gridded polygons were overlaid on several coral habitat basemaps: (1) shallow (1-30m) coral habitat maps developed by the National Oceanic and Atmospheric Administration's National Centers for Coastal Ocean Science Center for Coastal Monitoring and Assessment (NOAA NCCOS CCMA); (2) a high resolution MCE habitat map developed for the Marine Conservation District (MCD) by the University of the Virgin Islands; and (3) estimates of hardbottom habitat extent from NOAA NCCOS CCMA multi-beam, side-scan and LIDAR sounding datasets. Only gridded polygons intersecting with coral habitat in the aforementioned basemaps were retained for use in the dispersal model. These $1km^2$ reef polygons were limited geographically to the spatial extent of the highest resolution oceanographic model (ROMS), as the focus of this model is on local dispersal and connectivity in the northern USVI. Each reef polygon was assigned a depth of 0-10m, 11-20m, 21-30m, 31-40m or 41-50m. If a reef polygon intersected with habitat in multiple depth bins, a reef polygon for each depth bin (with the same horizontal extent) was retained. A total of 518 reef polygons were created for the model (Figure 4.1). The centroid of each reef polygon was used as the release location for

virtual larvae, and the horizontal extent of each reef polygon was used as settlement habitat.

Particle tracking module

The CMS tracked virtual larvae (particles therein) and recorded their positions over two years (2007-2008) of hydrographic forcing using a Lagrangian stochastic schemed described in Paris et al. (2013). If a competent particle passed over suitable settlement habitat, i.e., a reef polygon, that particle was considered to have settled to that location (node). In order to estimate vertical connectivity between habitats, habitat was considered "suitable" only if the larva and habitat polygon were located in the same 10m depth strata. This settlement condition allowed for fine-scale modeling of vertical connectivity. Additionally, reef habitat and larvae produced deeper than the 30m isobath were considered "mesophotic", and reef habitat and larvae produced in isobaths 30m or shallower were considered "shallow" (detail on code development for the CMS in appendix B).

Biological module - larval traits and behavior

For each species larvae were simulated in two scenarios: 1) as passive particles, and 2) as larvae which changed in specific gravity and size over time. Buoyancy characteristics were species-specific, and parameterized from literature (*M. faveolata*: Szmant and Meadows 2006; Vermeij et al. 2006; Tay et al. 2011; *P. astreoides*: Gleason et al. 2005, 2009) and from laboratory observations outlined in Chapter 2 (Table 4.2).

Simulated larvae (particles therein) were released from each node (Figure 4.1) according to species-specific reproductive seasons.

M. faveolata populations experience one to two mass spawning events per year in late summer, six to nine days after full moons (Szmant 1986, 1991; Szmant et al. 1997). In order to account for potential variability in spawning months, particles were released over four days 6-9 days after full moons at 21:00 in August, September and October of 2007 and 2008, for a total of 12 release times per year. All 518 nodes released 200 particles simultaneously at each release time, resulting in 2,486,400 simulated *M. faveolata* larvae per activity scenario.

P. astreoides colonies brood larvae internally and release nearly competent larvae in a loosely synchronized fashion throughout spring and summer, with peaks of larval release focused around new moons from March through August (Szmant 1986; Chornesky and Peters 1987; Mcguire 1998). Because *P. astreoides* are only found in very low densities below 40 m (see Chapter 2), all 50 m habitat was removed when modeling this species, leaving 377 reef polygons as larval production and settlement habitat. Particles were released over five days focused around new moons at 21:00, March through August in 2007 and 2008. All 377 nodes released 200 particles simultaneously at each of 30 release times, resulting in 4,524,000 simulated *P. astreoides* larvae per activity scenario.

These species-specific larval behavior parameters were used: 1) time from release to competency (Table 4.3), 2) maximum pelagic larval duration (PLD) (Table 4.3), and 3) egg/larval buoyancy (Table 4.2).

Model output and analysis

The output from the CMS contains information on individual successfully settling larva. This information includes the source (*i*) and settlement (*j*) nodes, the amount of time the particle was in the ocean (*age*), and the arrival time and the arrival depth. From this information migration matrices (M_T) were compiled which describe the cumulative settlement at node *j* of larvae originating from node *i*. Each migration of a larva (m_{ij}) can be scaled according to species-specific mortality rates. Mortality is expressed as half-life in seconds (*h*), and each larva's mortality is calculated individually as its exponential decay. In this way each migration, m_{ij}, is scaled as a probability ($P_{m_{ij}}$) from 0 to 1 based on the age of the particle (in seconds) at the time of settlement, using the following equation:

$$P_{m_{ij}} = \frac{1}{2^{age_{m_{ij}}/h}}$$

$P_{m_{ij}}$ can further be scaled by depth-specific production, K_i, which ranges from 0-1 at each production node, *i,* and thus M_T is defined as:

$$M_{T\,ij} = \sum_{c=1}^{c=C} P_{m_{ij_c}} * K_i$$

where *C* is the total number of larvae migrating from *i* to *j*. The resulting scaled matrix M_T contains cumulative probabilities of larval migration from any node *i* to any node *j*. Due to bias in the oceanographic model's flow velocities close to land, some reef polygons experience anomalously high settlement which can confound results. Outliers in M_T were identified by calculating the monthly interquartile range (IQR) of M_T, and

classifying any $M_{T_{ij}}$ greater than the third quartile (Q3) plus 3 * IQR as an outlier. These outliers were scaled to a maximum value of Q3 + 3 * IQR.

Analysis of M_T, referred to here as the raw migration matrix, in regards to comparisons of total settlement assumes that all local reef habitat is characterized (i.e. known). This assumption is rarely met, therefore in order to investigate connectivity without requiring this assumption a normalized matrix $\breve{M}$ is defined as:

$$\breve{M}_{T_{ij}} = \frac{M_{T\,ij}}{\sum_{j=1}^{j=J} M_{T\,ij}}$$

where *J* is the total number of potential settlement nodes (Sponaugle et al. 2012). In this normalized migration probability matrix, $\breve{M}_{T_{ij}}$ represents the probability that any successful individual larva released from node *i* will arrive at node *j*. In this case, where we are only concerned with the local retention of larvae, normalization has the potential to inflate the probability of migration from nodes with few or rare connections within the local connectivity network.

The model output was scaled by species-specific estimates of pelagic larval mortality and productivity (Table 4.3 and 4.4), yet the sensitivity of the model to these factors was unknown. In order to gauge the effects of parameterizing these factors empirically, sensitivity analyses were performed by estimating connectivity in 10,000 discrete scenarios of pelagic larval mortality and depth-specific productivity. Mortality and productivity were investigated simultaneously, and any interactive effects of these factors were noted. In these scenarios, pelagic larval mortality was expressed as a larval half-life which ranged from 1 to 30 days for *M. faveolata* and 1-10 days for *P. astreoides*. Depth-specific productivity varied with depth in 100 unique states (Figure 4.2). These

states were chosen to represent a gradient of 100 potential linear relationships of depth and productivity.

In each scenario mesophotic-shallow connectivity was estimated from M_T using a ratio describing mesophotic-shallow settlement compared to shallow-shallow settlement:

$$Mesophotic\ Contribution\ Ratio = \frac{Mesophotic \rightarrow Shallow\ settlement}{Shallow\ \rightarrow Shallow\ settlement}$$

This ratio indicates how many settlers of deep origin (>30m) to shallow habitat (10m-30m) the model predicts for every shallow-shallow settler, and is a comparison of mesophotic-shallow subsidy versus shallow larval retention to shallow habitat. If this ratio is estimated from the normalized matrix $\breve{M}_{T_{ij}}$, the result is a comparison of the probability of larval migration from mesophotic to shallow habitat versus the probability of shallow larval retention:

$$Probability\ of\ Mesophotic\ Contribution\ Ratio = \frac{Probability\ of\ Mesophotic \rightarrow Shallow\ arrival}{Probability\ of\ Shallow\ \rightarrow Shallow\ arrival}$$

Model output was also analyzed using literature and empirical estimates for both larval half-life (Table 4.3) and productivity (Chapter 2, Table 4.4) in order to estimate vertical connectivity in a meaningful way. Larval productivity is expressed as a function of adult colony density and adult fecundity per area, and each habitat polygon is assigned a productivity based on how these factors change with depth (Chapter 2). In the case of *M. faveolata*, maximum habitat productivity was at 40m, as opposed to *P. astreoides*, for which maximum habitat productivity was at 10m.

The dispersal model makes no initial references to depth-specific fertilization rates or post-settlement survivorship, which are major concerns for estimating levels of

deep-shallow connectivity. Little is known about fertilization in deep corals as compared to shallow corals (Levitan et al. 2004), but there is potential that fertilization in broadcasting species, which generally occurs at the air-sea boundary, could be reduced with depth. There is also evidence that coral larvae produced in deeper habitats may be more sensitive to ultraviolet radiation, and thus may have reduced survivorship or competitive ability in shallower habitats (Gleason and Wellington 1995; Wellington and Fitt 2003; Gleason et al. 2005). In order to test the effects of depth-specific fertilization and post-settlement survivorship on vertical connectivity and mesophotic contribution to shallow settlement, 10,000 discrete scenarios of fertilization and post-settlement survival were investigated. In these scenarios depth-specific fertilization ranged in comparison to a maximum rate. The fertilization rate at 10m was set as the maximum, and depth-specific fertilization was expressed by scaling migrations according to their depth of origin (Figure 4.3a, 4.4, Table 4.5). Fertilization varied with each increasing 10m depth bin by a power law applied to a differential (d_f) that ranged from 0-1. The fertilization at each depth bin (F_{bin}) was calculated based on the number of 10m steps that bin was away from the 10m isobath (*steps*) (Figure 4.3a, 4):

$$F_{bin} = {d_f}^{steps}$$

Similarly, post-settlement survivorship of each migrating larvae (S_{ij}) was modeled using a power law applied to a differential of 0-1 (d_s) to scale each migration according to the vertical distance between source and settlement habitat, again in 10m vertical steps (*steps*) (Figure 4.3b):

$$S_{ij} = {d_s}^{steps_{ij}}$$

Survivorship was only affected when a larva migrated into shallower habitat. Thus, if a larva migrated to a node at the same depth as its source node, post-settlement survivorship was maximum, 1 (d_s^0). If the larva migrated to habitat one depth bin shallower than the depth of its source node (*steps* = 1), post-settlement survivorship was scaled by d_s^1 (migrating two depth bins resulted in scaling by d_s^2, etc.). If a larva migrated into deeper habitat, post-settlement survivorship was modeled as 1 (d_s^0).) (Figure 4.3b, Table 4.5).

In order to estimate the number of generations necessary for local populations to be connected through larval exchange Johnson's algorithm was used to find the shortest path (node-to-node steps) between all pairs of habitat polygons (Johnson 1977). Coral "generations" are difficult to define because coral colonial organisms can be very long-lived, but in this case a coral generation is defined by a larval recruit developing into a reproductive adult. Additionally, the importance, or centrality, of each habitat polygon was estimated by calculating betweenness centrality (Freeman 1977). This measure of centrality also facilitates the identification of multigenerational corridors for larval connectivity (see Chapter 5).

Results

Local retention

The focus of the model results is on local retention. In general a majority of simulated larvae were advected out of the waters surrounding St. Thomas and the western portion of St. John. The fates of those larvae are not directly addressed in the following analyses. Despite this advection, monthly local retention, defined as larvae produced

within the model domain that settles within the model domain (Table 4.1), of *M. faveolata* larvae ranged from 3.72%-26.14% in the passive dispersal scenario, and from 4.25%-18.33 in the active dispersal scenario (Table 4.6, Figure 4.5). These ranges were not found to be significantly different from each other (paired t-test, $p = 0.348$). Monthly local retention of *P. astreoides* larvae was significantly higher in the active dispersal scenario (paired t-test, $p = 0.0001$), and ranged from 19.69%-50.02% and 26.21%-58.35% in the passive and active dispersal scenarios, respectively. Retention of *P. astreoides* larvae was significantly higher than that of *M. faveolata* in both passive and active dispersal scenarios (two-sample t-tests, $p < 0.0001$ in both cases) (Figure 4.6, Table 4.6).

Active changes in larval buoyancy had a consistent and significant positive effect on larval retention for *P. astreoides* (paired two-tail t-test, $p=0.0001$) (Figure 4.5, Table 4.7). The same cannot be said for *M. faveolata*, for which no significant effect of active buoyancy on local retention was found (paired two-tail t-test, $p>0.05$), and active buoyancy often reduced local retention (Figure 4.5, Table 4.7). The mean effect of active buoyancy in *P. astreoides* was an increase of 8.70% (±4.97%) in total larvae retained locally, and this effect was obvious in the first few hours of competence, during which time settlement nearly doubled in the active scenario as opposed to the passive scenario. After this time local retention in both active and passive scenarios was nearly identical (Figure 4.6). In *M. faveolata* the mean effect of active buoyancy was a reduction of 1.42% (±3.07%) in total larvae retained. Between years and scenarios, no significant differences in larval retention were found (pairwise paired t-tests, Table 4.8), and patterns of local retention over time appeared consistent between active and passive scenarios for

both species (see Figure 4.7.1-4.7.2 for overall means and appendix I for monthly sums and means). In the case of *M. faveolata*, peak local retention occurred in September in all scenarios and years, and retention was generally higher in 2007 as opposed to 2008.

The pattern of local retention over time in *P. astreoides* was different in 2007 and 2008. In 2007 peaks in local retention occurred in March and in late summer. In the passive scenario the late summer peak occurred in August, and in the active scenario that peak occurred in July and August. In 2008, in both scenarios, a peak in local retention occurred in May, and local retention was reduced in summer months (Figure 4.5).

Visual representations of vertical M_T and $\breve{M}_T$ can be seen in Figures 4.7.1-4.7.2. The matrices have been transformed in order to show vertical connectivity of larvae between depth bins. In this case M_T was summed by depth bin monthly (overall mean is shown), and $\breve{M}_T$ is averaged by depth bin monthly (overall mean is shown). Monthly vertical M_T and $\breve{M}_T$ can be found in appendix A.

Empirical parameterization and comparisons between scenarios and species

When the raw migration matrix, M_T, and the normalized matrix of probability of arrival, $\breve{M}_T$, are scaled using empirically estimated values of pelagic larval half-life and depth-specific fecundity (Tables 4.3 and 4.4), meaningful comparisons can be made between species and activity scenarios. Mean (±SD) monthly mesophotic contribution for *M. faveolata* was estimated as 0.423 (±0.141) and 0.361 (±0.094) mesophotic immigrants per shallow-shallow settler for passive and active scenarios, respectively. These means were not significantly different (paired t-test, $p = 0.301$). When *P. astreoides* larvae actively changed in size and specific gravity throughout dispersal (Table 4.2) it resulted

in significantly less (0.136 ±0.012) mesophotic contribution to shallow settlement than in the passive dispersal scenario (0.176 ±0.010) (paired t-test, p=0.0017). The monthly probability of mesophotic contribution was also significantly reduced by activity in *P. astreoides* (paired t-test, p=0.0003, Table 4.9).

Monthly *M. faveolata* mesophotic contribution to shallow settlement was significantly greater than that of *P. astreoides* only in the active scenario (independent two sample t-test, p=0.0039, Table 4.10). The comparison in the passive scenario failed a test of homoscedacity, and a Welch two sample t-test found no significant difference. Probability of *M. faveolata* mesophotic contribution was also significantly higher than that of *P. astreoides* in active scenarios (independent two sample t-tests, p=0. 522 in the passive scenario, p=0. 023 in the active scenario, Table 4.10).

Sensitivity analyses

Two sets of sensitivity analyses were performed. The first tested the sensitivity of the model's predictions of vertical connectivity to pelagic larval mortality and depth-specific productivity in order to give the empirical parameterization of these factors meaningful context. The second tested the sensitivity of the empirically parameterized model's predictions of vertical connectivity to unknown variability in depth-specific fertilization rates and post-settlement mortality.

Sensitivity of subsidy to pelagic mortality and productivity

To fully understand the implications of parameterizing the model with literature and observed estimates of pelagic larval mortality and depth-specific production (Tables

4.3 and 4.4), sensitivity analyses of the model's predictions of vertical connectivity (estimates of mesophotic contribution and the probability of mesophotic contribution) to pelagic larval mortality and depth-specific productivity were performed for each species and each dispersal scenario (Figures 4.8.1-4.8.2). For both species in all scenarios, mesophotic to shallow contribution and probability of contribution are robust to population-level changes in larval half-life. Only when mortality is very high, with larval half-lives less than two to three days, are mesophotic to shallow contributions and the probability of contributions affected negatively. Estimates of mesophotic contribution to shallow reefs are sensitive to depth-specific productivity. For both species, mesophotic to shallow contributions are on the order of 0.2-0.3 mesophotic to shallow immigrants for every shallow-shallow settler when productivity is near equal at all depths in both passive and active scenarios. Mesophotic to shallow contributions begin to increase exponentially as mesophotic productivity increases relative to shallow habitat. The most oppositely extreme productivity scenarios result in nearly an order of magnitude difference in mesophotic-shallow subsidy (Figures 4.8.1-4.8.2). Ultimately the sensitivity of mesophotic contributions to shallow settlement appears similar for both species.

Sensitivity of subsidy to depth-specific fertilization and post-settlement survivorship

The model's prediction of mesophotic contribution to shallow settlement is also sensitive to depth-specific rates of fertilization and post-settlement survivorship (Figures 4.9.1-4.9.2). In this case, settlers may actually be referred to as *recruits*, because the effects of post-settlement mortality are incorporated in the analysis. Mesophotic contribution is more sensitive to reduced fertilization at depth than to differential

survivorship in shallow habitat, but the two factors have the potential to interact and reduce mesophotic contribution non-linearly. For example, *M. faveolata* mesophotic contributions of between 1 and 10 immigrants for every 100 shallow-shallow recruits can be maintained when post-settlement survivorship differentials are as low as or lower than 0.1, which translates to post-settlement survivorship of larvae migrating from 40m to 10m being 0.1% that of larvae migrating from 10m to 10m. This is possible so long as fertilization differentials remain above ~0.6, which translates to a maximum of ~88% reduced fertilization at 40m as compared to 10m. A wide range of scenarios of reduced mesophotic *M. faveolata* fertilization and shallow survivorship result in mesophotic contributions greater than 0.01 (Figures 4.9.1-4.9.2), which implies considerable robustness of vertical connectivity in this model. *M. faveolata* vertical connectivity estimates in active and passive scenarios of dispersal demonstrate similar sensitivity to these factors, with mesophotic contributions being slightly lower in the active scenario, which was seen in the previous sensitivity analysis and in the analysis of vertical connectivity performed from empirical parameterization (Table 4.9). The sensitivity of *P. astreoides* mesophotic contribution is similar to that of *M. faveolata*; however mesophotic subsidies – as a proportion of shallow settlement – are generally lower for this species than for *M. faveolata.*

Multigenerational connectivity and habitat centrality

The minimum number of steps, or how many generations, the model predicts would be necessary to connect any two reef habitats (nodes) in the local USVI network of reef habitats was calculated for both species in each activity scenario. This estimate is

termed as "average shortest paths", and can be calculated using an adjacency matrix, which is a binary matrix, and describes network connections as being present or not present (1 or 0). An integer value is calculated for every connection *ij* that describes the minimum number of steps, or generations, that are required for those habitats to be connected through larval dispersal. Alternatively, the calculation of average shortest paths can be solved using edge weights, which define the strength of a connection (i.e. magnitude, probability, etc.). Because Johnson's algorithm (Johnson 1977) assumes that all possible habitat is included in the calculation of average shortest paths, edge weights were extracted from M_T, which has a similar assumption, and not from $\breve{M}_T$. The resulting weighted value for shortest path is essentially a *least-cost* path (or most efficient path), with positive real number values, as opposed to integers that can directly be related to the concept of generations. Comparisons of average shortest path can identify how quickly or extensively habitats in the network can be expected to be connected to one another, and can also be used to show the relative "ease" of connectivity in different directions, such as from mesophotic to shallow or vice versa.

Average shortest paths for the entire network (i.e. direction of mesophotic to shallow or vice versa were ignored) were compared within species (between passive and active scenarios) and also between species. All comparisons were highly significantly different despite overlapping standard deviations, due to very large *n* (n = 268,324, Welch two sample t-tests, $p<0.001$, Table 4.11). The network of *P. astreoides* had a significantly smaller average shortest path than that of *M. faveolata* (Welch two sample t-test, $p<0.001$, Table 4.11), which implies a higher degree of connectivity in the network of *P. astreoides*. Activity also significantly increased the average shortest in all cases

(Welch two sample t-test, $p<0.001$, Table 4.11), suggesting that activity does not increase local connectivity in either species, regardless of very different species-specific larval activity. Despite the statistical differences, all average shortest and least-cost paths were estimated between 1 and 2 for both species, all edge weighting, and all scenarios, which suggests on average all habitats in both species' local USVI habitat networks are connected within two generations.

Comparisons of average shortest paths in different vertical directions were made by averaging shortest paths to and from mesophotic and shallow habitat in order to estimate the degree of vertical connectivity. In this case, because trends in vertical connectivity were similar independent of edge weighting, and because using the adjacency matrix provides a measure that is easy to apply to ecological and evolutionary questions (generations), the adjacency matrix was used without edge weighting. Again, all comparisons were significantly different, both within and between species (n = ~43,000 – ~95,300, depending on comparison). In the case of *M. faveolata*, shallow to shallow connections had the shortest average shortest path, followed by shallow to mesophotic connections, mesophotic to shallow connections, and finally mesophotic to mesophotic connections. Activity reduced the average shortest paths and connectivity of the network compared to passive dispersal in all cases (Figure 4.10).

The network of *P. astreoides* displayed different vertical shortest path dynamics. Mesophotic to mesophotic connections had the smallest average shortest path, followed by shallow to shallow connections, mesophotic to shallow and shallow to mesophotic connections (passive scenario). The active scenario showed different dynamics, with

increasing average shortest paths mesophotic to mesophotic, shallow to shallow, shallow to mesophotic and mesophotic to shallow.

The betweenness centrality of each habitat node was calculated using the adjacency matrix and by using edge weights extracted from M_T (Figures 4.11.1-4.11.2). Because calculation of betweenness centrality assumes that all possible habitat is included in the calculations, $\widetilde{M}_T$ edge weights were not used. Without edge weights, shallow habitat, particularly between 10m and 30m, tend to have higher centralities than mesophotic habitat in the network of *M. faveolata*. In contrast, when migration edge weights are applied to the calculation of betweenness centrality, the relationship of centrality and depth changes. In this case maximum centrality occurs at a node at 40m in the passive scenario, and 30m in the active scenario. Habitat at 50m has very low estimates of centrality when edge weights are used.

Betweenness centrality does not vary as much with depth in the network of *P. astreoides* when edge weights are not used. In contrast, when edge weights are used shallow habitat (10m) has the highest centrality estimates. These estimates illustrate considerable differences in the local multigenerational connectivity of *M. faveolata* and *P. astreoides*.

Discussion

The goal of this study was to use biophysical dispersal modeling to gauge the potential of mesophotic reefs in the USVI to contribute coral larvae to local shallow settlement and recruitment in the context of the DRRH. It is necessary to perform this analysis using ratios of mesophotic and shallow settlement, and probabilities of arrival,

because the number of particles in the system is not realistic, and ignores the input of non-modeled habitat. The model predicts demographically significant mesophotic contributions to shallow settlement for both a spawning coral and a brooding coral, even under extreme scenarios of mesophotic larval post-settlement mortality and reduced fertilization (Figures 4.9.1-4.9.2). Empirical evidence of high mesophotic productivity bolsters these model predictions for *M. faveolata*. However, *P. astreoides* is not predicted to be more productive in mesophotic habitat than in shallow habitat, and yet the model predicts considerable mesophotic contribution for this species as well.

Although the ultimate fates of advected larvae and the input of larvae from upstream reefs are not directly addressed in the current model, it is important to recognize that vertical migration may occur on spatial scales larger than the one addressed here. A particularly interesting point is that mesophotic habitat tends to be peripheral to shallow habitat (Locker et al. 2010), which could suggest that larvae move over this habitat before reaching shallow reefs. It is then possible that recruitment to MCE from upstream sources is an important aspect of coral recruitment dynamics and population connectivity. The fates of advected mesophotic larvae have important implications for conservation and management; USVI MCE may not only be important for local population resilience, but also may be important larval source populations for downstream coral habitats, both shallow and mesophotic.

The effect of active buoyancy

Activity reduced local connectivity for both species, as can be seen in an increase in average shortest paths (Table 4.11, Figure 4.11) and a decrease in mesophotic

contribution to shallow settlement (Table 4.9). However, the mechanism through which this took place was different for each species. Active buoyancy caused a greater proportion of *M. faveolata* larvae to be advected from the system than in the passive scenario, and the opposite was true for *P. astreoides* (Tables 4.6, 4.7 and Figures 4.5, 4.6). Thus, activity in *P. astreoides* promotes settlement at or near natal habitat, reducing connectivity, whereas activity in *M. faveolata* promotes advection and also reduces local connectivity (but may increase connectivity on larger scales not addressed in this model).

The observed effect of *M. faveolata* active buoyancy may represent a discrepancy between laboratory observations of larval behavior and growth and the behaviors and developmental changes that occur *in situ*. It is possible that it is adaptively advantageous for larval activity to increase settlement close to natal reefs, which is the opposite of what was observed here for this species. This highlights the need for study of coral larval behavior in the field, which is particularly difficult. However *in situ* observation chambers have the potential to offer invaluable insight to predictions of patterns in coral settlement (Paris et al. 2008). An alternate explanation is that the negative effect of active *M. faveolata* larval buoyancy on local retention reflects the true ecology of this species in this geographic location, and that in reality the larval traits of this species encourage larval export and emigration to habitats not included in the model. Further study focusing on larval ecology and behavior of this species is necessary to make this distinction.

P. astreoides larvae are capable of settling rapidly post-planulation (McGuire 1997; Edmunds et al. 2001). Negative buoyancy that simulated bottom-seeking behavior began one hour post-planulation, and increased modeled local retention (Figure 4.5 and 4.6). The effect of activity in *P. astreoides* on larval retention occurred within the first 12

hours, and predominantly in the first few hours, of competence, during which time settlement was nearly doubled. After this time local retention in both active and passive scenarios is nearly identical (Figure 4.6), suggesting that early bottom-seeking behavior has the potential to dramatically increase settlement success in this species. Mesophotic contribution to shallow settlement, and the probability of mesophotic contribution, which is a ratio of average mesophotic-shallow probability of arrival versus shallow-shallow probability of arrival, both decreased with activity. Activity restricted dispersal and reduced the number of vertical connections between habitat nodes, decreasing the probability of mesophotic-shallow arrival relative to the probability of shallow-shallow arrival. Thus, in *P. astreoides*, activity increased local retention but decreased mesophotic subsidy to shallow habitat.

Inter- and intra-annual variability

Hydrographic conditions can vary considerably from one year to another, particularly in the late summer in the Caribbean, which is in the midst of hurricane season. In 2007 four separate tropical systems passed over or near the USVI during late summer, and in 2008 there were two, including Hurricane Omar which became a major hurricane in October. For this reason it is ideal to simulate larval dispersal over many years of hydrography in order to capture inter-annual variability in prevailing current velocities. Two years of high resolution hydrographic data were available for use in this study, and inter-annual variability in patterns of settlement was observed in both species. *M. faveolata* retention in the passive dispersal scenario was more than twice as high in

2007 than in 2008 in each month (Figure 4.5). During late summer in 2007 simulated larvae appeared to become entrained in a persistent sub-mesoscale eddy that returned larvae that may otherwise have been advected away from the USVI to USVI reef habitat. The remarkably high *M. faveolata* larval retention in September of 2007 (Figure 4.5) highlights both that recruitment events for this species may be stochastic (Miller et al. 2000; Edmunds and Elahi 2007) and that modeling dispersal using many years of hydrography may be necessary to predict realistic demographic estimates of local larval retention. However, the pattern of retention appears similar for *M. faveolata* between years, with peak retention occurring following September spawning. Reproductive histology and field observations in 2011 and 2012 suggest that a large portion of the USVI *M. faveolata* population spawned in September in both of those years, which may be an adaptive response to consistently enhanced local retention of larvae in this month (see Chapter 2 for more information on the reproductive ecology of both species).

In *P. astreoides* the pattern of intra-annual larval retention is nearly opposite, or out of phase, in 2007 and 2008 (Figure 4.5). In 2007 there is a three month dip in retention between April and June, and in 2008 there is a three month dip in retention between June and August. This again highlights the need to model dispersal using many years of hydrography, however total retention between 2007 and 2008 appears to be similar.

The model predicts that considerable magnitudes of larvae migrate between mesophotic and shallow habitat in the USVI. In fact, *M. faveolata* larval migration from 40m to 10m surpassed retention at 10m in September in both years (APPENDIX 1.1). The normalized probability of larval arrival at 10m from 40m was also higher than the

probability of arrival from 10m in some months, which suggests that the arrival of locally produced mesophotic larvae at shallow USVI reefs is likely not a rare occurrence. For *P. astreoides*, early larval competence and high productivity in shallow habitat increased larval retention at 10m (Figure 4.7.2).

Mesophotic contribution to shallow settlement

Mesophotic contributions were higher for *M. faveolata* than for *P. astreoides*, despite the fact that most *M. faveolata* larvae are advected from the system. Early competency in *P. astreoides* increased the proportion of shallow to shallow settlement, effectively reducing the contribution of mesophotic productivity to shallow settlement. On average, ¼ to nearly ⅓ of all locally produced *M. faveolata* larvae arriving at shallow habitat were of mesophotic origin (depending on activity scenario). This estimate was on the order of $^1/_{10}$ to $^1/_7$ for *P. astreoides*. This suggests that mesophotic larval supply to shallow USVI reefs is not negligible, and may be an important source of larval subsidy. It is also worth noting that mesophotic larval retention was consistently as high or higher than shallow larval retention for both species, suggesting that settlement in USVI mesophotic reef habitat may substantially consist of locally produced mesophotic larvae.

Pelagic larval mortality and depth-specific productivity

Using species- and depth- specific parameters should increase the efficacy of the model in describing vertical connectivity; however the sensitivity of the model to pelagic larval half-life and depth-specific productivity was unknown. The majority of larval settlement occurred within hours or several days of competence, and thus vertical

connectivity was affected very little by changes in pelagic larval mortality. Only when larval half-life was very short, on the order of hours to several days, was an effect noticeable. Estimates of vertical connectivity were highly sensitive to scenarios of depth-specific productivity, suggesting that precision in estimates of habitat extent, adult density and adult fecundity are essential to the development realistic models of dispersal (Hughes and Tanner 2000; Botsford et al. 2009). The use of empirical productivity estimates (Chapter 2) thus is not only warranted, but crucial to the accurate description of vertical connectivity in the USVI, and likely elsewhere.

Depth-specific post-settlement survivorship and fertilization

The potential for increased post-settlement mortality on larvae of deeper origin is arguably one of the greatest caveats to the DRRH, as it implies that mesophotic larvae might have difficulty replacing shallow corals, and that many coral populations may be speciating by depth. Deep corals likely produce lower concentrations of mycosporine-like amino acids (MMAs), which protect coral tissues from ultraviolet radiation, and this can result in lower concentrations of these proteins in eggs and larvae produced by deeper living colonies (Gleason and Wellington 1995; Wellington and Fitt 2003). This may imply that mesophotic corals have reduced reproductive success, particularly when mesophotic larvae enter shallow waters. Indeed, Bongaerts et al. (2010) suggest genetic divergence of *Seriatopora hystrix*, a brooding coral, by depth in eastern Australia; however Van Oppen et al. (2011) confounded these results by demonstrating genetic connectivity over depth in the same species, but on reefs in western Australia. Without further study, it's difficult to determine to what degree the genetic structure found on

eastern Australian reefs is due to local hydrologic forcing, post-settlement survivorship, or larval behavior. In the current study it has been shown that vertical larval connectivity is possible based on local hydrology, active and passive larval behavior, and a wide range of different productivity scenarios, however the effect of differential post-settlement larval survivorship has the potential to severely limit vertical connectivity.

Similarly, the reproductive success of corals may be limited by fertilization (Lasker et al. 1996). Distance and sperm-dilution can reduce fertilization in benthic invertebrates (Oliver and Babcock 1992; Babcock et al. 1994; Coma and Lasker 1997), and thus deeper living broadcast spawning corals may be limited by gamete dilution if those gametes must be near the sea surface to fertilize. Brooding species would likely not be affected unless adult density is reduced by depth.

To date, empirical estimates of any depth-related differences in post-settlement survivorship for *M. faveolata* or *P. astreoides* are unavailable beyond observations that mid-depth larvae experience higher mortality when exposed to UV radiation (Gleason and Wellington 1995; Wellington and Fitt 2003), and empirical comparisons of fertilization rates at different depths are particularly difficult to perform in the field. The sensitivity analysis performed in the current study provides ranges of differential post-settlement survivorship and fertilization rates that would still allow for demographically significant subsidy from mesophotic habitats to shallow habitats.

In this case, settlers are referred to as recruits because the effects of post-settlement mortality were considered. For both species, mesophotic contribution to shallow recruitment is more sensitive to fertilization than to post-settlement survivorship. This is because larvae that migrate from 40m to 30m or 20m will have lower post-

settlement mortality than larvae moving from 40m to 10m, and the fact that a range of depths are considered "shallow habitat" buffers the effect of differential post-settlement survivorship. Both species demonstrate mesophotic contributions of above 0.01, or 1 mesophotic recruit for every 100 retained shallow recruits, in a wide range of scenarios of greatly reduced mesophotic fertilization and shallow post-settlement survivorship of mesophotic larvae. Indeed, there is potential that local mesophotic contribution in the USVI is considerably robust. In the case of *P. astreoides*, the assumption that fertilization may be reduced with increasing depth may not be accurate, because sperm are neutrally buoyant and fertilization occurs within the coral tissues, not at the sea surface. Therefore, differential fertilization can be ignored for this species, and mesophotic subsidy remains quite high for a large range of differential post-settlement survivorship scenarios. For both species, it is difficult to identify "most likely" scenarios in this sensitivity analysis, however extreme scenarios where fertilization rates or post-settlement survivorship at 40 m are 0.000001-0.01% (differentials of 0.01 and 0.1, respectively) of rates at 10 m are likely unrealistic. Thus, subsidies of 1-10 mesophotic recruits for every 100 retained shallow-shallow recruits for both species is likely a conservative realistic estimate. However, further study of the effects of depth on the fertilization of broadcast spawning corals and the post-settlement survivorship of mesophotic larvae is certainly necessary in order to fully understand vertical connectivity in this system.

Colony isolation due to habitat fragmentation and the effect of isolation on fertilization rates has not been directly addressed in this analysis. Habitat degradation in shallow environments may depress fertilization by isolating conspecifics, which can limit fertilization due to dilution of gametes and reducing the probability that conspecific

gametes will encounter one-another (Oliver and Babcock 1992; Babcock et al. 1994; Levitan 2000; Levitan et al. 2004). This adds credit to the reasoning that understanding habitat quality is integral to understanding population connectivity (Moilanen 1998; Hanski and Ovaskainen 2000; Urban and Keitt 2001; Kininmonth et al. 2010).

Multigenerational connectivity

It is important to recognize that the DRRH does not require mesophotic and shallow habitats to be connected directly through larval exchange, but rather that mesophotic reefs contribute to the demography of coral reefs in general, and shallow reefs in particular. It is possible that multigenerational larval pathways connect mesophotic and shallow reefs even where direct larval pathways between the two habitats are missing or rare. Within a network, investigation of multigenerational connectivity through shortest path analysis and by estimating node and edge betweenness can also identify particularly well-connected or poorly-connected habitats. Doing so has the potential to inform management decisions when delineating management areas.

Shortest paths analysis can be indicative of the degree to which nodes are connected, and the predominant direction they are connected in. For instance, average shortest paths analysis of the USVI *M. faveolata* network suggests that migrating from any shallow habitat to any other shallow habitat requires, on average, the fewest steps (Figure 4.10), and thus these nodes are expected to be better connected to one-another. Connecting all mesophotic habitat requires the most steps, and connecting shallow and mesophotic habitats has less cost when it occurs in the shallow to deep direction. Despite the fact that *M. faveolata* mesophotic contribution to shallow settlement is higher than

that of *P. astreoides* (Table 4.10, active scenarios), the network of *P. astreoides* is significantly smaller than that of *M. faveolata*, as estimated by average shortest paths (Table 4.12, Figure 4.10), suggesting fewer habitats are isolated from larval exchange, and potentially a higher degree of genetic connectivity. Essentially, despite lower direct mesophotic subsidy to shallow settlement, mesophotic and shallow *P. astreoides* populations may be more connected than *M. faveolata* populations in the USVI.

Betweenness centrality can identify multigenerational corridors and habitats essential to the structure of the network. Betweenness centrality calculated using edge weights is likely more informative than when edge weights are not used, as the magnitude of connections are taken into account, and habitats that exchange more larvae will be more central. Very little habitat deeper than 40m appears to be central to the local connectivity network of *M. faveolata*. However, it is important to recognize that the analysis excludes habitat that may, in reality, be providing important larval subsidy. That being said, some habitat plays more important roles in the local network than others, and for *M. faveolata* habitat nodes with high betweenness centrality occur in the 30m and 40m depth bins. This suggests that these deeper habitats may behave as corridors of connectivity across the network, and this may be due to increased productivity at these depths. In the network of *P. astreoides*, shallow habitat, particularly habitat above 10m, appears to be much more central than deeper habitat. This is likely due to high productivity and a high degree of larval exchange among nodes at 10m. This may suggest that these two species have unique local management requirements, and it implies that local habitat fragmentation may affect populations of these species very differently.

Conclusions

Bongaerts et al. (2010a) directly identifies knowledge gaps that limit the applications of DRRH. One of those knowledge gaps, the reproductive capabilities of mesophotic corals, was addressed directly in Chapter 2, and the results were applied to this study which directly addresses another, the connectivity of mesophotic and shallow populations. The migration of larvae from mesophotic habitat into shallow habitat was a consistent feature of the connectivity networks of both species. As was hypothesized, higher larval productivity in mesophotic habitats increased mesophotic larval subsidy to shallow reef areas, suggesting that as shallow coral reefs become depopulated mesophotic subsidy likely becomes more significant.

The analyses performed in this study of mesophotic-shallow subsidy sensitivity to factors such as pelagic larval mortality, depth-specific productivity, depth-specific fertilization rates and post-settlement survivorship offer a robust evaluation of the potential for vertical connectivity in the USVI. The results also provide future research addressing these factors with benchmarks for application. The degree of mesophotic-shallow connectivity in different geographic locations, and at different spatial scales than the one studied here, is dependent on local hydrologic forcing and species-specific adult and larval traits; and thus, the degree to which the DRRH will apply to the management of coral reefs will not be constant in space and time. Studies such as this one provide important insight into the potential of realized connectivity between habitats with different or changing characteristics. As climate change and coastal development continues to fragment habitat the competitive dynamics for settling coral larvae may be difficult to predict, and studies of genetic population connectivity may not be indicative

of future settlement on coral reefs. Although projections of coral reef futures may be uncertain, the DRRH provides some hope that with intelligent management and protection, coral populations may have some potential to safeguard themselves in a challenging environment.

Table 4.1. Definitions of terms used, including terms relating to larval ecology and terms related to graph theoretical analysis of connectivity networks.

Glossary of terms	
Migration	The movement of a larva from one habitat, or node, to another
Recruit	A larva that has settled and survived any post-settlement mortality
Recruitment	The act of a larva recruiting, or generally refers to the accumulation of recruits, or the degree or magnitude of that accumulation
Settler	A larva that has encountered settlement habitat and completed its pelagic larval phase
Settlement	The act of a larva settling, or may refer to the number or magnitude of settlers in a specific habitat
Larval subsidy	The supply of settlers from exogenous sources. In this case, mesophotic larval subsidy to shallow reefs is the supply of settlers from mesophotic reefs to shallow areas
Local retention	The percent or proportion of larvae produced within the model domain that also settle within the model domain
Mesophotic contribution ratio	A ratio describing the settlement in shallow areas that is due to mesophotic larval input (subsidy) as compared to shallow larval retention
Probability of mesophotic contribution ratio	A ratio describing the probability of mesophotic larval arrival in shallow areas as compared to the probability of shallow larval retention
Network/connectivity network	An arrangement of habitats that are intersected by larval exchange
Node	A point or vertex that describes the location of reef habitat. A node is assigned a depth between 0 m and 50 m
Edge	A connection between two habitats that represents larval exchange in a specific direction
Shortest path	The minimum number of steps through connected habitats, or generations, required to connect two habitats
Average shortest path	The mean minimum number of steps, or generations, required to connect every node in a network to every other node
Betweenness centrality	A measure of the importance of a habitat or node to the integrity of a network. Highly central habitats are likely to behave has corridors for multigenerational connectivity

Table 4.2. Species-specific changes in larval size and specific gravity used to describe larval movement in active dispersal scenarios.

M. faveolata			
Time (s)	Specific gravity	Size (cm)	Source
7200	1021	0.0014	Chapter 2 observations
208800	1021	0.003	Szmant and Meadows (2006), Vermeij et al (2006)
288800	1022.5	0.00025	Szmant and Meadows (2006), Vermeij et al (2006)
525600	1024	0.00025	Vermeij et al (2006)
end	1025	0.0002	

P. astreoides			
Time	Specific gravity	Size	Source
3600	1016	0.001	Chapter 2 observations
86400	1024	0.001	Gleason et al. (2009)
end	1025	0.001	

Table 4.3. Species-specific larval traits.

	Days (seconds)			
	Time to competency	Max PLD	Half-life	Source
M. faveolata	6 (518400)	30 (2592000)	8.3 (720000)	Vermeij et al. (2006)
P. astreoides	1 (86400)	10 (864000)	6.5 (561600)	Edmunds et al. (2001)

Table 4.4. Depth-specific habitat productivity based on empirical reproductive study of *M. faveolata* and *P. astreoides*. Productivity is a product of adult coral cover and fecundity per area. Values are scaled to the maximum value.

Depth	*M. faveolata*	*P. astreoides*
10	0.307692	1
20	0.384615	0.306383
30	0.923077	0.53617
40	1	0.378723
50	0.076923	-

Table 4.5. Modeled effects of depth on fertilization and vertical migration on post-settlement survivorship. Effects were calculated according to a power law applied to differentials that ranged from 0-1. See Figures 4.3 and 4.4 for more information.

	Fertilization (d_f) Proportional to fertilization rate at 10m					Post-settlement survivorship (d_s) Proportional to 10m-10m surivorship			
	Depth					Vertical distance traveled towards surface			
Differential	10m	20m	30m	40m	50m	10m	20m	30m	40m
d	d_f^0	d_f^1	d_f^2	d_f^3	d_f^4	d_s^1	d_s^2	d_s^3	d_s^4
1	1	1	1	1	1	1	1	1	1
0.9	1	0.9	0.81	0.729	0.6561	0.9	0.81	0.729	0.6561
0.8	1	0.8	0.64	0.512	0.4096	0.8	0.64	0.512	0.4096
0.7	1	0.7	0.49	0.343	0.2401	0.7	0.49	0.343	0.2401
0.6	1	0.6	0.36	0.216	0.1296	0.6	0.36	0.216	0.1296
0.5	1	0.5	0.25	0.125	0.0625	0.5	0.25	0.125	0.0625
0.4	1	0.4	0.16	0.064	0.0256	0.4	0.16	0.064	0.0256
0.3	1	0.3	0.09	0.027	0.0081	0.3	0.09	0.027	0.0081
0.2	1	0.2	0.04	0.008	0.0016	0.2	0.04	0.008	0.0016
0.1	1	0.1	0.01	0.001	0.0001	0.1	0.01	0.001	0.0001
0	1	0	0	0	0	0	0	0	0

Table 4.6. Local retention and the effect of scenario for each month and year for *M. faveolata* and *P. astreoides*. Local retention was consistently higher for the brooding coral *P. astreoides*, and the effect of active buoyancy on local retention was consistently positive for this species.

	Passive retention	Active retention	Effect of activity
M. faveolata			
2007			
Aug	11.19%	8.61%	-2.58%
Sep	26.14%	18.34%	-7.80%
Oct	10.64%	11.01%	+0.37%
2008			
Aug	5.01%	5.97%	+0.96%
Sep	10.68%	10.66%	-0.02%
Oct	3.72%	4.25%	+0.54%
Mean	11.23%	9.81%	-1.42%
(SD)	(7.28%)	(4.51%)	(3.07%)
P. astreoides			
2007			
Mar	44.81%	52.26%	+7.46%
Apr	26.57%	43.46%	+16.89%
May	38.71%	40.25%	+1.54%
Jun	33.04%	41.89%	+8.84%
Jul	38.00%	58.35%	+20.34%
Aug	50.02%	56.87%	+6.85%
2008			
Mar	38.69%	42.15%	+3.45%
Apr	45.05%	53.57%	+8.53%
May	49.53%	58.94%	+9.41%
Jun	31.13%	37.84%	+6.71%
Jul	19.69%	26.21%	+6.52%
Aug	23.88%	31.69%	+7.81%
Mean	36.59%	45.29%	+8.70%
(SD)	(9.52%)	(10.26%)	(4.97%)

Table 4.7. Paired t-tests on local retention between dispersal scenarios and within species, and independent two sample t-tests on local retention within dispersal scenarios, but between species. There was no detectable effect of scenario on local retention for *M. faveolata*, whereas there was a significant effect for *P. astreoides*. *P. astreoides* had significantly higher local retention.

	Mean	SD	*df*	*t*	*P* (two-tailed)
M. faveolata					
Passive	11.23%	7.98%	5	-1.0345	0.3483
Active	9.81%	4.94%			
P. astreoides					
Passive	36.59%	9.94%	5	5.8035	0.0001**
Active	45.29%	10.71%			
Passive					
M. faveolata	11.23%	7.98%	16	2.1199	<0.0001***
P. astreoides	36.59%	9.94%			
Active					
M. faveolata	9.81%	4.94%	16	2.1199	<0.0001***
P. astreoides	45.29%	10.71%			

Table 4.8. Results of pairwise two-tailed paired t-tests on local retention between dispersal scenarios and years. *P* represents the passive particle scenario, and *A* represents the active particle scenario. Although there is a significant difference for *M. faveolata* between the 2008 passive scenario and the 2007 active scenario, this is likely not important to the interpretation of the results. Local retention in active scenarios was significantly different from passive scenarios within years for *P. astreoides*. "A" denotes active scenarios and "P" denotes passive scenarios.

M. faveolata				
	2007 P	2008 P	2007 A	2008 A
2007 P	-	-	-	-
2008 P	0.0853	-	-	-
2007 A	0.2969	0.0412 *	-	-
2008 A	0.1083	0.2239	0.0667	-
P. astreoides				
	2007 P	2008 P	2007 A	2008 A
2007 P	-	-	-	-
2008 P	0.5997	-	-	-
2007 A	0.0151 *	0.1236	-	-
2008 A	0.6771	0.0004 **	0.4162	-

Table 4.9. The results of paired t-tests on mesophotic contribution (from M_T) and the probability of mesophotic contribution (from $\breve{M}_T$), with the comparison being between active and passive scenarios. No significant difference was found between active and passive scenarios in *M. faveolata*, whereas passive scenarios resulted in significantly higher mesophotic contribution and probability of contribution to shallow settlement. Means and (SD) are shown. P denotes passive scenarios, A denotes active scenarios.

Species	Passive	Active	*df*	*t*	*P*	*Contrast*
M. faveolata						
M_T	0.423 (0.141)	0.361 (0.094)	5	1.1520	0.3014	NA
$\breve{M}_T$	0.591 (0.033)	0.562 (0.052)	5	2.5706	0.0832	NA
P. astreoides						
M_T	0.176 (0.010)	0.136 (0.012)	11	4.3924	0.0017*	P > A
$\breve{M}_T$	0.570 (0.069)	0.450 (0.096)	11	2.2010	0.0002**	P > A

Table 4.10. The results of independent two sample t-tests of mean monthly mesophotic contribution (from M_T) and the probability of mesophotic contribution (from $\widetilde{M}_T$) in different scenarios between species. All comparisons are independent two sample t-tests, with the exception of the passive (M_T) comparison which failed a test of homogeneity of variance. This comparison is a Welch two sample t-test.

M. faveolata v. *P. astreoides*	df	t	*P*	Contrast
M_T				
Passive	16	1.772	0.136	NA
Active	16	3.374	0.0039**	*M. faveolata* > *P. astreoides*
$\widetilde{M}_T$				
Passive	16	-.655	0.5218	NA
Active	16	-2.5257	0.0225*	*M. faveolata* > *P. astreoides*

Table 4.11. Average shortest path comparisons (Welch two sample t-tests) between active and passive scenarios for each species. Comparisons are shown using an adjacency matrix (presence/absence of connections) and the raw migration matrix M_T as edge weights, Activity increased the size of the network in all cases.

	Passive	Active	*P*
M. faveolata			
Adjacency	1.620 (0.001)	1.681 (0.001)	<0.0001***
M_T	1.595 (0.001)	1.658 (0.001)	<0.0001***
P. astreoides			
Adjacency	1.268 (0.020)	1.402 (0.022)	<0.0001***
M_T	1.251 (0.019)	1.383 (0.021)	<0.0001***

Table 4.12. Vertical average shortest path comparisons (Welch two sample t-tests) between species for passive (A) and active (B) dispersal scenarios. All comparisons were highly significant, with average shortest paths being smaller in the network of *P. astreoides* in all comparisons. *M* denotes mesophotic and *S* denotes shallow (i.e. *M-S* represents the average shortest paths from mesophotic to shallow habitat). See Figure 4.10.

A.

		M. faveolata			
	Direction	M-S	S-M	S-S	D-D
P. astreoides	M-S	<0.0001***	-	-	-
	S-M	-	<0.0001***	-	-
	S-S	-	-	<0.0001***	-
	D-D	-	-	-	<0.0001***

B.

		M. faveolata			
	Direction	M-S	S-M	S-S	D-D
P. astreoides	M-S	<0.0001***	-	-	-
	S-M	-	<0.0001***	-	-
	S-S	-	-	<0.0001***	-
	D-D	-	-	-	<0.0001***

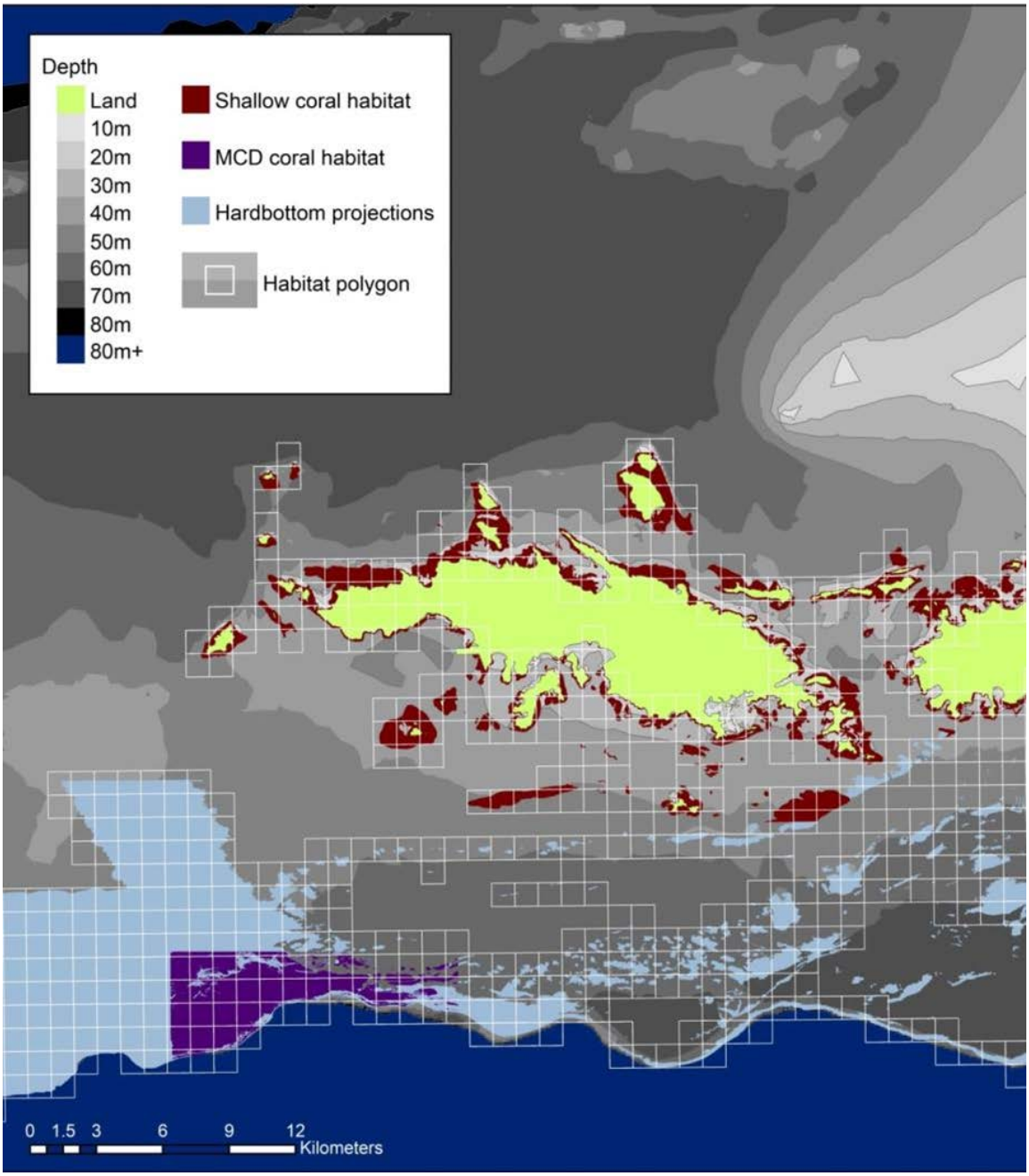

Figure 4.1. Spatial extent of the USVI ROMS model. The model is centered over the island of St. Thomas. Extensive mesophotic coral habitat exists on the deep insular shelf south of St. Thomas. Shallow benthic habitats (red) and habitats in the Marine Conservation District, shown in purple, are well classified, whereas hardbottom projections, shown in light blue, are un-verified predictions of coral habitat extent. White squares represent 1km^2 habitat polygons used in dispersal modeling. A total of 518 polygons were used when modeling the dispersal of *M. faveolata*, and 377 were used when modeling the dispersal of *P. astreoides*.

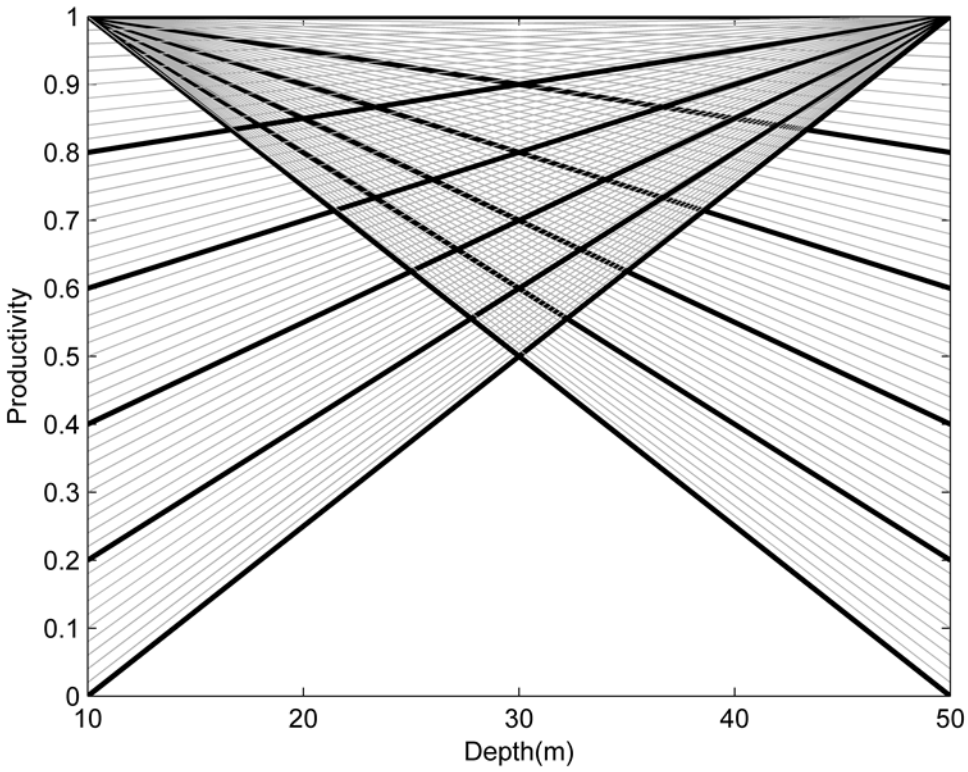

Figure 4.2. Productivity scenarios were chosen to represent a gradient of 100 potential linear relationships of depth and productivity. These scenarios were used to test the sensitivity of mesophotic contribution to shallow settlement.

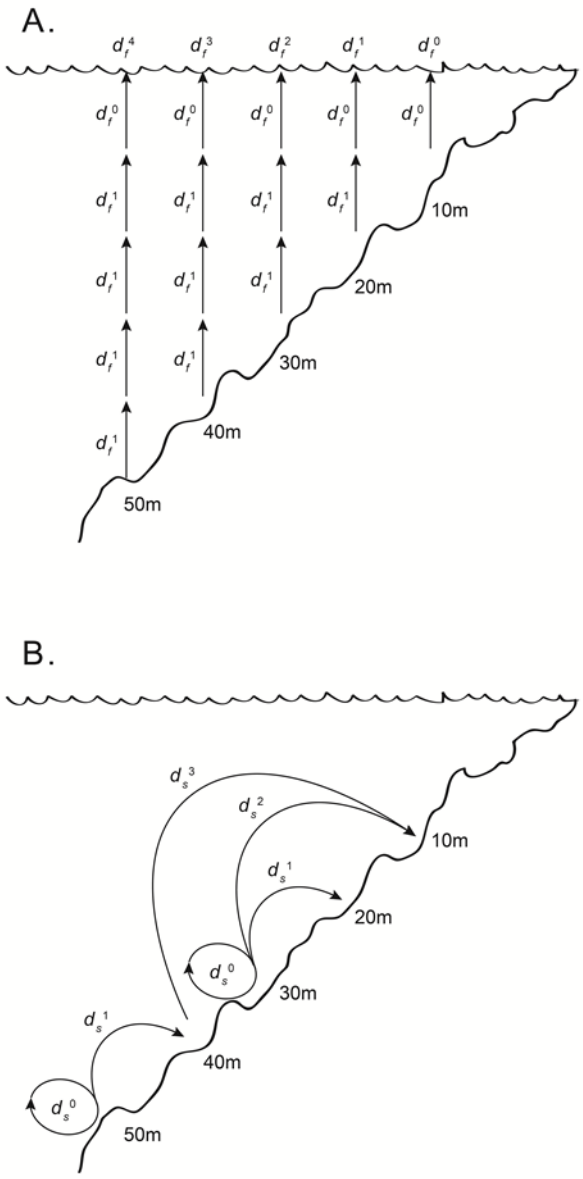

Figure 4.3. (A) Rationale of the design of 100 unique fertilization scenarios based on depth for sensitivity analysis of mesophotic contributions to shallow recruitment. Every 10m gametes must travel to reach the sea surface decreases fertilization by a factor of d_f^1, and d_f^1 ranges from 0-1. See Figure 4.3 and Table 4.3 for more information. (B) An illustration of the rationale behind the design of 100 unique post-settlement survivorship scenarios based on the vertical distance between production and settlement habitat. Every 10m a larva migrates upward (shallower) post-settlement survivorship is scaled by a factor of d_s^1, which ranges from 0-1. Survivorship of larvae migrating into deeper habitat is not affected.

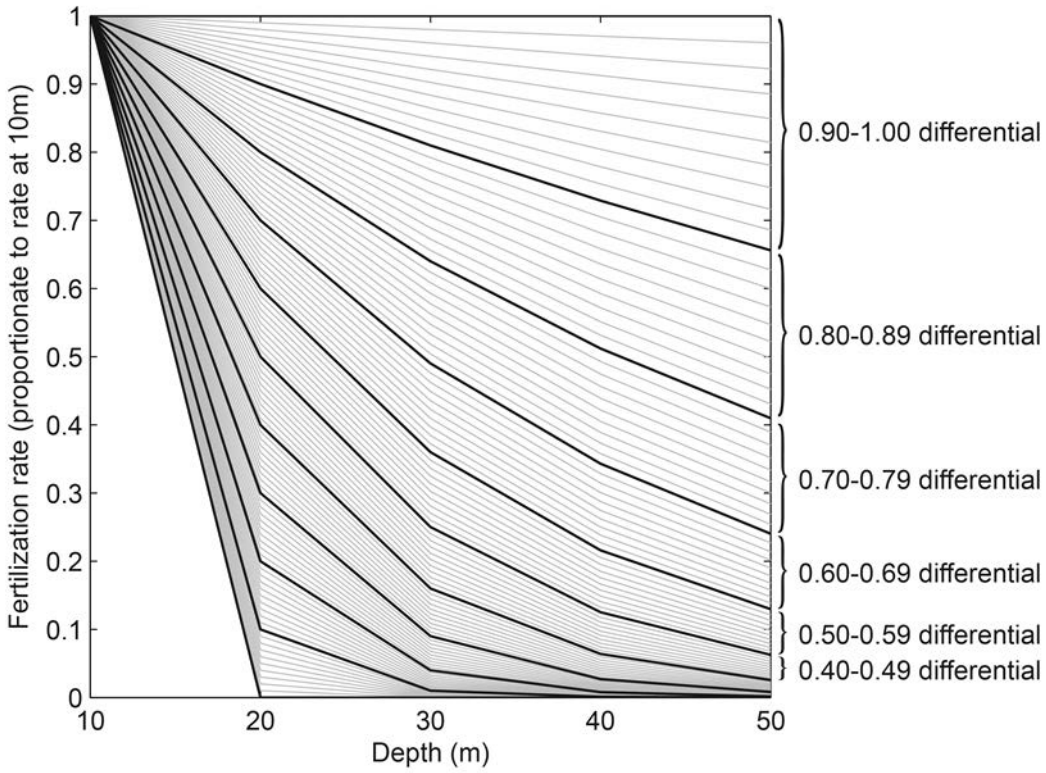

Figure 4.4. Fertilization scenarios used in sensitivity analysis of mesophotic contributions to shallow recruitment. Fertilization is scaled at each increasing depth bin according to a power law applied to a differential d_f which ranges from 0-1. See Figure 4.2a and Table 4.3 for more information.

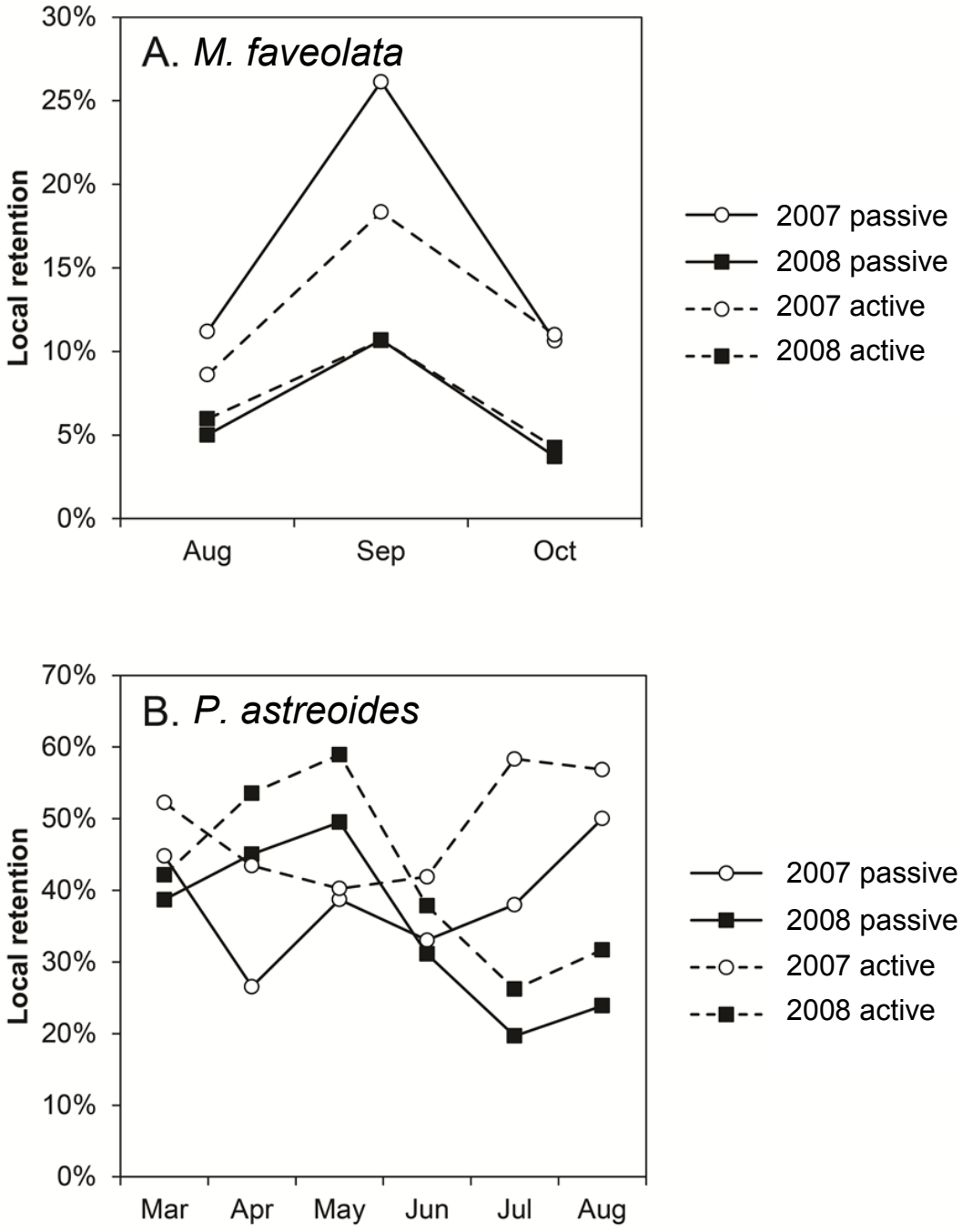

Figure 4.5. Local retention of larvae of (A.) *M. faveolata* and (B.) *P. astreoides* in all modeled months in 2007 and 2008. Retention was generally higher for *P. astreoides*, and activity increased retention in *P. astreoides*. *M. faveolata* retention was highest in September in both years. "P" indicates passive dispersal and "A" indicates active buoyancy scenarios.

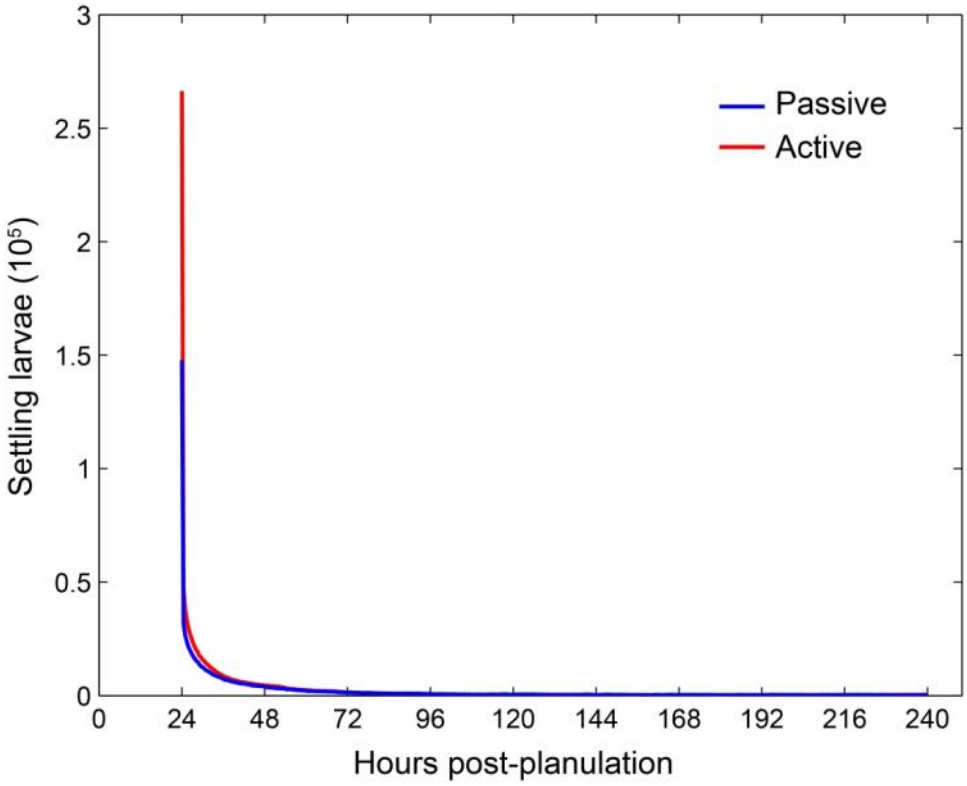

Figure 4.6. Settlement of *P. astreoides* and hours post-planulation. In both active and passive scenarios settlement occurs predominantly within the first 48 hours after competency is reach (24 hours). Activity nearly doubles settlement just as competency is reached because larvae are nearer to the benthos (settlement habitat) due to negative buoyancy which mimics bottom-searching behavior.

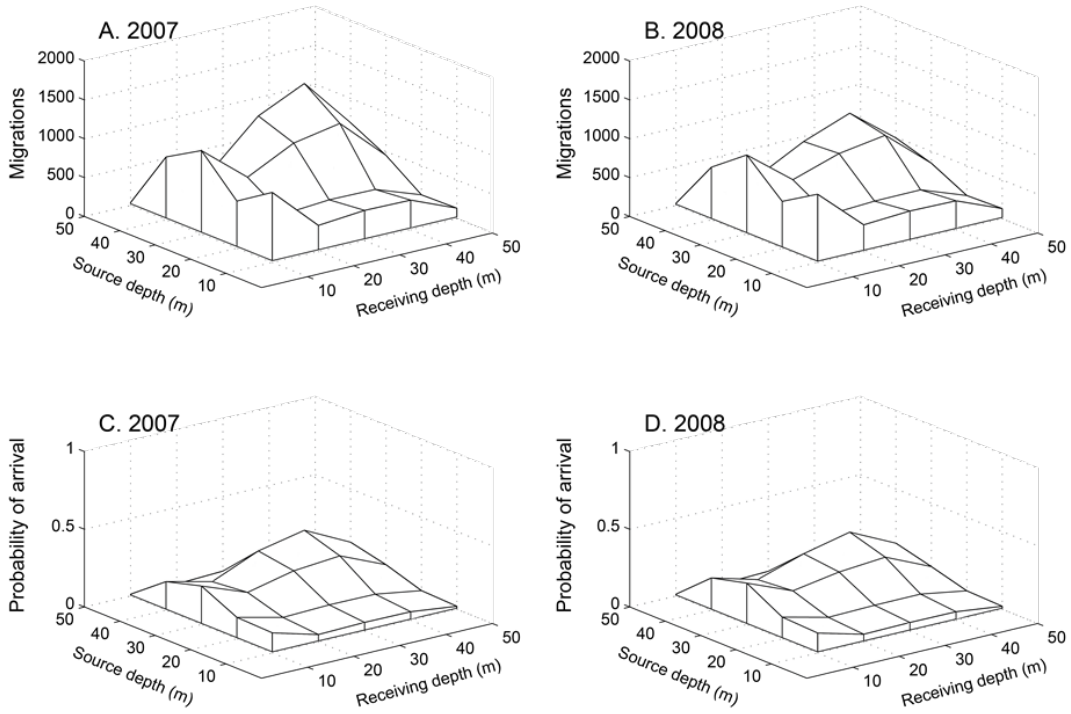

Figure 4.7.1. *M. faveolata* vertical M_T (A = 2007, B = 2008) and $\breve{M}_T$ (C = 2007, D = 2008). A and B show mean monthly migrations from any depth bin to any other. The patterns between years are consistent, with many larvae migrating from mesophotic to mesophotic habitat (40m-40m). There also appears to be a large number of larvae migrating from 30m and 40m to 10m C and D show mean probabilities of arrival at any depth bin from any other. Mean probabilities of arrival are highest from 40m to all depths.

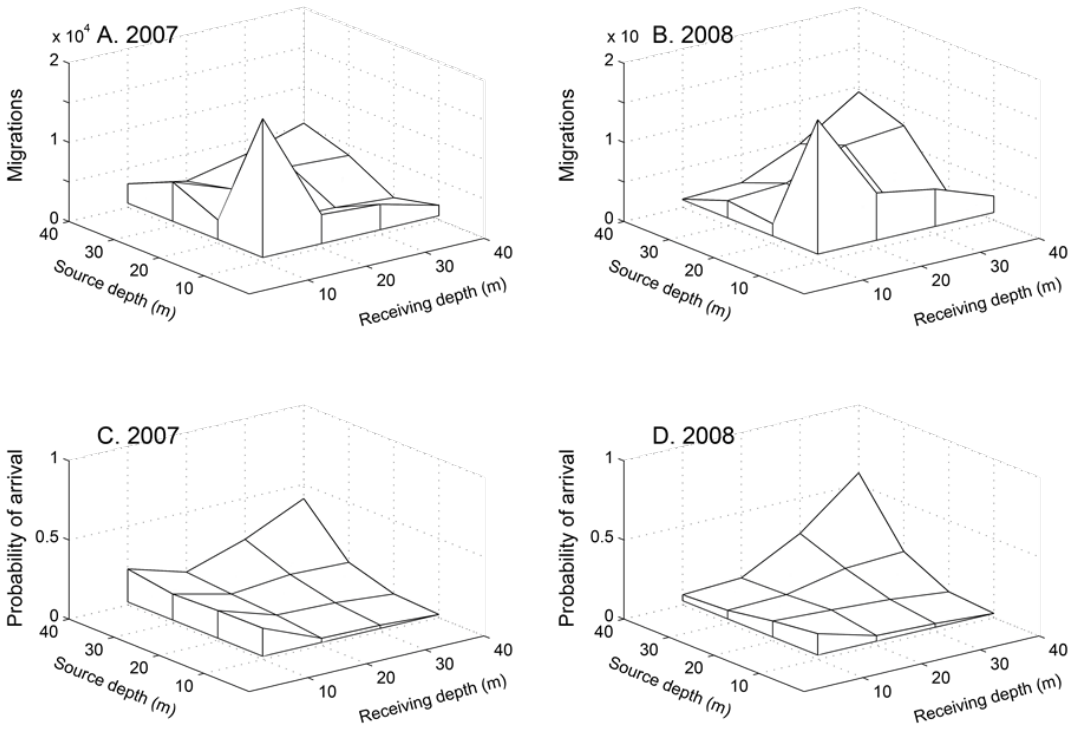

Figure 4.7.2. *P. astreoides* vertical M_T (A = 2007, B = 2008) and $\breve{M}_T$ (C = 2007, D = 2008). A and B show mean monthly migrations from any depth bin to any other. The patterns between years are consistent, with many larvae migrating from shallow to shallow habitat (10-10m). There also appears to be a large number of larvae migrating from 30m and 40m to 30m and 40m in 2008. C and D show mean probabilities of arrival at any depth bin from any other. Mean probabilities of arrival changes considerably between 2007 and 2008, with mesophotic-shallow arrival more probable in 2007 than in 2008, and mesophotic-mesophotic arrival most probable in 2008. Probability of shallow-mesophotic arrival is low in both years.

M. faveolata

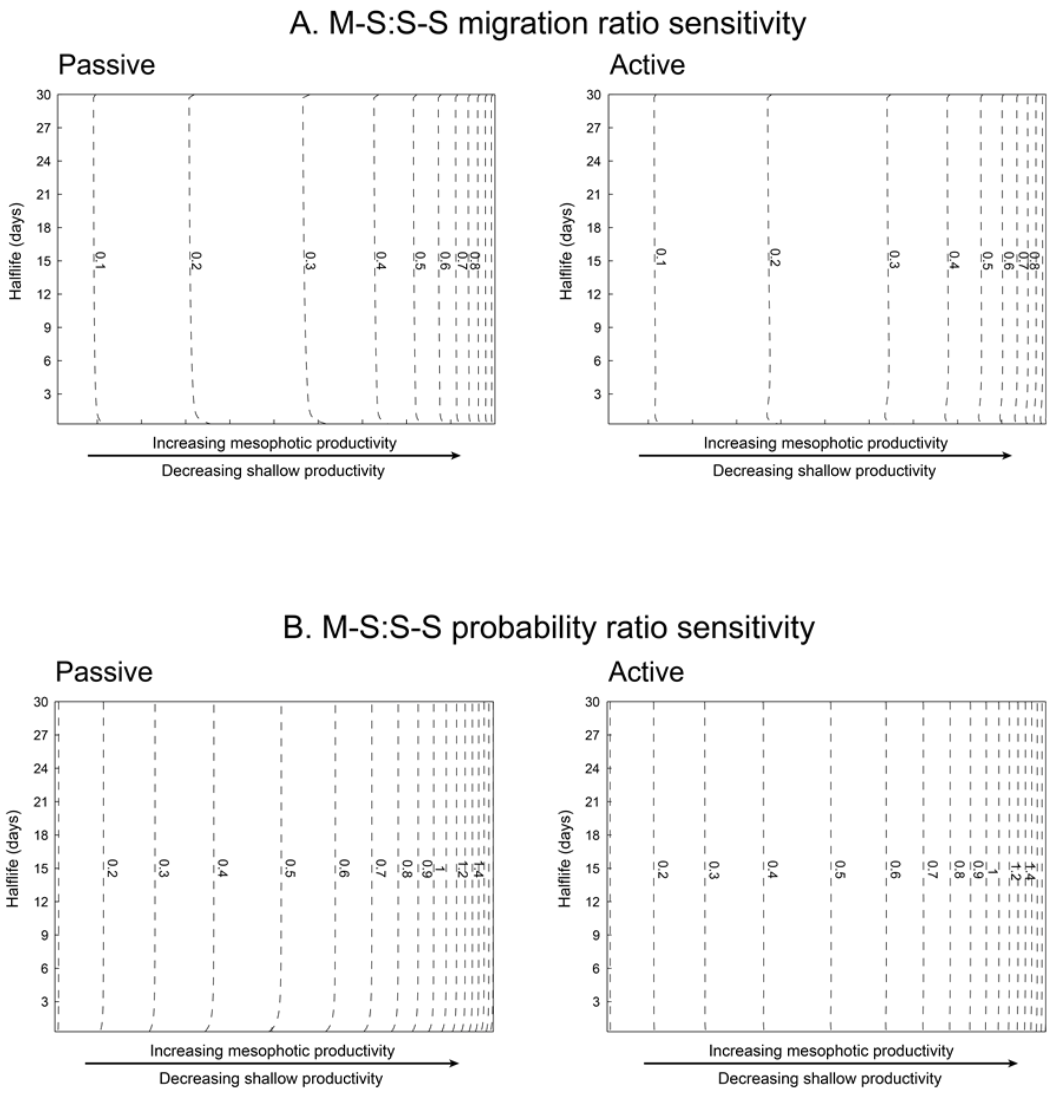

Figure 4.8.1. *M. faveolata* sensitivity analyis of (A) mesophotic contribution to shallow settlement and (B) probability of mesophotic contribution to pelagic larval mortality and depth-specific productivity in both passive and active dispersal scenarios. Mortality is expressed as larval half-life on the y-axis, and the x-axis represents 100 different linear scenarios of depth-specific production, which are illustrated in Figure 4.2. Equal fecundity at all depths is halfway across the x-axis. Contours represent ranges of mesophotic contribution (A) and probability of mesophotic contribution (B). Mesophotic contribution to shallow settlement is robust to changes in pelagic larval mortality, and increases exponentially as productivity increases with depth. *M* denotes mesophotic habitat and *S* denotes shallow habitat.

P. astreoides

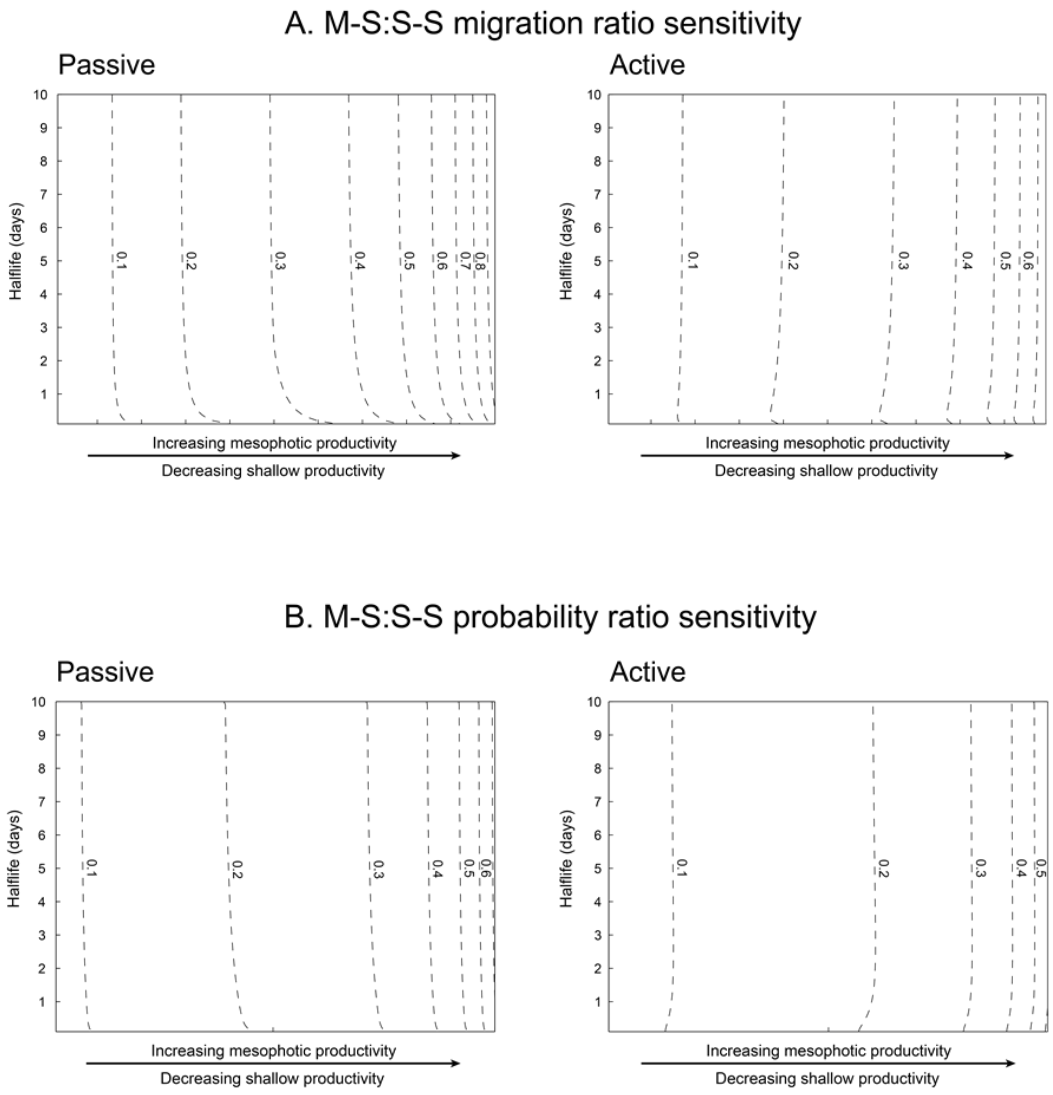

Figure 4.8.2. *P. astreoides* sensitivity analyis of (A) mesophotic contribution to shallow settlement and (B) probability of mesophotic contribution to pelagic larval mortality and depth-specific productivity in both passive and active dispersal scenarios. Mortality is expressed as larval half-life on the y-axis, and the x-axis represents 100 different linear scenarios of depth-specific production, which are illustrated in Figure 4.2. Equal fecundity at all depths is halfway across the x-axis. Contours represent ranges of mesophotic contribution (A) and probability of mesophotic contribution (B). Mesophotic contribution to shallow settlement is robust to changes in pelagic larval mortality, and increases exponentially as productivity increases with depth. *M* denotes mesophotic habitat and *S* denotes shallow habitat.

M. faveolata

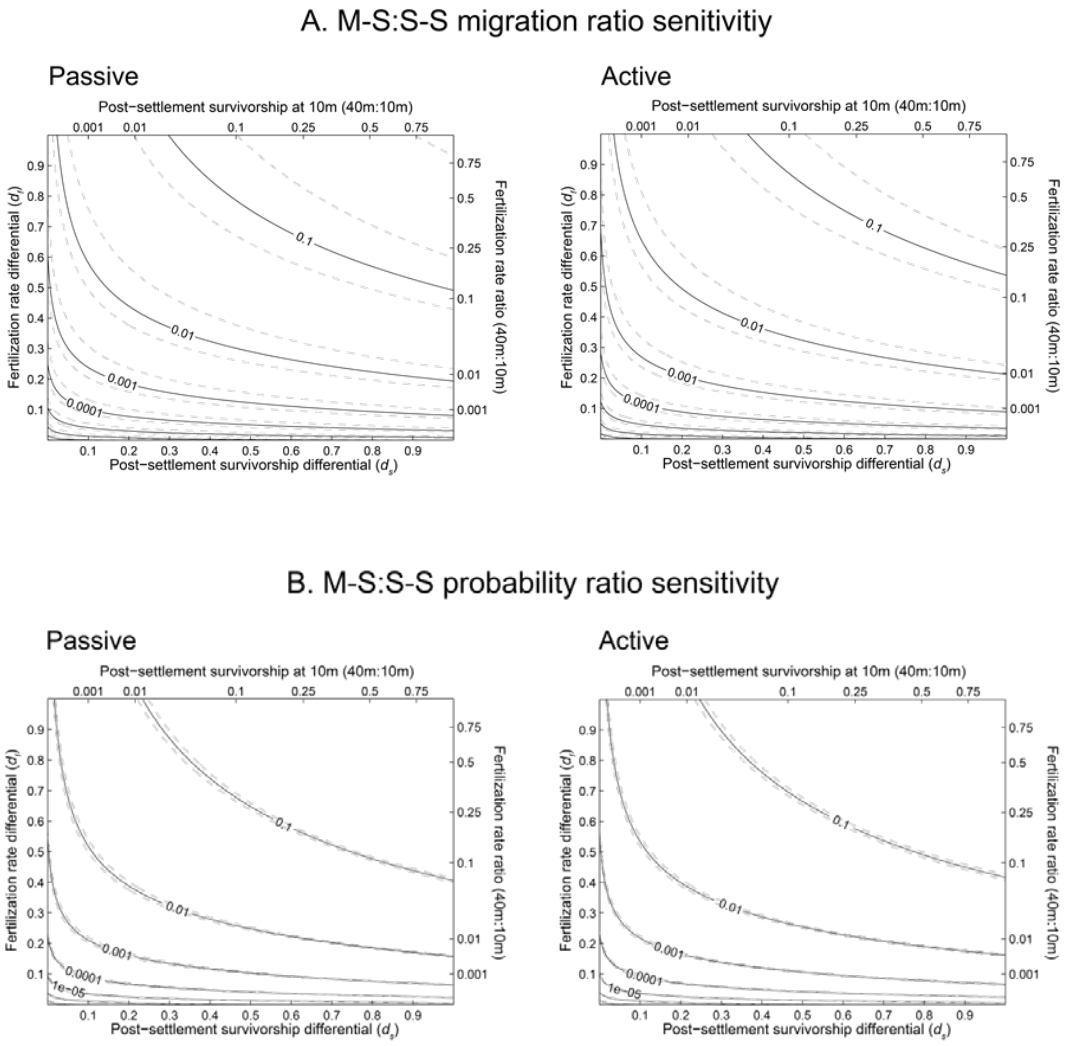

Figure 4.9.1. *M. faveolata* sensitivity analyis of (A) mesophotic contribution to shallow settlement and (B) probability of mesophotic contribution to shallow settlement to depth-specific fertilization and depth-specific post-settlement survivorship. Primary x- and y-axes are differentials that range from 0 to 1. Secondary axes compare the fertilization rate at 40m as compared to at 10m (y-axis, d_f^3: d_f^0), and post-settlement survivorship of larvae produced at 40m and settling at 10m as compared to post-settlement survivorship of larvae produced and retained at 10m (x-axis, d_s^3:d_s^0). Mesophotic contribution to shallow settlement is more sensitive to reductions in mesophotic fertilization potential than to reductions in mesophotic post-settlement surviorship in shallow habitat. See Figures 4.3 and 4.4 for more information regarding fertilization rate and post-settlement survivorship differentials and modeled scenarios. *M* denotes mesophotic habitat and *S* denotes shallow habitat.

P. astreoides

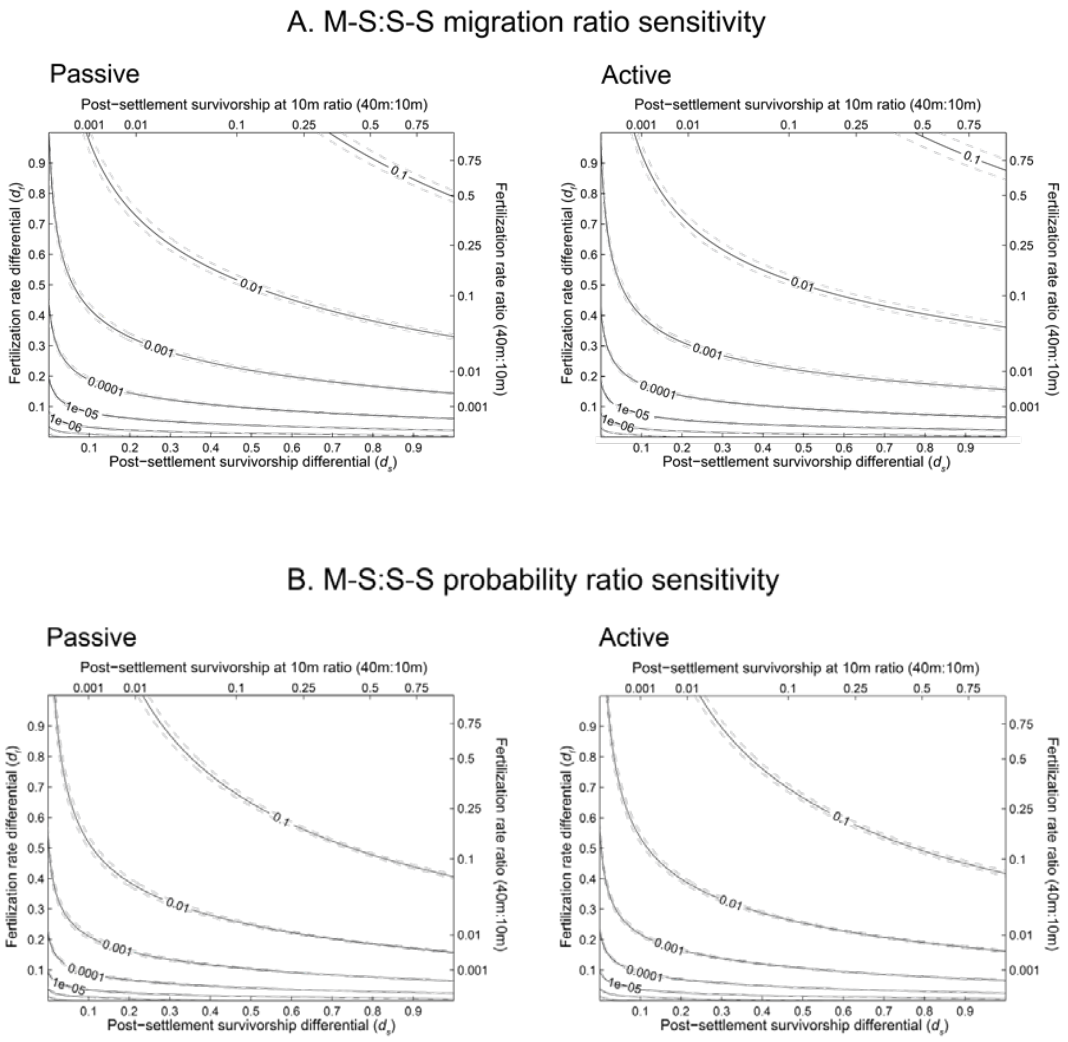

Figure 4.9.2. *P. astreoides* sensitivity analyis of (A) mesophotic contribution to shallow settlement and (B) probability of mesophotic contribution to shallow settlement to depth-specific fertilization and depth-specific post-settlement survivorship. Primary x- and y-axes are differentials that range from 0 to 1. Secondary axes compare the fertilization rate at 40m as compared to at 10m (y-axis, d_f^3: d_f^0), and post-settlement survivorship of larvae produced at 40m and settling at 10m as compared to post-settlement survivorship of larvae produced and retained at 10m (x-axis, d_s^3:d_s^0). Mesophotic contribution to shallow settlement is more sensitive to reductions in mesophotic fertilization potential than to reductions in mesophotic post-settlement surviorship in shallow habitat. See Figures 4.3 and 4.4 for more information regarding fertilization rate and post-settlement survivorship differentials and modeled scenarios. *M* denotes mesophotic habitat and *S* denotes shallow habitat.

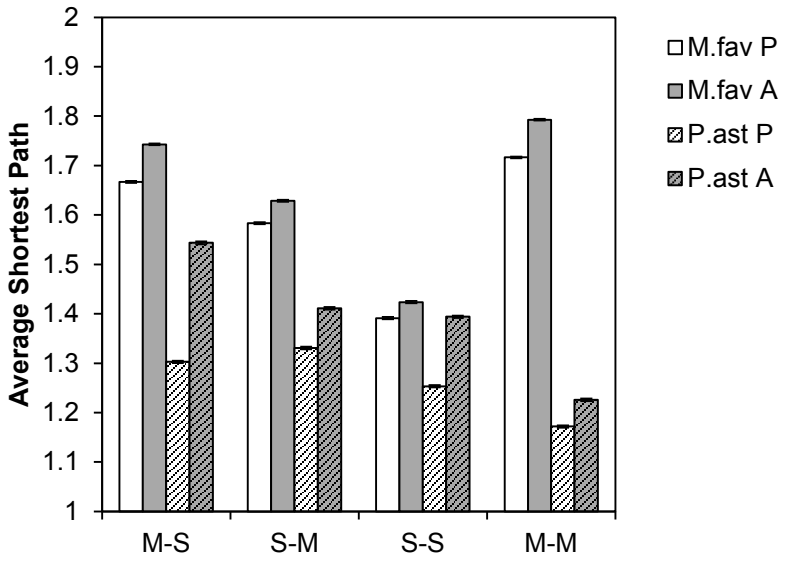

Figure 4.10. Average shortest paths for vertical connectivity in different directions in the networks of *M. faveolata* and *P. astreoides*. Average shortest paths was calculated from the adjacency connectivity networks for these species, and thus can be thought of as "generations". Standard error bars are shown, however they are too small to resolve. The average shortest paths in the network of *P. astreoides* are significantly smaller than that of *M. annularis* (Welch's two-sample t-tests, $p<0.0001$, Table 4.11) . All nodes in both species' networks are connected, on average, within two generations. Average shortest paths may indicate the "ease" or "rate" at which populations are connected through multigenerational pathways. *M* denotes mesophotic and *S* denotes shallow (i.e. *M-S* represents the average shortest paths from mesophotic to shallow habitat). A shortest path of zero represents self-recruitment, which is ignored in this analysis. Thus, the y-axis begins is shown with a minimum of 1. See Table 4.12.

M. faveolata

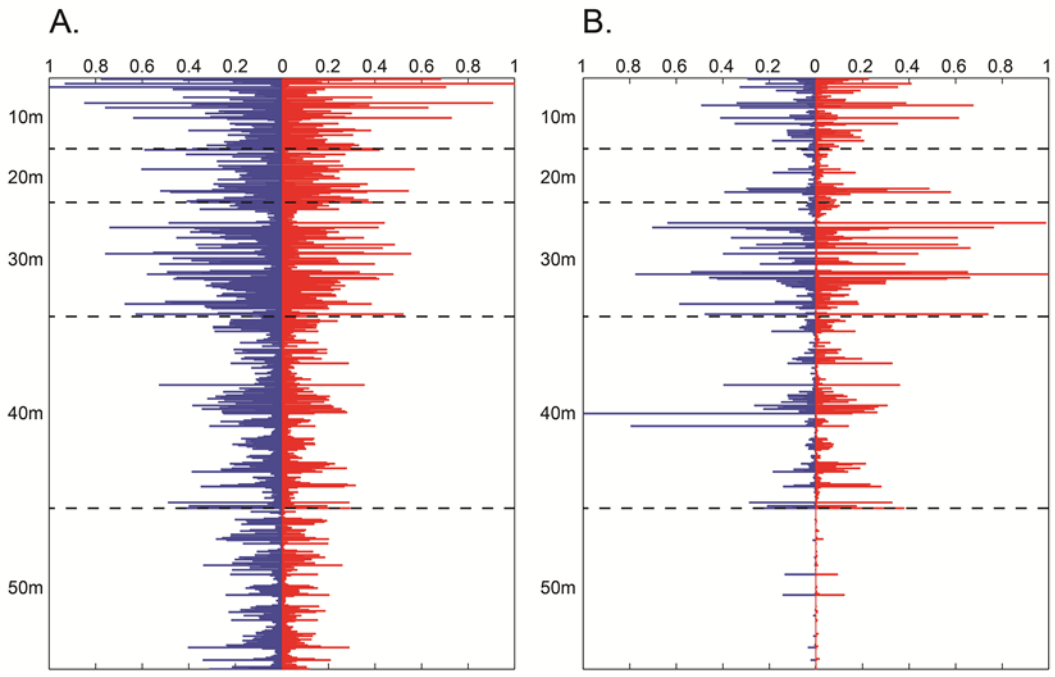

Figure 4.11.1. *M. faveolata* network estimates of node betweenness centrality calculated using (A) the adjacency matrix and (B) edge weights extracted from M_T. Blue denotes node centrality in the passive scenario, and red denotes centrality of the same node in the active scenario. Centrality scales with depth when edge-weights are ignored, but this relationship disappears when edge weights are used. Instead, habitat between 30m and 40m appears much more central to network integrity, likely due to higher productivity (and thus, more migrations leaving) at these depths.

P. astreoides

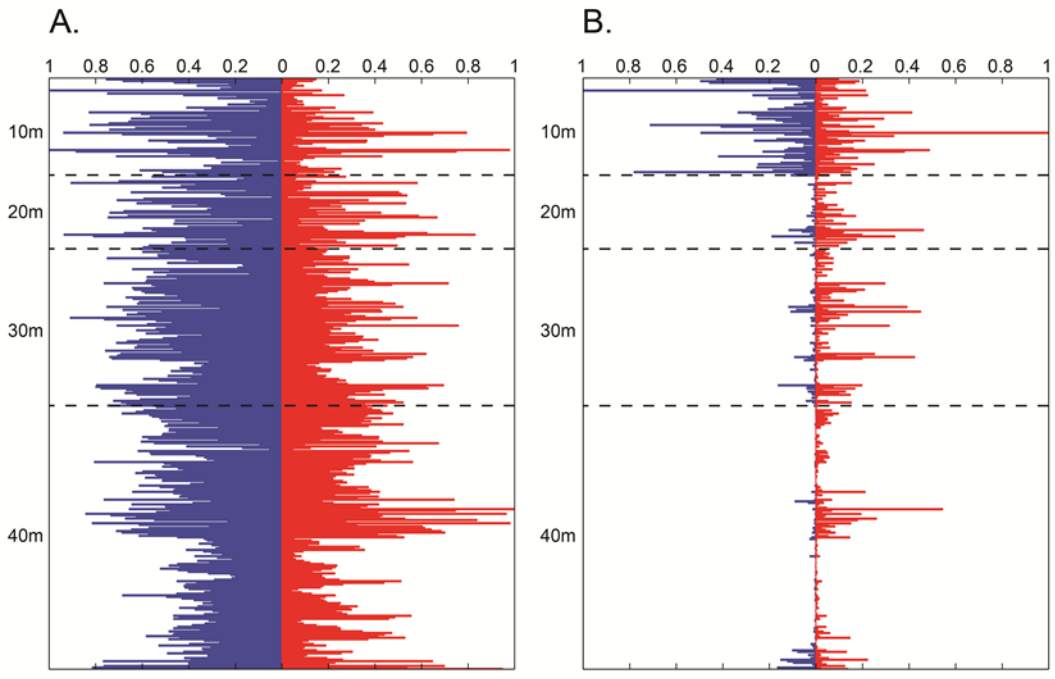

Figure 4.11.2. *P. astreoides* network estimates of node betweenness centrality calculated using (A) the adjacency matrix and (B) edge weights extracted from M_T. Blue denotes node centrality in the passive scenario, and red denotes centrality of the same node in the active scenario. Centrality has little relationship with depth when edge-weights are ignored, but this relationship changes when edge weights are used. Habitat shallower than 10m appears much more central to network integrity, likely due to higher productivity at 10m and high larval retention in this species.

Chapter 5: Consistency and inconsistency in multispecies population network dynamics of coral reef ecosystems

Background

Understanding the dispersal dynamics of pelagic larvae in the oceans and how those dynamics affect the resilience, recovery and management of marine resources continues to be a fundamental challenge at the forefront of marine ecology and policy (Sale et al. 2005). For many coral reef species the pelagic larval phase is the only opportunity for migration, and import and export of larvae among connected populations is essential for metapopulation maintenance (Moilanen 1998; Hanski and Ovaskainen 2000; Hanski 2003). Contrary to theoretical expectations (Largier 2003), larval dispersal direction and magnitude in real-world situations are often asymmetric and heterogeneous (Vuilleumier and Possingham 2006, and citations within). Adult sexual strategy (Paris et al. 2005), larval behavior (Leis and McCormick 2002; Paris and Cowen 2004), larval mortality (Cowen 2000; Vikebø et al. 2007) and persistent oceanographic features (Graham and Largier 1997; Limouzy-paris et al. 1997; Bassin et al. 2005; Sponaugle et al. 2005; Lipphardt et al. 2006) have all been shown to differentially affect recruitment and connectivity of marine larvae across the seascape.

For management purposes, reef areas are often described as either being a sink or a source of larval recruits. Sources are thought of as consistent suppliers of larvae, and sinks receive recruits from one or more sources. Resource managers, therefore, are often concerned with the sources of larvae coming into their managed areas, and productive larval sources are generally considered good candidates for protection because of their

contributions to population resilience and structure, particularly in areas that are harvested. The integration of larval
dispersal connectivity into management planning is commonly considered advantageous (Cowen 2000; Gaines et al. 2003; Sale et al. 2005; Christie et al. 2010). However, as ubiquitous as these concepts are in the scientific and management communities, very little empirical evidence exists describing source-sink dynamics because evidence of larval connectivity can be difficult to acquire.

Multispecies ecosystem-based management is a robust management approach when attempting to maintain ecosystem services and functional redundancy (Gislason et al. 2000; Pauly et al. 2002; Browman and Stergiou 2004). However, this approach is complicated by the fact that different marine species and their larvae have traits and behaviors that may expand or contract their potential dispersal capabilities. In an ideal world, management would benefit from simultaneous consideration of the dispersal abilities of every species of management concern. Some species might be selected because of their direct commercial importance to fisheries (Harrison et al. 2012), whereas others might facilitate production and biodiversity because of their role as ecosystem engineers, such as macroalgae and corals (Bozec et al. 2012). Here we estimate the source-sink dynamics of five diverse Caribbean coral reef associated species in order to identify regions of potential importance to metacommunity persistence and management consideration. The persistence of a population can be defined as its replacement over space and time through all possible larval exchange pathways over multiple generations (Botsford et al. 2009). The simplest kind of replacement consists of larvae returning to their natal population (i.e., local retention, *sensu* Paris and Cowen [2004]); a more

complex example might include larval pathways that connect populations through multiple generations, presumably through cut-nodes or corridors (Rozenfeld et al. 2008; Treml et al. 2008; Treml and Halpin 2012). We investigate any differential network dynamics among study species from local-scale larval exchanges to regional-scale connectivity and characterize consistent and inconsistent patterns of source-sink dynamics in the Caribbean.

Materials and methods

Model initialization

To investigate the network dynamics of larval dispersal in the Caribbean we used a multi-scale biophysical model, the Connectivity Modeling System (CMS, Paris et al. [2013]). The CMS simulated larval transport among populations and the larval flux between Caribbean regions over half a decade (2004 – 2008) for three species of coral reef fishes, the yellowtail snapper *Ocyurus chrysurus*, the stoplight parrotfish *Sparisoma viride*, and the bluehead wrasse *Thalassoma bifasciatum*, and two scleractinian corals, the boulder star coral *Montastraea annularis* and the mustard hill coral *Porites astreoides*. *O. chrysurus* and *S. viride* are targeted for harvesting in many Caribbean fisheries, and *T. bifasciatum* is a model species with a plastic pelagic larval duration (PLD) (Swearer et al. 1999; Swearer 2001; Sponaugle et al. 2006; Hamilton et al. 2008; Munday et al. 2009) and has been the subject of genetic population study (Purcell et al. 2006). The carbonate skeletons of scleractinian corals form the framework and habitat of coral reefs. There are two major life history strategies in scleractinian corals including brooding and broadcast spawning. These alternative strategies have implications for the dispersal of planulae

larvae, and so we include an example of each; the brooder *P. astreoides* and the broadcaster *M. annularis*.

The CMS couples ocean current, GIS-based habitat, and biological submodels. The biological submodel includes traits such as spawning frequency, PLD, larval ontogenetic vertical shifts and mortality (Paris et al. 2007). To maximize accuracy in larval dispersion calculations a hierarchy of coupled nested models were used, all based in the community code of the HYbrid Coordinate Ocean Model (HYCOM) (Bleck 2002). Starting from the larger domain, these included the HYCOM-Global 1/12 degree horizontal resolution (ca. 7 km grid), the Gulf of Mexico GoM-HYCOM 1/25 degree horizontal resolution (ca. 4 km grid), and finally the Florida Keys FKeyS-HYCOM 1/100 degree horizontal resolution (ca. 900 m grid) (Kourafalou & Kang 2012). All three models used 20 vertical layers.

For this study 3202 8km^2 coral reef habitat polygons ("nodes" therein) were developed from Caribbean coral reef extent datasets (Millenium Coral Reef Mapping Project, Andrefouet et al. [2005]; Reefs at Risk, Burke et al. [2011]). These nodes had dual functions as spawning/larval release and settlement/nursery habitats of local populations. Habitat nodes were sub-grouped *a priori* into 23 Caribbean regions based on previous connectivity studies (Cowen et al. 2006; Bustamente and Paris 2008) to facilitate the description of Caribbean network dynamics. Regions ranged in size from containing roughly 22 to 3000 square kilometers of reef habitat and 16 to 703 coral reef nodes (Figure 5.1). The CMS tracked larvae (particles therein) and recorded their positions (Paris et al. 2013). If a competent particle passed over suitable settlement habitat, i.e., a habitat node, that particle was considered to have recruited to that node.

This study assumes homogenous productivity at each reef node and makes no reference to post-settlement effects on recruitment success.

Spawning and larval traits were used to scale the number of particles released. The total number of particles released was computed to saturate all possibilities of dispersal for a given competency period, mortality rate and release frequency. Thus, species-specific differences in the number of particles released from each node are based on computational minimums, not on species-specific reproductive output. For the fish species, 100 simulated larvae were released from each node on the first of every month. Simulated larvae were released for each coral species according to limited species-specific reproductive seasons. *P. astreoides* is a brooding coral that releases competent larvae throughout spring and summer, with peaks of larval release focused around new moons from March through August (Szmant 1986; Chornesky and Peters 1987; Mcguire 1998). 100 particles were released from each node on new moons from March through August each year.

M. annularis populations experience one to two mass spawning events per year in late summer, six to eight days after full moons (Szmant 1986, 1991; Szmant et al. 1997). Depending on the calendar date of full moons in late summer, particles were released in two late summer months (August, September or October) each year. A total of 500 particles were released from each node, each selected month, distributed over five days with peaks on the seventh night after full moon.

Species-specific larval behavior parameters were used for each fish and coral species, including time from release to competency, maximum PLD, flexion ages (for fish), vertical distributions, and mortality rates (Table 5.1). Mortality rates were

calculated *a priori* as larval half-lives, such that approximately 50% of unsettled larvae would be surviving after half the maximum PLD.

For each species, the model generated transition matrices of *P* dimension (3202x3202) with element p_{ij} representing the number of particles originating at any node *i* that migrate to any other node *j*. Probabilities of migration *M* are generated by normalizing transition matrix *P* (i.e., number of surviving particles arriving in each node s_{ij}) by the total arrival from node *i*:

$$M = \frac{P}{\sum p_i} \qquad \text{eqn 1}$$

The matrix *M* ("connectivity matrix" *sensu* Cowen et al. [2006]), does not reflect the relative magnitude of settlement among nodes, rather the probability that a larva spawned from node *i* settles successfully at another node *j*, connecting thus the population *i* to *j*. Connectivity matrices M_r (23x23) were similarly developed at the regional-scale representing the probability of larval migration from any region *I* to any other region *J.* Without information on spawning production and the size of the population, the magnitude of larval fluxes cannot be realistically quantified. Yet, we can accurately quantify the probability of migration M_r which were used in connectivity network analyses.

Network analyses

Graph theoretical network analyses were performed at the regional-level for each species. Average shortest path is a descriptive network statistics that estimates the diameter, or level of connectivity, of a connectivity network (Albert and Barabási 2002).

The statistic requires that a network be strongly connected, meaning that all nodes must be connected to a single network (no isolated nodes or sub-networks).

Betweenness centrality (*BC*) is a measure indicating the degree to which a node serves to connect other nodes in the network, such as a corridor or stepping stone to multi-generational connectivity (Rozenfeld et al. 2008; Treml et al. 2008; Treml and Halpin 2012). *BC* counts the fraction of shortest paths between pairs of nodes that pass through node *i*.

$$BC(i) = \sum_{s \neq i \neq t} \frac{\sigma_{st}(i)}{\sigma_{st}} \qquad \text{eqn 2}$$

Where σ_{st} denotes the total number of shortest paths between nodes *s* and *t*, and $\sigma_{st}(i)$ denotes the number of those that pass through node *i*. *BC* can be thought of as a measure of the importance of a node in maintaining the structure of the network, and has been used to identify critical patches for the maintenance of connectivity in complex landscapes (Estrada and Bodin 2008). Each region's *BC* was calculated within the networks of each species.

Regional analyses

There are many ways to visualize dynamic networks; however extracting node-specific information can be difficult, particularly in multispecies networks. The following are analyses designed to communicate source-sink relationships within and among regions for multiple species. Mean regional source-sink indices (*SS*) were calculated for

each species as the positive or negative difference in larvae being exported from and larvae being imported to a region, divided by the sum of import and export for that species in that region.

$$SS = \frac{(R_{out} - R_{in})}{(R_{out} + R_{in})} \qquad \text{eqn 3}$$

Where *R* represents the successful recruitment into or out of a region. A value of zero would indicate that the region experiences nearly equal import and export of recruiting larvae. Negative index values indicate that a region receives (imports) more exogenous recruits than it produces, and thus the region is a net sink. Positive index values indicate that the region is a net source. Indices of higher magnitude (positive or negative) indicate larger discrepancies between import and export, and regions with high index values may represent strong or consistent sources or sinks.

The number of connections a node or region shares is often used as a measure of connectivity. However, this measure may not indicate the network significance of those regions. Source and sink connection diversity indices were calculated for each region using a modified Shannon's diversity index (*S'*):

$$S' = -\sum_{i=1}^{C_d} (p_i \ln p_i) \qquad \text{eqn 4}$$

Where *C* is equal to the number of connections (*d* represents direction, and denotes whether *C* is the in- or out-degree of the region) and p_i is the probability that any given connection is to or from a region *i*.

This index takes take into account not only the number of connections in a region, but also the evenness of those connections. Thus regions with many sources providing near equal proportions of the region's total recruitment will have higher index values. Regions for which inputs are low or highly uneven will have lower index values. The

exponent of this index, $e^{s'}$ represents the true diversity of connections (Hill 1973; Jost 2006). The discussion here focuses on upstream (source) connections only.

Results

Over 82 million simulated larvae (particles) were tracked over a five year simulation time, resulting in over 25 million source-sink connections. The connectivity network of each species can be graphed using vertices and edges (Figure 5.2), where each vertex represents a region and each edge represents a larval pathway.

Connectivity and network comparisons

The networks of all three fish species are strongly connected and have only one component (Figure 5.2 and Table 5.2). For all three species the average shortest path is under 2 node-to-node steps, suggesting that, on average, every region has the potential to be connected in two steps; or, in this simulation, in two generations. The network of *T. bifasciatum* has a significantly shorter average shortest path than any other modeled species (one way ANOVA, p=.003), indicating higher degrees of connectivity in comparison to the other two fish species or the coral species. The maximum PLD of *T. bifasciatum* is 53% greater than the parrotfish *S. viride* and is associated with a 19% increase in network connectivity (Tables 5.1 and 5.2). The modeled PLDs of *O. chrysurus* and *S. viride* were similar with only a 7.8% difference, but their flexion ages were quite different at 11-18 days and 7 days respectively. Yet, despite differences in flexion ages, the differences in network diameter were negligible at <1% and not statistically significant (Table 5.2, independent t-test, p>.05). All fish species demonstrate

high probabilities of dispersal in the Bahamas and northeast Caribbean, as well as in the central Caribbean (Figure 5.2).

The connectivity networks of the corals differ from those of the fish, as well as from each other. The network of the brooder *P. astreoides* is highly fragmented, and self-recruitment is dominant in every region (Figure 5.2). Of the five species modeled, *P. astreoides* is the only species that has an unconnected network, meaning that distinct metapopulations are confined to subgraphs in the network and might not exchange larvae. Because this network is unconnected, network diameter calculations result in diameters of infinity (Table 5.2). The spawning coral *M. annularis* has a network intermediary to that of *P. astreoides* and the three fish species in terms of fragmentation and degree of connectivity. Although the graph is a connected graph, one region (Gulf of Mexico) does not receive larvae from any other region, meaning this graph is not strongly connected. The diameter and connectivity of the *M. annularis* network cannot be calculated without eliminating the Gulf of Mexico. The network of *M. annularis* has fewer connections than the fish species and the average shortest path is significantly longer than any fish species (independent t-tests, all $p<.001$, Table 5.2). The maximum PLD of *T. bifasciatum* is 160% longer than that of *M. annularis* and its network is 33+% more connected.

Networks of fish species have similar pattern of regional *BC*, with regions of high centrality in the central Caribbean, including Mexican reefs, Jamaica and the Colombian Archipelago. Regions with low *BC* for fish include Belize, Nicaragua, Turks and Caicos and Florida reefs. Corals share a set of highly central regions unique from fish, including the Bahamas, Cuban reefs and Hispaniola. The network of *M. annularis* has shares central regions with fish species as well, suggesting intermediate network dynamics

between *P. astreoides* and fish (Figure 5.4c). Regions with high centrality for all species include the Bahamas, Northcentral Cuba and Hispaniola. Differences in *BC* among fish species exist in many regions despite similarities in maximum PLD and time to competency.

Source-sink dynamics

Thirteen of the twenty-three regions have species-specific mean *SS'* indices, acting as a sink for some species and a source for others, including, for instance, the Colombian Archipelago and Honduras (Figure 5.4a). Of those regions, ten of them have similar index directions for all fish species, while one or both coral species has an opposite index direction. Mean *SS'* index directions for fish species differ only in three regions: the Bahamas, which is a net source for *S. viride* and not the other two fish species; Venezuela, which is a net sink only for *S. viride*; and Honduras, which is a net source only for *T. bifasciatum*. The remaining ten – nearly half of all – regions show consistent mean index values in either the source or sink direction for all species. Consistent sources for all species include Turks and Caicos, Northwest Cuba, Southwest Cuba, the Nicaraguan Rise Islands and Belize. Consistent sinks for all species include Florida reefs, Northcentral Cuba, Southeast Cuba, the Gulf of Honduras (excluding *T. bifasciatum*), and Mexico.

Variability in mean *SS'* index over the five years studied is represented by standard deviation, and can be seen in Figure 5.4b. In general, coral species have higher variability in this index. Regions with index directions consistent across all species tend

to have lower variability during the five year study period, with a notable exception of the Turks and Caicos Islands. Similarly, high magnitude mean *SS'* index values by region and species are often associated with lower variability.

Upstream connection diversity and isolation

The proportion of self- regional-recruitment is defined here has the proportion of settling larvae within each region that originated from reefs within that region. Although there is high variability, species with longer maximum PLDs and time to competency tend to have lower self- regional-recruitment and those regions tend to have a higher number of source connections. A decreasing linear relationship exists between the proportion of self- regional-recruitment and true diversity of upstream connections ($e^{S'}$) (Figure 5.4b, $R^2 = .80$), suggesting that lower self-regional-recruitment correlates with higher upstream connection diversity, and isolation correlates with a low diversity of larval inputs. Maximum $e^{S'}$ values decreases with maximum PLD and time to competency (Table 5.2 and Figure 5.3b, bounding boxes). *P. astreoides*, the most isolated species in all regions, has probabilities of self- regional-recruitment ranging from 0.87 to 1, and also has the fewest sources and lowest diversity of sources at all regions (maximum $e^{S'}$ of 1.31). In contrast, regions in *T. bifasciatum*'s network experience proportions of self- regional-recruitment ranging from as low as .12 to .93 and $e^{S'}$ ranging from 1.28 to 6.11, indicating considerable variability in the recruitment dynamics of this species among regions (Figures 5.3 and 5.4d).

For all species, South Cuba, Puerto Rico, the Windward Islands, Venezuela, Nicaragua, Belize and the Gulf of Mexico experience high self- regional-recruitment and

low upstream connection diversity. For fish species, recruitment in Northcentral Cuba, the Colombian Archipelago, Cayman Islands, Honduras and Mexico is primarily from exogenous upstream reefs, and the diversity of those upstream sources is high (Figures 5.3b and 5.4d, also see Jamaica and Northwest Cuba). The same is true of Northwest Cuba and Grand Bahama for *T. bifasciatum*.

Discussion

The effects of larval traits on connectivity

Foster et al. (2012) demonstrated that larval exchange projections for *M. annularis* made with the CMS (Paris et al. 2013) had a high degree of consensus with empirical genetic population data, with notable discrepancies likely due to habitat conditions not included in the model, such as low salinity runoff. We have expanded this model to include the larval exchange probabilities of five coral reef-associated species in order to gain insight into multispecies network dynamics. In doing so, we have shown that network dynamics are largely species-specific due to diverse reproductive and larval traits. Graph theoretic analyses of the connectivity networks of the five studied species statistically confirm some common assertions regarding maximum PLD and dispersive capabilities in marine organisms. The fish species modeled have small network diameters of less than 2 steps, which suggest that there is scope for significant geographic mixing over multiple generations. In the case of *T. bifasciatum*, this assertion is supported by previous population genetic studies that found no explicit spatial pattern to genetic variations in this fish in the Caribbean basin (Purcell et al. 2006). *T. bifasciatum* has the longest maximum PLD of the modeled species together with deepest vertical migration,

and its network is predicted to be richer in connections, have a smaller diameter (higher connectivity), and generally experience lower proportional self- regional-recruitment and higher source diversity than the other five species. Correspondingly, the network of *P. astreoides*, which has the shortest maximum PLD and time to competency of modeled species, also has the most fragmented network. In general, connectivity decreases with shorter maximum PLD and time to competency.

When comparing the similar connectivity networks of *S. viride* and *O. chrysurus* – which have comparable maximum PLDs but differing time to competency, flexion ages and vertical distributions – the effects of non-PLD larval characteristics on connectivity are not statistically obvious using network diameter analyses, but can be seen as regional variations in recruitment magnitude and *BC*. Due to larval behavior, the relationship between dispersal distance and PLD is non-linear (Shanks 2009), and shorter time to competency should increase the probability of recruiting nearer to natal reefs, which increases the probability of self-recruitment. Flexion ages determine the timing of species-specific ontogenetic shifts in larval vertical distribution, which can expose pelagic larvae to horizontal and vertical flow velocities that may serve to retain or disperse larvae (Paris and Cowen 2004), leading to species-specific network connectivity. Even for species with similar maximum PLD, such as *S. viride* and *O. chrysurus*, these differences in larval biology can create networks with regions that have functionally different roles and centralities. Although the networks of these two species appear similar, in many cases the removal of regions may have significantly different effects on multi-generational basin-scale connectivity.

BC is an estimate of the relative importance of a region in a network. There is high consistency in regional *BC* among fish species, and *M. annularis* shares patterns of *BC* with fish species in the central Caribbean. This is likely due to overlap in maximum PLD, whereas the shorter larval duration of *P. astreoides* restricts the connectivity of this species in the Colombian Archipelago and Jamaica (Figure 5.4c). The networks of coral species also share a set of highly central regions, including Bahamian reefs, Cuban regions and Hispaniola. These regions behave as stepping stones to multigenerational connectivity for corals. Shorter time to competency restricts connectivity and enhances local retention, and connections with these highly central regions facilitate the multigenerational connectivity in the more fragmented networks of coral species.

It is important to recognize that this study does not address any species-specific post-settlement mortality. Scaling connectivity by post-settlement mortality would reduce connectivity for all species, especially those with high predicted post-settlement mortality, such as *M. annularis* (Hughes and Tanner 2000; Edmunds and Elahi 2007). However, the shapes of each species' connectivity network (Figure 5.2) and the regional centralities within those networks would likely not change significantly if connectivity were scaled by spatially homogenous species-specific mortality rates. In reality, it is possible that post-settlement mortality is not homogenous over space, which could change the connectivity relationships both within and between regions. Additionally, it is possible that larvae settling at different times within their competency period have differential settlement success, which could also alter the connectivity network. For more information on modeling the effects of post-settlement mortality on vertical coral connectivity, see Chapter 4.

Source-sink dynamics

The Bahamas, Venezuela and Honduras are the only regions in which fish *SS'* indices may be in opposite directions. In all other regions, the magnitude of index values may differ but fish species have similar source-sink dynamics, suggesting that the adult replacement dynamics in these regions may be similar. This is likely due to persistent current regimes and relatively similar larval characteristics among these species (as compared to the coral species).

The two coral species have very different larval traits, and thus the source-sink dynamics are considerably different for each species. Because these source-sink patterns are so different, it is expected that real-world recruitment patterns for these species would be quite different as well (Glynn and Colley 2008).

Variability in source-sink dynamics is higher for corals than for fish throughout the five year study period. The most obvious reason for this is that the limited spawning window for coral species exposes settling larvae to higher environmental variability from year to year, as opposed to fish which settle year-round in this model. In the case of *P. astreoides*, low levels of larval exchange may also create variability in source-sink dynamics for this species. Both coral species have short time to competency, and the probability of self- regional-recruitment is high in most cases. This may imply that larval exchange occurs in pulses determined by variability in hydrodynamics, leading to higher variability in source-sink dynamics.

In regions where mean *SS'* indices are in the same direction for all species, variation in *SS'* index values tends to be lower for all species. This is also true for regions and species with high magnitude index values. This may imply that the arrangement and

orientation of these regions in the seascape, as well as consistent hydrodynamic and eddy features, may be more responsible for the source-sink dynamics at these regions than larval traits.

Source diversity and isolation

The number of upstream connections providing larvae to a region may not be the best indicator of levels of connectivity or population resilience. For example, in Jamaica *M. annularis* has 12 upstream connections, meaning that more than half of the regions in the Caribbean contribute to recruitment there. However, the probability of self-recruitment for this coral in Jamaica is higher than 0.94, suggesting that an overwhelming proportion of recruits come from Jamaica itself. Although upstream connections are rich (Figure 5.3a), the diversity of those connections is low (Figures 5.3b and 5.4d). How demographically significant are those upstream connections? The connection diversity index *S*' provides a metric that describes both the richness and evenness of source connections, which has implications for the recovery potential of a region after perturbation; a region with diverse upstream connections should be less vulnerable to variability in larval supply or a reduction in local reproductive success. Alternatively, regions with high proportions of self-recruitment are potentially vulnerable to recruitment failure should local reproductive success decline, and such regions are potentially vulnerable to isolation due to network fragmentation. Self- regional-recruitment and the diversity of source connections are strongly linearly correlated. Regions that rely less on locally produced larvae generally rely instead on diverse sets of sources. Populations that experience exogenous larval subsidies have increased recovery potential due to the

"rescue effect" (Brown and Kodric-Brown 1977; Hanski 1982; Gotelli 1991). More diverse subsidies (higher *S*') should correlate to a higher probability of rescue.

In some cases, regions are isolated physically which results in a high proportion of self- regional recruitment and low source diversity for all species. Alternatively, species with short time to competency or short PLD may be isolated in regions that are otherwise well-connected physically. The ecological result is the same; isolation likely limits rescue potential (Hanski 2001). Regions at the other extreme that experience low proportions of self-recruitment rely heavily on exogenous source populations, and severe network variability or an inhospitable pelagic environment could cause recruitment failure while isolated regions may be less affected.

Management implications

Regions and species with similar network dynamics may benefit from similar management focuses. For example, populations with low self-recruitment and high source diversity may benefit most from the maintenance of upstream populations. Oppositely, regions and species that predominantly receive locally produced recruits may benefit most from the maintenance of local adult reproductive populations. Because there is evidence that coral recovery and recruitment can be enhanced through the rebuilding of fish biomass (Mumby and Harborne 2010), the management of isolated coral populations may not be decoupled from that of the management of local and upstream fish populations.

Variability in connectivity and network characteristics, both among and within species, represents a challenge to successful multispecies management. Networks of

marine protected areas arranged to incorporate dispersal kernel probabilities are considered ideal for the protection of marine species (Steneck et al. 2009), however kernels vary with species and location, and the high degree of complexity of marine larval connectivity has not been fully integrated into marine protected area design. Here we propose that areas (reefs, countries, regions, etc.) that are important for multispecies connectivity and network stability should be a focus of marine protection. In the current study several regions have high *BC* for all or most species, including Hispaniola, Northcentral Cuba and some smaller regions in the central Caribbean, such as the Colombian Archipelago and Jamaica. These regions are likely important for multi-generational connectivity for all modeled species, partly due to the physical location of these regions in the seascape. Preserving and maintaining suitable settlement and reproductive habitat at highly central regions may be critical to metapopulation maintenance. Areas that consistently provide larvae to downstream reefs, especially if they behave as sources for multispecies assemblages, are especially valuable. Because marine reserves cannot protect organisms from major physical disturbances such as storms or bleaching events, management benefits from spreading risk across the seascape (Allison et al. 2003; Mumby et al. 2011b), and the protection of regions that have natural resilience due to consistent and diverse larval inputs may represent good investments of resources.

Our study suggests that estimating diversity of exogenous recruitment may provide a proxy of recolonization potential. Multispecies network dynamics reveals stability (e.g. sources and corridors) pertinent to regional level management but also dissimilarities in networks calling for local management. In most cases management will

and should occur at scales finer than discussed here, however the analyses used are applicable at all spatial scales. Larval connectivity models and network theory will continue to contribute valuable information to the management and protection of marine habitats, especially as the potential for further reef fragmentation and other physical changes to the environment alter both the habitat and the biology of coral reef organisms and their larvae.

Table 5.1. Species parameters and proportional settlement (ignoring any post-settlement mortality). Flexion determines the age at which major ontogenetic shifts occur in these fish species, including changes in mean depth of larvae (Paris and Cowen 2004). Fish larvae were released on the 1st of every month each year. Coral larvae were released according to restricted reproductive seasons and spawning events. Total larvae released is over the five year simulation time. Note that higher proportional settlement in corals is due to a short time to competency.

Model parameters

Species	Time to competency (days)	Maximum PLD (days)	Flexion age (days)	Release frequency	Total larvae released (millions)	Proportion of larvae settled
T. bifasciatum	38	78	11	Monthly	18.89	0.18
O. chrysurus	25	47	11-18	Monthly	18.89	0.16
S. viride	34	51	7	Monthly	18.89	0.14
M. annularis	6	30	-	Seasonal	16.01	0.40
P. astreoides	2	7	-	Seasonal	9.61	0.38

Table 5.2. Graph theoretical estimates of network connectivity (diameter) for each species. Diameter values are in "steps", and suggest how many node-to-node steps are required to span the network. Lower numbers indicate higher network connectivity. Coral network diameter estimates result in infinity values because they are not strongly connected. If the Gulf of Mexico (GOM) region is removed, the connectivity network of *M. annularis* becomes strongly connected. Thus, all values after a slash denote calculation omitting GOM. The network of *M. annularis* is significantly larger (independent t-test, all p=<.001). *T. bifasciatum* has a significantly shorter average shortest path (one way ANOVA, p=.003). SCC indicates strongly connected components

Network analyses

	Diameter		
	Longest shortest path	Average shortest path	# SCCs
T. bifasciatum	3/3	1.4249 [a]/1.3680 [a]	1
O. chrysurus	4/3	1.7589 [b]/1.667 [b]	1
S. viride	4/4	1.7609 [b]/1.6732 [b]	1
M. annularis	∞/4	∞/2.0498 [c]	2
P. astreoides	∞/∞	∞/∞	11

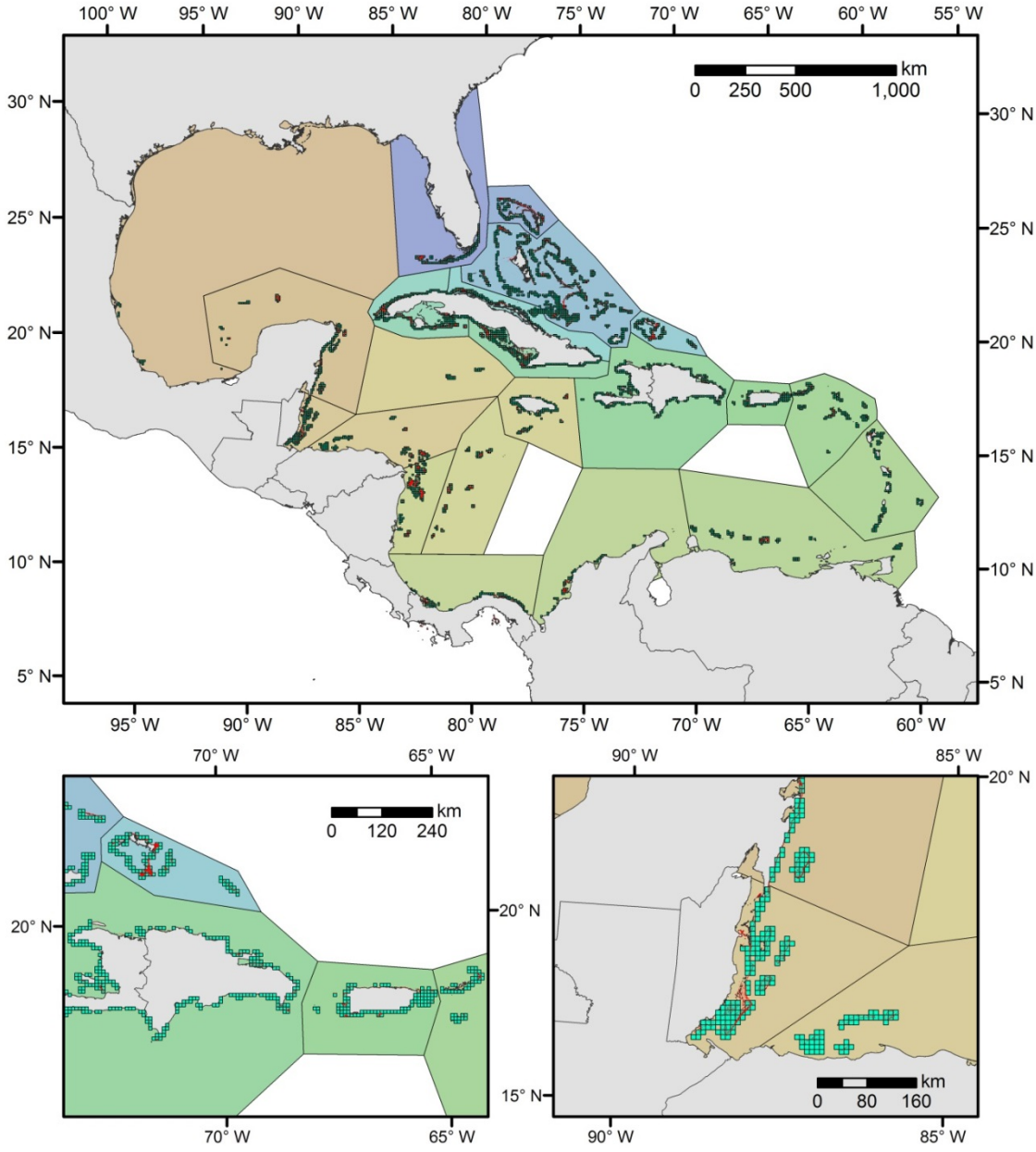

Figure 5.1. Spatial representation of coral reef extent, polygons and regions. 3,202 8 km^2 habitat nodes (blue) were developed for the Caribbean from coral reef extent datasets (red). Larger colored polygons represent 23 *a priori* Caribbean regions. Top, Caribbean-wide. Left, Hispaniola, Puerto Rico, Turks and Caicos. Right, Belize.

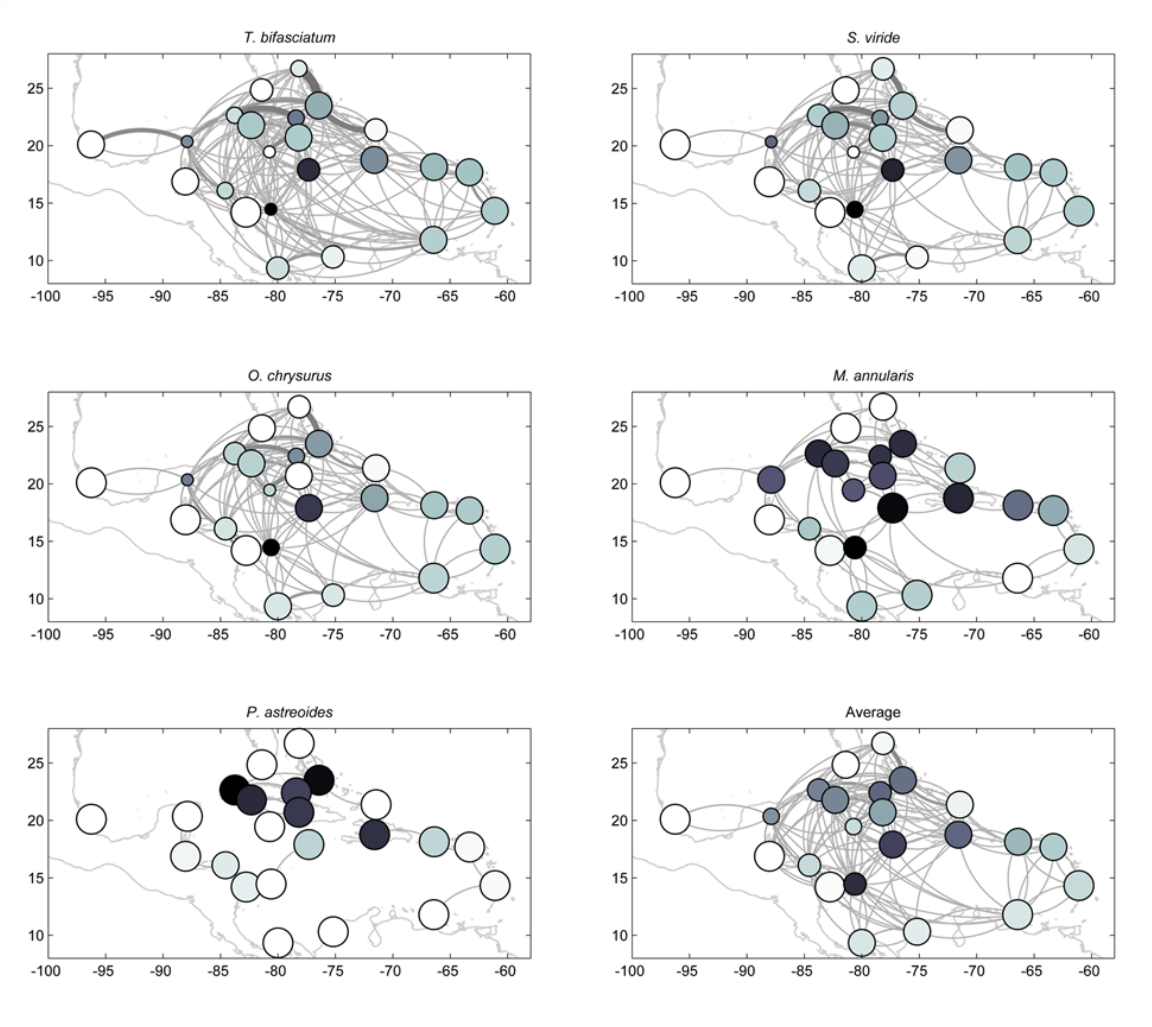

Figure 5.2. Network graphs for the five studied species, and an averaged network. Vertices represent regions and edges represent larval exchange (clockwise along arc). The size of the vertex indicates the proportion of self- regional-recruitment and the shade of the vertex indicates the *BC* of that node (darker shades indicate higher values). The thickness of the edge represents probability of migration (threshold of .001 to illustrate connections of demographic significance).

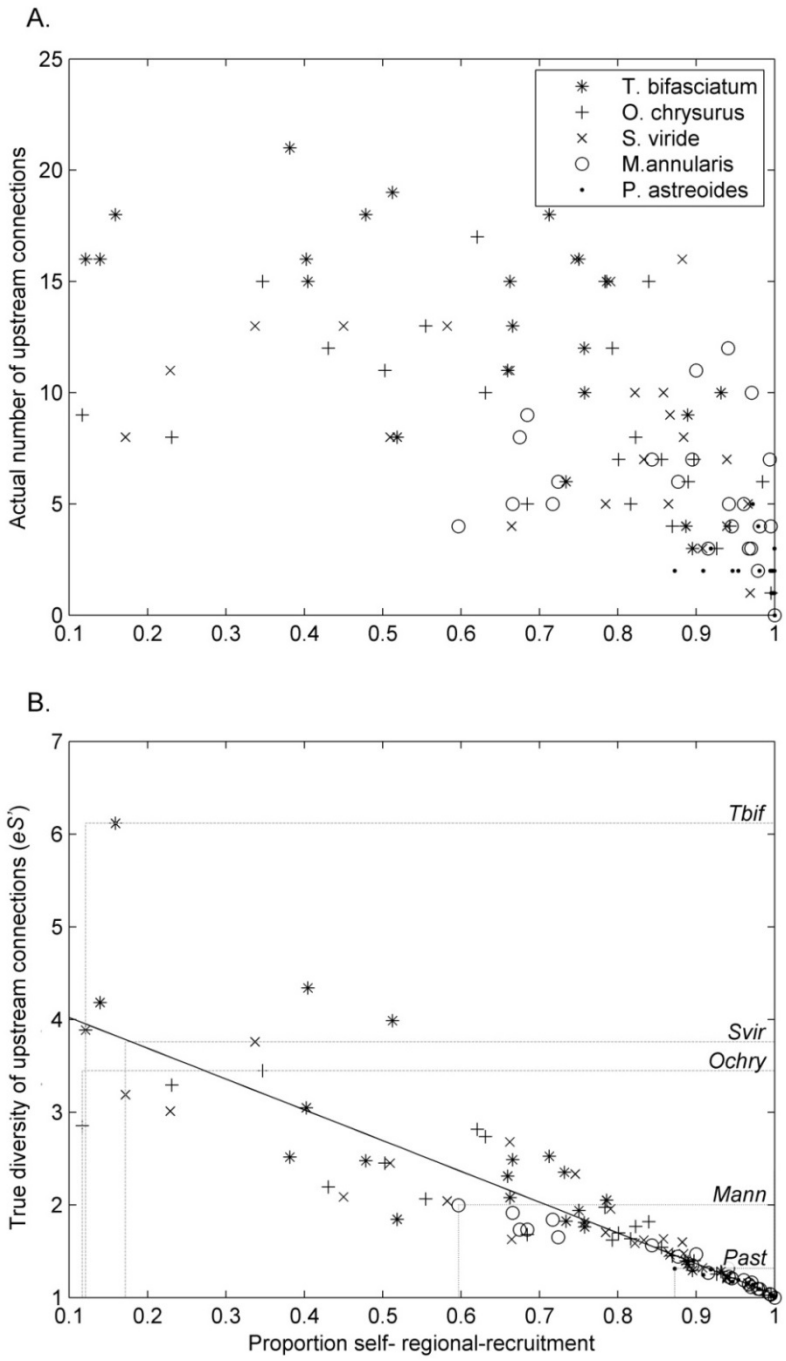

Figure 5.3. A) Number of upstream connections (region and species) versus the proportion of self- regional-recruitment. B) True diversity of upstream connections (region and species) versus the proportion of self- regional-recruitment. A linear relationship ($R^2 = .80$) suggests source diversity is negatively correlated with the proportion of self- regional-recruitment. Dotted boxes indicate the lower threshold of self- regional-recruitment and upper threshold of upstream connection diversity for each species.

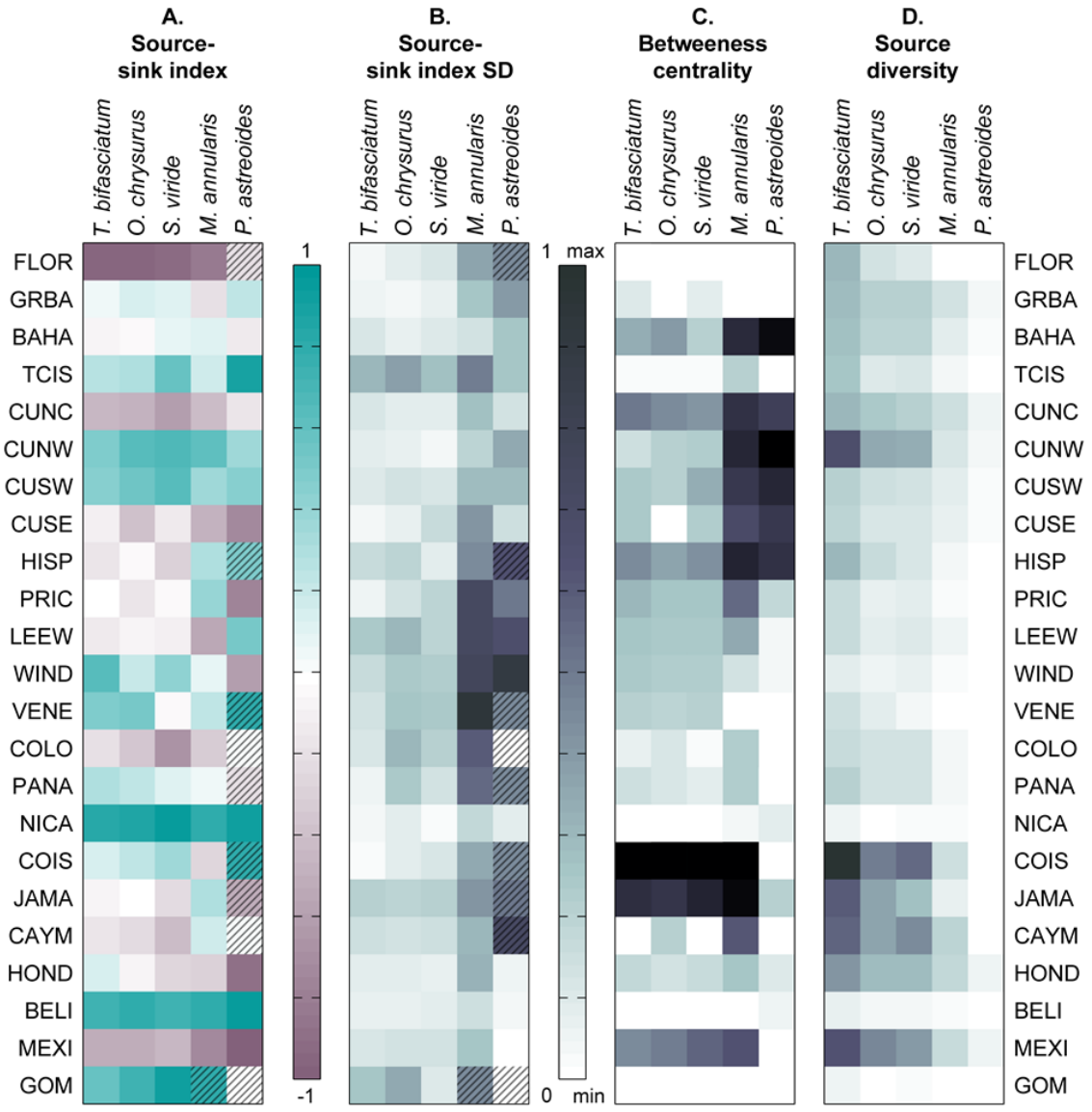

Figure 5.4. A) mean *SS'* indices by species for each region. Positive values indicate greater export than import (source), and negative values indicate greater import than export (sink). Values near zero indicate near equal import and export. B) SD of *SS'* indices over the five year modeling time. Hatched boxes represent nodes that have no connections in at least one direction in at least one year. C) Relative *BC* for each region and species. High values suggest importance for network stability and may indicated corridors for multigenerational connectivity. Note that corals and fish have distinct patterns of *BC*, and the network of *M. annularis* shares attributes with fish in some regions. D) Source diversity has implications for regional population persistence for each species.

References

Albert R, Barabási A-L (2002) Statistical mechanics of complex networks. Reviews of Modern Physics 74:47–97

Allison G, Gaines S, Lubchenco J, Possingham HP (2003) Ensuring persistence of marine reserves: Catastrophes require adapting and insurance factor. Ecological Applications 13:8–24

Andrefouet S, Muller-Karger FE, Robinson JA, Kranenburg CJ, Torres-Pulliza D, Spraggins SA, Murch B (2005) Global assessment of modern coral reef extent and diversity for regional science and management applications: A view from space.

Armstrong R (2007) Deep zooxanthellate coral reefs of the Puerto Rico: US Virgin Islands insular platform. Coral Reefs 26:945–945

Armstrong R, Singh H, Torres J, Nemeth R, Can a, Roman C, Eustice R, Riggs L, Garciamoliner G (2006) Characterizing the deep insular shelf coral reef habitat of the Hind Bank marine conservation district (US Virgin Islands) using the Seabed autonomous underwater vehicle. Continental Shelf Research 26:194–205

Aronson RB, Bruckner A, Moore JA, Precht WF, Weil E (2008) Montastraea faveolata and Montastraea franksii. IUCN 2012. IUCN Red List of Threatened Species. Version 2012.2.

Atkinson MJ, Carlson B, Crow GL (1995) Coral growth in high-nutrient, low-pH seawater: A case study of corals cultured at the Waikiki Aquarium, Honolulu, Hawaii. Coral Reefs 14:215–223

Babcock R, Mundy C, Whitehead D (1994) Sperm diffusion models and in situ confirmation of long-distance fertilization in the free- spawning asteroid Acanthaster planci. The Biological Bulletin 186:17–28

Bak R, Nieuwland G, Meesters E (2005) Coral reef crisis in deep and shallow reefs: 30 years of constancy and change in reefs of Curacao and Bonaire. Coral reefs 24:475–479

Baker a, Glynn P, Riegl B (2008) Climate change and coral reef bleaching: An ecological assessment of long-term impacts, recovery trends and future outlook. Estuarine, Coastal and Shelf Science 80:435–471

Baker PA, Weber JN (1975) Coral growth rate: Variation with depth. Physics of the Earth and Planetary Interiors 10:135–139

Bare a. Y, Grimshaw KL, Rooney JJ, Sabater MG, Fenner D, Carroll B (2010) Mesophotic communities of the insular shelf at Tutuila, American Samoa. Coral Reefs 29:369–377

Barnes DJ, Lough JM (1993) On the nature and causes of density banding in massive coral skeletons. Journal of Experimental Marine Biology and Ecology 167:91–108

Bassin CJ, Washburn L, Brzezinski M, McPhee-Shaw E (2005) Sub-mesoscale coastal eddies observed by high frequency radar: A new mechanism for delivering nutrients to kelp forests in the Southern California Bight. Geophysical Research Letters 32:L12604

Baums IB, Miller MW, Szmant AM (2003) Ecology of a corallivorous gastropod, Coralliophila abbreviata, on two scleractinian hosts. I: Population structure of snails and corals. Marine Biology 142:1083–1091

Baums IB, Paris CB, Cherubin LM, Che LM (2006) A bio-oceanographic filter to larval dispersal in a reef-building coral. Physical Oceanography 51:1969–1981

Beuck L, Vertino A, Stepina E, Karolczak M, Pfannkuche O (2007) Skeletal response of Lophelia pertusa (Scleractinia) to bioeroding sponge infestation visualised with micro-computed tomography. Facies 53:157–176

Bleck R (2002) An oceanic general circulation model framed in hybrid isopycnic-Cartesian coordinates. Ocean Modelling 37:55–88

Bongaerts P, Ridgway T, Sampayo EM, Hoegh-Guldberg O (2010a) Assessing the "deep reef refugia" hypothesis: Focus on Caribbean reefs. Coral Reefs 29:309–327

Bongaerts P, Riginos C, Ridgway T, Sampayo EM, van Oppen MJH, Englebert N, Vermeulen F, Hoegh-Guldberg O (2010b) Genetic divergence across habitats in the widespread coral Seriatopora hystrix and its associated Symbiodinium. PloS one 5:e10871

Bosscher H (1993) Computerized tomography and skeletal density of coral skeletons. Coral Reefs 12:97–103

Bosscher H, Meesters EH (1992) Depth Related Changes in the Growth Rate of Montastrea annularis. 507–512

Bosscher H, Schlager W (1992) Computer-Simulation of Reef Growth. Sedimentology 39:503–512

Botsford LW, White JW, Coffroth M -a., Paris CB, Planes S, Shearer TL, Thorrold SR, Jones GP (2009) Connectivity and resilience of coral reef metapopulations in marine protected areas: Matching empirical efforts to predictive needs. Coral Reefs 28:327–337

Bozec Y-M, Yakob L, Bejarano S, Mumby PJ (2012) Reciprocal facilitation and non-linearity maintain habitat engineering on coral reefs. Oikos 122:428–440

Bridge TCL, Done TJ, Beaman RJ, Friedman A, Williams SB, Pizarro O, Webster JM (2010) Topography, substratum and benthic macrofaunal relationships on a tropical mesophotic shelf margin, central Great Barrier Reef, Australia. Coral Reefs 30:143–153

Browman HI, Stergiou KI (2004) Marine Protected Areas as a central element of ecosystem-based management : Defining their location , size and number Tuning the ecoscope for the Ecosystem Approach to Fisheries. Marine Ecology Progress Series 271–272

Brown J, Kodric-Brown A (1977) Turnover Rates in Insular Biogeography : Effect of Immigration on Extinction. Ecology 58:445–449

Buddemeier RW, Kinzie III RA (1975) The chronometric reliability of contemporary corals. In: Rosenburg G.D., Runcoorn S.K. (eds) Growth Rhythms and the History of the Earth's Rotation. John Wiley & Sons Ltd, London, pp 135–147

Burke L, Reytar K, Spalding M, Perry A (2011) Reefs at risk revisited. World Resources Institute, Washington

Bustamente G, Paris C (2008) World Heritage Sites and marine population connectivity. In: Grober-Dunsmore R., Keller B. (eds) Caribbean connectivity: Implications for marine protected area management. U.S. Department of Commerce, NOAA, National Marine Sanctuary Program, NMSP-08-07, Silver Spring, MD, pp 102–117

Carpenter KE, Abrar M, Aeby G, Aronson RB, Banks S, Bruckner A, Chiriboga A, Cortés J, Delbeek JC, Devantier L, Edgar GJ, Edwards AJ, Fenner D, Guzmán HM, Hoeksema BW, Hodgson G, Johan O, Licuanan WY, Livingstone SR, Lovell ER, Moore JA, Obura DO, Ochavillo D, Polidoro BA, Precht WF, Quibilan MC, Reboton C, Richards ZT, Rogers AD, Sanciangco J, Sheppard A, Sheppard C, Smith J, Stuart S, Turak E, Veron JEN, Wallace C, Weil E, Wood E (2008) One-third of reef-building corals face elevated extinction risk from climate change and local impacts. Science 321:560–3

Chalker BE (1981) Simulating light-saturation curves for photosynthesis and calcification by reef-building corals. Marine Biology 63:135–141

Cherubin LM, Nemeth RS, Idrisi N (2011) Flow and transport characteristics at an Epinephelus guttatus (red hind grouper) spawning aggregation site in St. Thomas (US Virgin Islands). Ecological Modelling 222:3132–3148

Chornesky E, Peters E (1987) Sexual reproduction and colony growth in the scleractinian coral Porites astreoides. The Biological Bulletin 172:161–177

Christie MR, Johnson DW, Stallings CD, Hixon M a (2010) Self-recruitment and sweepstakes reproduction amid extensive gene flow in a coral-reef fish. Molecular ecology 19:1042–57

Collingham Y, Huntley B (2000) Impacts of habitat fragmentation and patch size upon migration rates. Ecological Applications 10:131–144

Coma R, Lasker HR (1997) Effects of spatial distribution and reproductive biology on in situ fertilization rates of a broadcast-spawning invertebrate. Biological Bulletin 193:20

Cowen R, Paris C, Olson D, Fortuna J (2003) The role of long distance dispersal versus local retention in replenishing marine populations. Gulf and Caribbean Research 14:129–137

Cowen RK (2000) Connectivity of marine populations: Open or closed? Science 287:857–859

Cowen RK, Paris CB, Olson DB, Fortuna JL (2002) The role of long distance dispersal versus local retention in replenishing marine populations. Journal of Gulf and Caribbean Science 14:129–137

Cowen RK, Paris CB, Srinivasan A (2006) Scaling of connectivity in marine populations. Science 311:522–7

Cowen RK, Sponaugle S (2009) Larval dispersal and marine population connectivity. Annual Review of Marine Science 1:443–466

Crabbe MJC, Mendes JM, Warner GF (2002) Lack of recruitment of non-branching corals in Discovery Bay is linked to severe storms. Bulletin of Marine Science 70:939–945

Crabbe MJC, Smith DJ (2003) Computer modelling and estimation of recruitment patterns of non-branching coral colonies at three sites in the Wakatobi Marine Park, S.E. Sulawesi, Indonesia; implications for coral reef conservation. Computational Biology and Chemistry 27:17–27

Darwin C (1889) The structure and distribution of coral reefs. Smith, Elder & Co., London

Dodge RE, Aller RC, Thomson J (1974) Coral growth related to resuspension of bottom sediments. Nature 247:574–576

Done TJ (1983) Coral Zonation: Its Nature and Significance. In: Barnes D., Clouston B. (eds) Perspectives on Coral Reefs. Australian Institute of Marine Science, pp 107–147

Dunstan P, Dustan P (1979) Distribution of zooxanthellae and photosynthetic chloroplast pigments of the reef-building coral Montastrea annularis Ellis and Solander in relation to depth on a West Indian coral reef. Bulletin of Marine Science 29:79–95

Dustan P (1975) Growth and form in the reef-building coral Montastrea annularis. Marine Biology 33:101–107

Edinger EN, Limmon G V, Jompa J, Widjatmoko W, Heikoop JM, Risk MJ (2000) Normal coral growth rates on dying reefs: Are coral growth rates good indicators of reef health? Marine Pollution Bulletin 40:404–425

Edmunds PJ, Elahi R (2007) The demographics of a 15-year decline in cover of the Caribbean reef coral Montastraea annularis. Ecological Monographs 77:3–18

Edmunds PJ, Gates RD, Gleason DF (2001) The biology of larvae from the reef coral Porites astreoides , and their response to temperature disturbances. Marine Biology 139:981–989

Estrada E, Bodin Ö (2008) Using network centrality measures to manage landscape connectivity. Ecological Applications 18:1810–1825

Felis T, Patzold J, Loya Y, Wefer G (1998) Vertical water mass mixing and plankton blooms recorded in skeletal stable carbon isotopes of a Red Sea coral. Journal of Geophysical Research 103:731–739

Fleischmann EM (1989) The measurement and penetration of ultraviolet radiation into tropical marine water. Limnology and Oceanography 34:1623–1629

Foster NL, Paris CB, Kool JT, Baums IB, Stevens JR, Sanchez J a, Bastidas C, Agudelo C, Bush P, Day O, Ferrari R, Gonzalez P, Gore S, Guppy R, McCartney M a, McCoy C, Mendes J, Srinivasan A, Steiner S, Vermeij MJ a, Weil E, Mumby PJ (2012) Connectivity of Caribbean coral populations: Complementary insights from empirical and modelled gene flow. Molecular ecology 21:1143–57

Freeman LC (1977) A set of measures of centrality based on betweenness. Sociometry 40:35–41

Gaines SD, Gaylord B, Largier JL (2003) Avoiding current oversights in marine reserve design. Ecological Applications 13:32–46

Gardner T a, Côté IM, Gill J a, Grant A, Watkinson AR (2003) Long-term region-wide declines in Caribbean corals. Science 301:958–60

Gislason H, Sinclaire M, Sainsbury K, O'Boyle R (2000) Symposium overview: Incorporating ecosystem objectives within fisheries management. ICES Journal of Marine Science 57:468–475

Gleason DF, Danilowicz BS, Nolan CJ (2009) Reef waters stimulate substratum exploration in planulae from brooding Caribbean corals. Coral Reefs 28:549–554

Gleason DF, Edmunds PJ, Gates RD (2005) Ultraviolet radiation effects on the behavior and recruitment of larvae from the reef coral Porites astreoides. Marine Biology 148:503–512

Gleason DF, Wellington GM (1995) Variation in UVB sensitivity of planula larvae of the coral Agaricia agaricites along a depth gradient. Marine Biology 123:693–703

Glynn PW (1996) Coral reef bleaching: Facts, hypotheses and implications. Global Change Biology 1:177–509

Glynn PW, Colley SB (2008) Survival of Brooding and Broadcasting Reef Corals Following Large Scale Disturbances : Is There Any Hope for Broadcasting Species During Global Warming ? Proceedings of the 11th International Coral Reef Symposium

Goldberg W (1983) Cay Sal Bank: A biologically impoverished physically controlled environment. Atoll Research Bulletin 271:1–36

Goreau TF (1959) The Ecology of Jamaican Coral Reefs I. Species Composition and Zonation. Ecology 40:67–90

Gotelli NJ (1991) Metapopulation models: The rescue effect, the propogule rain, and the core-satellite hypothesis. The American Naturalist 138:768–776

Graham WM, Largier JL (1997) Upwelling shadows as nearshore retention sites: The example of northern Monterey Bay. Continental Shelf Research 17:509–532

Graus RR, Macintyre IG (1976) Light control of growth form in colonial reef corals: Computer simulation. Science 193:895–7

Graus RR, Macintyre IG (1982) Variation in growth forms of the reef coral Montastrea annularis (Ellis and Solander): A quantitative evaluation of growth response to light distribution using computer simulation. Smithsonian Contributions to Marine Science 12:441–464

Guzman HM, Burns KA, Jackson JBC (1994) Injury, regeneration and growth of Caribbean reef corals after a major oil spill in Panama. Marine ecology progress series 105:231–241

Guzman HM, Cipriani R, Jackson JBC (2008) Historical decline in coral reef growth after the Panama Canal. Ambio 37:342–6

Hamilton SL, Regetz J, Warner RR (2008) Postsettlement survival linked to larval life in a marine fish. Proceedings of the National Academy of Sciences of the United States of America 105:1561–6

Hanski I (1982) Dynamics of regional distribution: The core and satellite species hypothesis. Nordic Society Oikos 38:210–221

Hanski I (2001) Spatially realistic theory of metapopulation ecology. Biological Conservation 372–381

Hanski I (2003) Metapopulation theory for fragmented landscapes. Theoretical Population Biology 64:119–127

Hanski I, Ovaskainen O (2000) The metapopulation capacity of a fragmented landscape. Nature 404:755–8

Harrison HB, Williamson DH, Evans RD, Almany GR, Thorrold SR, Russ GR, Feldheim K a, van Herwerden L, Planes S, Srinivasan M, Berumen ML, Jones GP (2012) Larval export from marine reserves and the recruitment benefit for fish and fisheries. Current Biology 22:1023–8

Harrison PL, Wallace CC (1990) Reproduction, dispersal and recruitment of scleractinian corals. In: Dubinsky Z. (eds) Coral Reefs. Ecosystems of the World V 25. Elsevier Science Publishing Company, Inc., Amsterdam, pp 133–207

Hill MO (1973) Diversity and Evenness : A Unifying Notation and Its Consequences. Ecology 54:427–432

Hoegh-Guldberg O, Mumby PJ, Hooten a J, Steneck RS, Greenfield P, Gomez E, Harvell CD, Sale PF, Edwards a J, Caldeira K, Knowlton N, Eakin CM, Iglesias-Prieto R, Muthiga N, Bradbury RH, Dubi A, Hatziolos ME (2007) Coral reefs under rapid climate change and ocean acidification. Science 318:1737–42

Hudson JH (1981) Growth rates in Montastraea annularis: A record of environmental change in Key Largo Coral Reef Marine Sanctuary, Florida. Bulletin of Marine Science 31:444–459

Hudson JH, Shinn EA, Halley RB, Lidz B (1976) Sclerochronology: A tool for interpreting past environments. Geology 4:361–364

Hughes TP, Baird AH, Bellwood DR, Card M, Connolly SR, Folke C, Grosberg R, Hoegh-Guldberg O, Jackson JBC, Kleypas J, Lough JM, Marshall P, Nystrom M, Palumbi SR, Pandolfi JM, Rosen B, Roughgarden J (2003a) Climate change, human impacts, and the resilience of coral reefs. Science 301:929–933

Hughes TP, Baird AH, Bellwood DR, Connolly SR, Folke C, Grosberg R, Hoegh-Guldberg O, Jackson JBC, Kleypas J, Lough JM, Marshall P, Nystrom M, Palumbi SR, Pandolfi JM, Rosen B, Roughgarden J, Aronson RB, Bruno JF, Precht WF, Glynn PW, Harvell CD, Kaufman L, Rogers CS, Shinn EA, Valentine JF (2003b) Causes of coral reef degradation - Response. Science 302:1503–1504

Hughes TP, Rodrigues MJ, Bellwood DR, Ceccarelli D, Hoegh-Guldberg O, McCook L, Moltschaniwskyj N, Pratchett MS, Steneck RS, Willis B (2007) Phase shifts, herbivory, and the resilience of coral reefs to climate change. Current Biology 17:360–365

Hughes TP, Tanner JE (2000) Recruitment failure, life histories, and long-term decline of Caribbean corals. Ecology 81:2250–2263

Huston M (1985) Variation in coral growth rates with depth at Discovery Bay, Jamaica. Coral Reefs 4:19–25

Jackson JBC, Kirby MX, Berger WH, Bjorndal KA, Botsford LW, Bourque BJ, Bradbury RH, Cooke R, Erlandson J, Estes JA, Hughes TP, Kidwell S, Lange CB, Lenihan HS, Pandolfi JM, Peterson CH, Steneck RS, Tegner MJ, Warner RR (2001) Historical overfishing and the recent collapse of coastal ecosystems. Science 293:629–638

James N, Ginsburg RN (1980) The morphology, sediments and organisms of the deep barrier reef and fore-reef. The Seward Margin of Belize Barrier and Atoll Reefs: Morphology, Sedimentology, Organism Distribution and Late Quaternary History. Blackwekk Publishing Ltd., Oxford, UK,

Johnson DB (1977) Efficient algorithms for shortest paths in sparse networks. Journal of the ACM 24:1–13

Jost L (2006) Entropy and diversity. Oikos 113:363–375

Kahng SE, Garcia-Sais JR, Spalding HL, Brokovich E, Wagner D, Weil E, Hinderstein L, Toonen RJ (2010) Community ecology of mesophotic coral reef ecosystems. Coral Reefs 29:255–275

Keppel G, Van Niel KP, Wardell-Johnson GW, Yates CJ, Byrne M, Mucina L, Schut AGT, Hopper SD, Franklin SE (2012) Refugia: Identifying and understanding safe havens for biodiversity under climate change. Global Ecology and Biogeography 21:393–404

Kininmonth S, Drechsler M, Johst K, Possingham H (2010) Metapopulation mean life time within complex networks. Marine Ecology Progress Series 417:139–149

Kinzie III RA (1973) The zonation of West Indian gorgonians. Bulletin of Marine Science 23:93–155

Knowlton N, Weil E, Weigt LA, Guzmán HM (1992) Sibling species in Montastraea annularis, coral bleaching, and the coral climate record. Science 255:330–3

Kojis BL, Quinn NJ (1984) Season and depth variation in fecundity of Acropora palifera at two reefs in Papua New Guinea. Coral Reefs 3:165–172

Kough AS, Paris CB, Butler MJ (2013) Larval Connectivity and the International Management of Fisheries. PLoS ONE 8:e64970

Kruszyński KJ, Kaandorp J a., Liere R (2007) A computational method for quantifying morphological variation in scleractinian corals. Coral Reefs 26:831–840

Largier JL (2003) Considerations in estimating larval dispersal distances from oceanographic data. Ecological Applications 13:71–89

Lasker HRH, Brazeau D a., Calderon J, Coffroth MA, Coma R, Kim K (1996) In situ rates of fertilization among broadcast spawning gorgonian corals. The Biological Bulletin 190:45

Leichter J, Genovese S (2006) Intermittent upwelling and subsidized growth of the scleractinian coral Madracis mirabilis on the deep fore-reef slope of Discovery Bay, Jamaica. Marine Ecology Progress Series 316:95–103

Leichter J, Shellenbarger G, Genovese S, Wing S (1998) Breaking internal waves on a Florida (USA) coral reef: A plankton pump at work? Marine Ecology Progress Series 166:83–97

Leichter J, Stokes M, Genovese S (2008) Deep water macroalgal communities adjacent to the Florida Keys reef tract. Marine Ecology Progress Series 356:123–138

Leichter JJ, Stewart HL, Miller SL (2003) Episodic nutrient transport to Florida coral reefs. Limnology and Oceanography 48:1394–1407

Leis JM, McCormick MI (2002) The biology, behavior and ecology of the pelagic larval stage of coral reef fishes. In: Sale P.F. (eds) Coral Reef Fishes: Dynamics and Diversity in a Complex Ecosystem. Academic Press, San Diego, California, USA, pp 171–199

Lesser MP, Slattery M, Leichter JJ (2009) Ecology of mesophotic coral reefs. Journal of Experimental Marine Biology and Ecology 375:1–8

Levitan D (2000) Sperm velocity and longevity trade off each other and influence fertilization in the sea urchin Lytechinus variegatus. Proceedings of the Royal Society B 267:531-534

Levitan D, Fukami H, Jara J, Kline D, McGovern T (2004) Mechanisms of reproductive isolation among sympatric broadcast-spawning corals of the Montastraea annularis species complex. Evolution 58:308–323

Lewis JB (1977) Processes of organic production on coral reefs. Biological Reviews 52:305–347

Liddell WD, Ohlhorst SL (1988) Hard Substrata Community Patterns , North Jamaica1. Palaios 3:413–423

Limouzy-paris CB, Graber HC, Jones DL, Ropke AW, Richards WJ (1997) Translocation of larval coral reef fishes via sub-mesoscale spin-off eddies from the Florida current. Bulletin of Marine Science 60:966–983

Lipphardt BL, Small D, Kirwan a. D, Wiggins S, Ide K, Grosch CE, Paduan JD (2006) Synoptic Lagrangian maps: Application to surface transport in Monterey Bay. Journal of Marine Research 64:221–247

Locker SD, Armstrong R a., Battista T a., Rooney JJ, Sherman C, Zawada DG (2010) Geomorphology of mesophotic coral ecosystems: Current perspectives on morphology, distribution, and mapping strategies. Coral Reefs 29:329–345

Lough J, Barnes D (2000) Environmental controls on growth of the massive coral Porites. Journal of Experimental Marine Biology and Ecology 245:225–243

Loya Y (1972) Community structure and species diversity of hermatypic corals at Eilat , Red Sea. Marine Biology 13:100–123

Mayer AG (1915) Ecology of the Murray Island Coral Reef. Proceedings of the National Academy of Sciences of the United States of America 1:211–214

McGuire MP (1997) The biology of the coral Porites astreoides: Reproduction, larval settlement behavior and responses to ammonium enrichment. Disseration

Mcguire MP (1998) Timing of larval release by Porites astreoides in the northern Florida Keys. Coral Reefs 17:369–375

Menza C, Kendall M, Hile S (2008) The deeper we go the less we know. Revista De Biologia Tropical 56:11–24

Menza C, Kendall M, Rogers C, Miller J (2007) A deep reef in deep trouble. Continental Shelf Research 27:2224–2230

Miller J, Muller E, Rogers C, Waara R, Atkinson a., Whelan KRT, Patterson M, Witcher B (2009) Coral disease following massive bleaching in 2005 causes 60% decline in coral cover on reefs in the US Virgin Islands. Coral Reefs 28:925–937

Miller MW, Weil E, Szmant AM (2000) Coral recruitment and juvenile mortality as structuring factors for reef benthic communities in Biscayne National Park, USA. Coral Reefs 19:115–123

Moilanen A (1998) Metapopulation dynamics: Effects of habitat quality and landscape structure. Ecology 79:2503

Moore AM, Arango HG, Di Lorenzo E, Cornuelle BD, Miller AJ, Neilson DJ (2004) A comprehensive ocean prediction and analysis system based on the tangent linear and adjoint of a regional ocean model. Ocean Modelling 7:227–258

Mumby PJ, Elliott I a, Eakin CM, Skirving W, Paris CB, Edwards HJ, Enríquez S, Iglesias-Prieto R, Cherubin LM, Stevens JR (2011a) Reserve design for uncertain responses of coral reefs to climate change. Ecology letters 14:132–40

Mumby PJ, Harborne AR (2010) Marine reserves enhance the recovery of corals on Caribbean reefs. PloS one 5:e8657

Mumby PJ, Vitolo R, Stephenson DB (2011b) Temporal clustering of tropical cyclones and its ecosystem impacts. Proceedings of the National Academy of Sciences of the United States of America 108:17626–17630

Munday PL, Leis JM, Lough JM, Paris CB, Kingsford MJ, Berumen ML, Lambrechts J (2009) Climate change and coral reef connectivity. Coral Reefs 28:379–395

Muscatine L, Porter JW, Kaplan IR (1989) Resource partitioning by reef corals as from stable isotope composition. Marine Biology 100:185–193

Naumann MS, Niggl W, Laforsch C, Glaser C, Wild C (2009) Coral surface area quantification–evaluation of established techniques by comparison with computer tomography. Coral Reefs 28:109–117

Nemeth RS, Smith TB, Blondeau J, Kadison E, Calnan JM, Gass J (2008) Characterization of deep water reef communities within the Marine Conservation District, St. Thomas, U.S. Virgin Islands: Final report. Caribbean Fisheries Management Council

Okubo A (1980) Diffusion and Ecological Problems: Mathematical Models. Biomathematics, Vol. 10. Springer-Verlag, Berlin-Heidelberg-New York, pp 254

Oliver J, Babcock R (1992) Aspects of the fertilization ecology of broadcast spawning corals: Sperm dilution effects and in situ measurements of fertilization. Biological Bulletin 183:409

Van Oppen MJH, Bongaerts P, Underwood JN, Peplow LM, Cooper TF (2011) The role of deep reefs in shallow reef recovery: An assessment of vertical connectivity in a brooding coral from west and east Australia. Molecular Ecology 20:1647–60

Pandolfi J, Budd A (2008) Morphology and ecological zonation of Caribbean reef corals: The Montastraea "annularis" species complex. Marine Ecology Progress Series 369:89–102

Pandolfi JM, Bradbury RH, Sala E, Hughes TP, Bjorndal KA, Cooke RG, McArdle D, McClenachan L, Newman MJH, Paredes G, Warner RR, Jackson JBC (2003) Global trajectories of the long-term decline of coral reef ecosystems. Science 301:955–958

Pandolfi JM, Connolly SR, Marshall DJ, Cohen AL (2011) Projecting coral reef futures under global warming and ocean acidification. Science 333:418–22

Pandolfi JM, Jackson JBC, Baron N, Bradbury RH, Guzman HM, Hughes TP, Kappel C V, Micheli F, Ogden JC, Possingham HP, Sala E (2005) Are US coral reefs on the slippery slope to slime? Science 307:1725–1726

Paris C, Chérubin L, Cowen R (2007) Surfing, spinning, or diving from reef to reef: Effects on population connectivity. Marine Ecology Progress Series 347:285–300

Paris CB, Cowen RK (2004) Direct evidence of a biophysical retention mechanism for coral reef fish larvae. Limnology and Oceanography 49:1964–1979

Paris CB, Cowen RK, Claro R, Lindeman KC (2005) Larval transport pathways from Cuban snapper (Lutjanidae) spawning aggregations based on biophysical modeling. Marine Ecology Progress Series 296:93–106

Paris CB, Cowen RK, Lwiza KMM, Wang D, Olson DB (2002) Multivariate objective analysis of the coastal circulation of Barbados, West Indies: Implication for larval transport. Deep-Sea Research 49:1363–1386

Paris CB, Guigand CM, Irisson J, Fisher R, Alessandro D (2008) Orientation with No Frame of Reference (OWNFOR): A Novel System to Observe and Quantify Orientation in Reef Fish Larvae. In: Grober-Dunsmore R., Keller B.D. (eds) Caribbean connectivity: Implications for marine protected area management. Proceedings of a Special Symposium, 9-11 November 2006, 59th Annual Meeting of the Gulf and Caribbean Fisheries Institute. Marine Sanctuaries Conservation Series ONMS-08-07. U.S. Department of Commerce, National Oceanic and Atmospheric Administration, Office of National Marine Sanctuaries, Silver Spring, MD, Belize City, Belize, pp 54–64

Paris CB, Helgers J, van Sebille E, Srinivasan A (2013) Connectivity Modeling System: A probabilistic modeling tool for the multi-scale tracking of biotic and abiotic variability in the ocean. Environmental Modelling & Software 42:47–54

Pauly D (1995) Anecdotes and the shifting baseline syndrome of fisheries. Trends in Ecology & Evolution 10:430

Pauly D, Christensen V, Guénette S, Pitcher TJ, Sumaila UR, Walters CJ, Watson R, Zeller D (2002) Towards sustainability in world fisheries. Nature 418:689–95

Pelc R a, Warner RR, Gaines SD, Paris CB (2010) Marine Reserves Special Feature: Detecting larval export from marine reserves. Proceedings of the National Academy of Sciences of the United States of America 107:18266–71

Pomar L (2001) Types of carbonate platforms: A genetic approach. Basin Research 13:313–334

Prada C, Hellberg ME (2013) Long prereproductive selection and divergence by depth in a Caribbean candelabrum coral. Proceedings of the National Academy of Sciences of the United States of America 2012:1–6

Purcell JFH, Cowen RK, Hughes CR, Williams D a (2006) Weak genetic structure indicates strong dispersal limits: A tale of two coral reef fish. Proceedings of the Royal Society B 273:1483–90

Richmond RH (1987) Energetic relationships and biogeographical differences among fecundity, growth and reproduction in the reef coral pocillopora damicornis. Bulletin of Marine Science 41:594–604

Riegl B, Piller WE (2003) Possible refugia for reefs in times of environmental stress. International Journal of Earth Sciences 92:520–531

Rinkevich B, Loya Y (1987) Variability in the pattern of sexual reproduction of the coral Stylophora pistillata at Eilat, Red Sea: A long-term study. Biological Bulletin 173:335–344

Risk MJ, Sammarco PW, Schwarcz HP (1994) Cross-continental shelf trends in δ13C in coral on the Great Barrier Reef. Marine Ecology Progress Series 106:121–130

Roche RC, Abel R a., Johnson KG, Perry CT (2010a) Quantification of porosity in Acropora pulchra (Brook 1891) using X-ray micro-computed tomography techniques. Journal of Experimental Marine Biology and Ecology 396:1–9

Roche RC, Abel RL, Johnson KG, Perry CT (2010b) Spatial variation in porosity and skeletal element characteristics in apical tips of the branching coral Acropora pulchra (Brook 1891). Coral Reefs 30:195–201

Rozenfeld AF, Arnaud-Haond S, Hernández-García E, Eguíluz VM, Serrão E a, Duarte CM (2008) Network analysis identifies weak and strong links in a metapopulation system. Proceedings of the National Academy of Sciences of the United States of America 105:18824–9

Sale PF, Cowen RK, Danilowicz BS, Jones GP, Kritzer JP, Lindeman KC, Planes S, Polunin NVC, Russ GR, Sadovy YJ, Steneck RS (2005) Critical science gaps impede use of no-take fishery reserves. Trends in Ecology & Evolution 20:74–80

Schindelin J, Arganda-Carreras I, Frise E, Kaynig V, Longair M, Pietzsch T, Preibisch S, Rueden C, Saalfeld S, Schmid B, Tinevez J-Y, White DJ, Hartenstein V, Eliceiri K, Tomancak P, Cardona A (2012) Fiji: An open-source platform for biological-image analysis. Nature Methods 9:676–82

Shanks AL (2009) Pelagic larval duration and dispersal distance revisited. The Biological Bulletin 216:373–85

Shchepetkin AF (2003) A method for computing horizontal pressure-gradient force in an oceanic model with a nonaligned vertical coordinate. Journal of Geophysical Research 108:3090

Shchepetkin AF, McWilliams JC (2005) The regional oceanic modeling system (ROMS): A split-explicit, free-surface, topography-following-coordinate oceanic model. Ocean Modelling 9:347–404

Shinn EA (1966) Coral growth-rate, and environmental indicator. Journal of Paleontology 40:233–240

Slattery M, Lesser MP, Brazeau D, Stokes MD, Leichter JJ (2011) Connectivity and stability of mesophotic coral reefs. Journal of Experimental Marine Biology and Ecology 408:32–41

Smith TB, Blondeau J, Nemeth RS, Pittman J, Calnan JM, Kadison E, Gass J, Pittman SJ (2010) MCE: Benthic structure and cryptic mortality in a Caribbean mesophotic coral reef bank system, the Hind Bank Marine Conservation District, U.S. Virgin Islands. Coral Reefs 29:289–308

Smith TB, Brandt ME, Calnan JM, Kadison E, Taylor M, Rothenberger J (2013) Convergent mortality responses of Caribbean coral species to seawater warming. Ecosphere in press

Smith TB, Kadison E, Henderson L, Gyory J, Brandt ME, Calnan JM, Kammann M, Wright V, Nemeth RS, Rothenberger J (2011) The United States Virgin Islands Territorial Coral Reef Monitoring Program. 2011 Annual Report.

Smith TB, Nemeth RS, Blondeau J, Calnan JM, Kadison E, Herzlieb S (2008) Assessing coral reef health across onshore to offshore stress gradients in the US Virgin Islands. Marine Pollution Bulletin 56:1983–91

Sponaugle S, Grorud-Colvert K, Pinkard D (2006) Temperature-mediated variation in early life history traits and recruitment success of the coral reef fish Thalassoma bifasciatum in the Florida Keys. Marine Ecology Progress Series 308:1–15

Sponaugle S, Lee T, Kourafalou V, Pinkard D (2005) Florida Current frontal eddies and the settlement of coral reef fishes. Limnology and Oceanography 50:1033–1048

Sponaugle S, Paris C, Walter K, Kourafalou V, D'Alessandro E (2012) Observed and modeled larval settlement of a reef fish to the Florida Keys. Marine Ecology Progress Series 453:201–212

Staaterman E, Paris CB, Helgers J (2012) Orientation behavior in fish larvae: A missing piece to Hjort's critical period hypothesis. Journal of Theoretical Biology 304:188–96

Steneck RS (2006) Staying Connected in a Turbulent World. Science 311:480–1

Steneck RS, Paris CB, Arnold SN, Ablan-Lagman MC, Alcala a. C, Butler MJ, McCook LJ, Russ GR, Sale PF (2009) Thinking and managing outside the box: Coalescing connectivity networks to build region-wide resilience in coral reef ecosystems. Coral Reefs 28:367–378

Swearer SE (2001) Self-recruitment in coral-reef fish populations. University of California, Santa Barbara, CA,

Swearer SE, Caselle JE, Lea DW, Warner RR (1999) Larval retention and recruitment in an island population of a coral-reef fish. Nature 402:799–802

Szmant A (1986) Reproductive ecology of Caribbean reef corals. Coral Reefs 5:43–54

Szmant AAM (1991) Sexual reproduction by the Caribbean reef corals Montastrea annularis and M. cavernosa. Marine Ecology Progress Series 74:13–25

Szmant AM (1985a) Sexual reproduction of Favia fragum (Esper): Lunar patterns of Gametogenesis, embryogenesis and planularion in Puerto Rico. Bulletin of Marine Science 37:880–892

Szmant AM (1985b) The effect of colony size on the reproductive ability of the Caribbean coral Montastrea Annularis (Ellis and Solander). Proceedings of the Fifth International Coral Reef Congress 4:295–300

Szmant AM, Meadows MG (2006) Developmental changes in coral larval buoyancy and vertical swimming behavior: Implications for dispersal and connectivity. Proceedings of 10th International Coral Reef Symposium 431–437

Szmant AM, Weil E, Miller MW, Colon DE (1997) Hybridization within the species complex of the scleractinan coral Montastraea annularis. Marine Biology 129:561–572

Tay YC, Guest JR, Chou LM, Todd P a. (2011) Vertical distribution and settlement competencies in broadcast spawning coral larvae: Implications for dispersal models. Journal of Experimental Marine Biology and Ecology 409:324–330

Tilman D, May RM, Lehman CL, Nowak MA (1994) Habitat destruction and the extinction debt. Nature 371:65–66

Treml EA, Halpin PN (2012) Marine population connectivity identifies ecological neighbors for conservation planning in the Coral Triangle. Conservation Letters 5:441–449

Treml EA, Halpin PN, Urban DL, Pratson LF (2008) Modeling population connectivity by ocean currents, a graph-theoretic approach for marine conservation. Landscape Ecology 23:19–36

Underwood JN, Smith LD, Van Oppen MJH, Gilmour JP (2007) Multiple scales of genetic connectivity in a brooding coral on isolated reefs following catastrophic bleaching. Molecular Ecology 16:771–84

Urban D, Keitt T (2001) Landscape connectivity: A graph-theoretic perspective. Ecology 82:1205–1218

Vago R, Shai Y, Ben-Zion M, Dubinsky Z, Achituv Y (1994) Computerized tomography and image analysis: A tool for examining the skeletal characteristics of reef-building organisms. Limnology and Oceanography 39:448–452

Van Veghel MLJ (1994) Reproductive characteristics of the polymorphic Caribbean reef building coral Montastrea annularis. I . Gametogenesis and spawning behavior. Marine Ecology Progress Series 109:209–219

Venn AA, Weber FK, Loram JE, Jones RJ (2008) Deep zooxanthellate corals at the high latitude Bermuda Seamount. Coral Reefs 28:135–135

Vermeij MJA, Fogarty ND, Miller MW (2006) Pelagic conditions affect larval behavior, survival, and settlement patterns in the Caribbean coral Montastraea faveolata. Marine Ecology Progress Series 310:119–128

Vikebø F, Jørgensen C, Kristiansen T, Fiksen Ø (2007) Drift, growth, and survival of larval Northeast Arctic cod with simple rules of behaviour. Marine Ecology Progress Series 347:207–219

Villinski JT (2003) Depth-independent reproductive characteristics for the Caribbean reef-building coral Montastraea faveolata. Marine Biology 142:1043–1053

Vize PD (2006) Deepwater broadcast spawning by Montastraea cavernosa, Montastraea franksi, and Diploria strigosa at the Flower Garden Banks, Gulf of Mexico. Coral Reefs 25:169–171

Vuilleumier S, Possingham HP (2006) Does colonization asymmetry matter in metapopulations? Proceedings. Biological sciences / The Royal Society 273:1637–42

Warner JC, Sherwood CR, Arango HG, Signell RP (2005) Performance of four turbulence closure models implemented using a generic length scale method. Ocean Modelling 8:81–113

Weil E, Knowlton N (1994) A Multi-Character Analysis of the Caribbean Coral Montastraea Annularis (Ellis and Solander, 1786) and its Two Sibling Species, M. Faveolata (Ellis and Solander, 1786) and M. Franksi (Gregory, 1895). Bulletin of Marine Science 55:151–175

Wellington GM, Fitt WK (2003) Influence of UV radiation on the survival of larvae from broadcast-spawning reef corals. Marine Biology 143:1185–1192

Wellington GM, Glynn PW, Strong AE, Navarrete SA, Wieters E, Hubbard D (2001) Crisis on coral reefs linked to climate change. Eos, Transactions American Geophysical Union 82:1–1

West JM, Salm R V. (2003) Resistance and resilience to coral bleaching: Implications for coral reef conservation and management. Conservation Biology 17:956–967

Wilkinson C (2008) Status of Coral Reefs of the World: 2008. Global Coral Reef Monitoring Network and Reef and Rainforest Research Centre, Townsville, Australia

Wilkinson C, Souter D (2008) Status of Caribbean Coral Reefs after Bleaching and Hurricanes in 2005. Global Coral Reef Monitoring Network and Reef and Rainforest Research Centre, Townsville, Australia

Van Woesik R (2009) Calm before the spawn: Global coral spawning patterns are explained by regional wind fields. Proceedings. Biological sciences / The Royal Society 277:715–22

Wolgast LJ, Zeide B (1983) Reproduction of trees in a variable environment. Botanical Gazette 144:260–262

Xu D, Cui J, Bansal R, Hao X, Liu J, Chen W, Peterson BS (2009) The ellipsoidal area ratio: An alternative anisotropy index for diffusion tensor imaging. Magnetic resonance imaging 27:311–23

Appendix A. This appendix contains monthly vertical migration matrices (M_T) and normalized probability of arrival matrices ($\breve{M}_T$) for *M. faveolata* and *P. astreoides* in 2007 and 2008. They are included here for reference, and to illustrate intra- and inter-annual variability in larval retention and vertical migration.

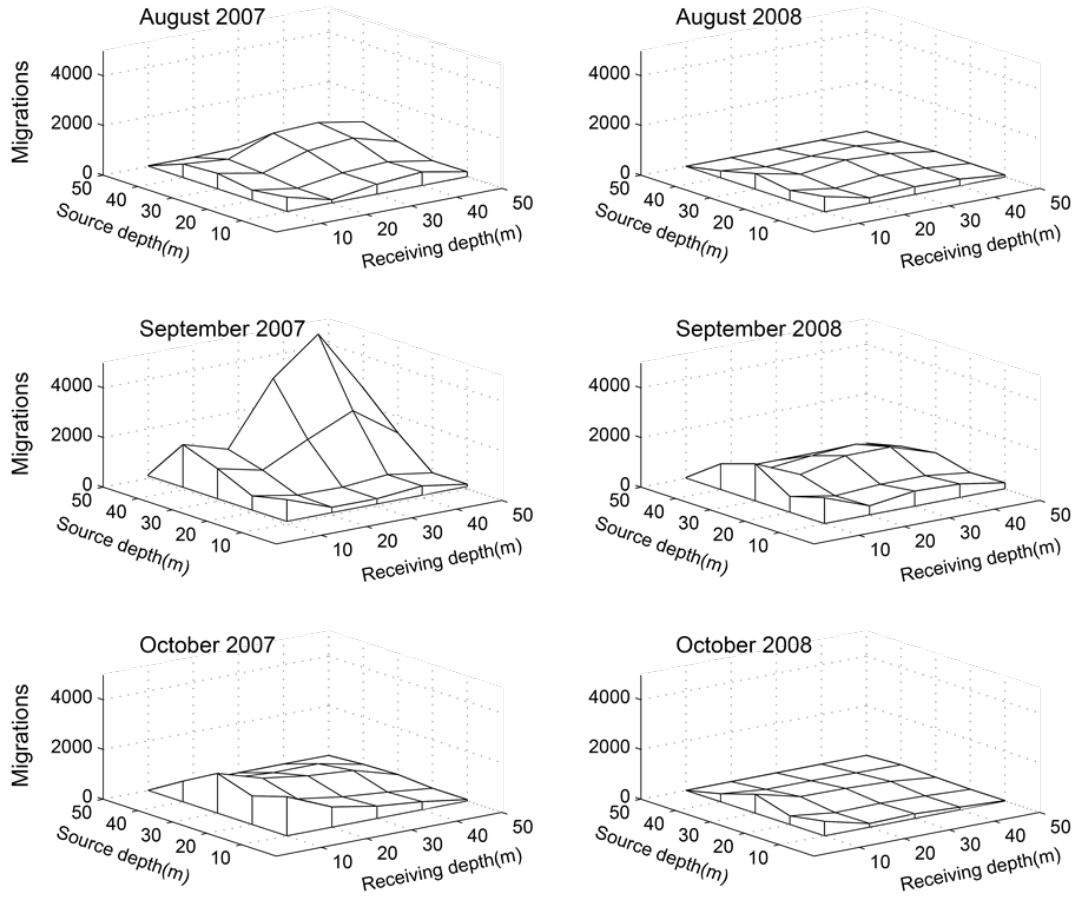

A.01. *M. faveolata* – M_T – passive scenario

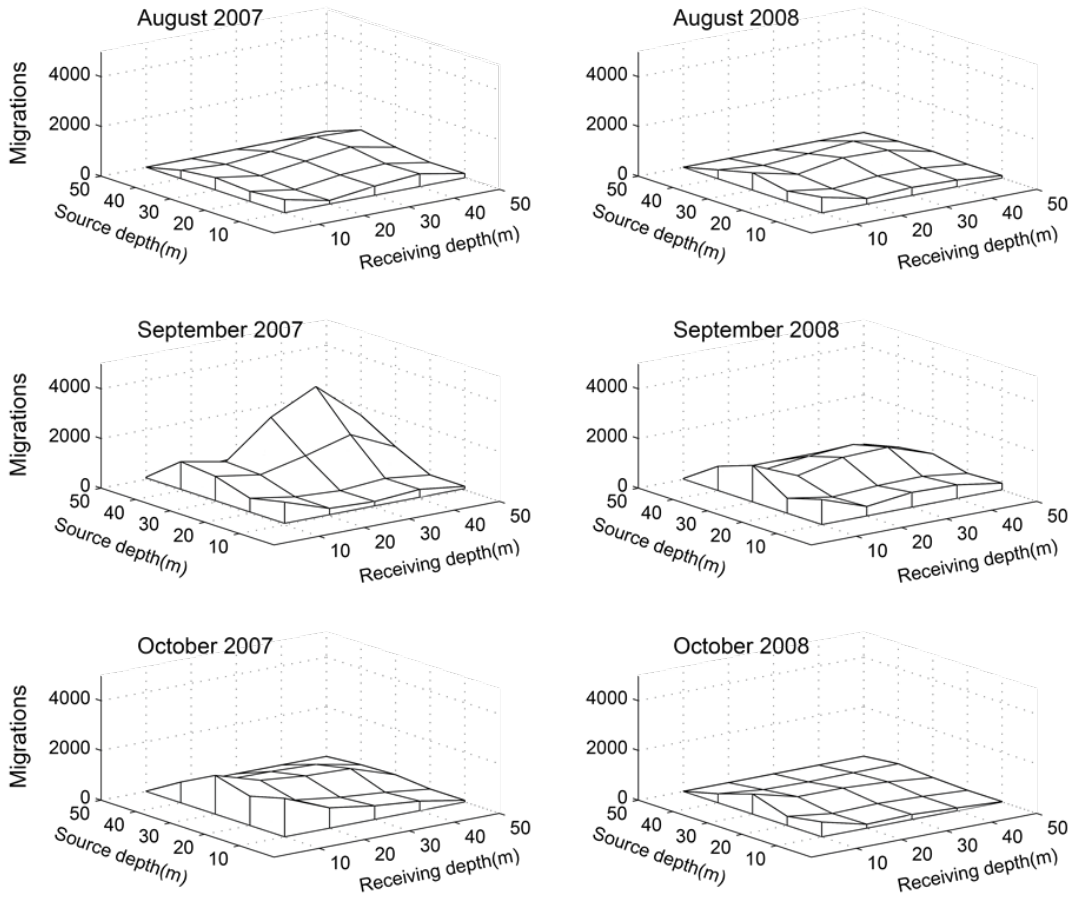

A.02. *M. faveolata* – M_T – active scenario

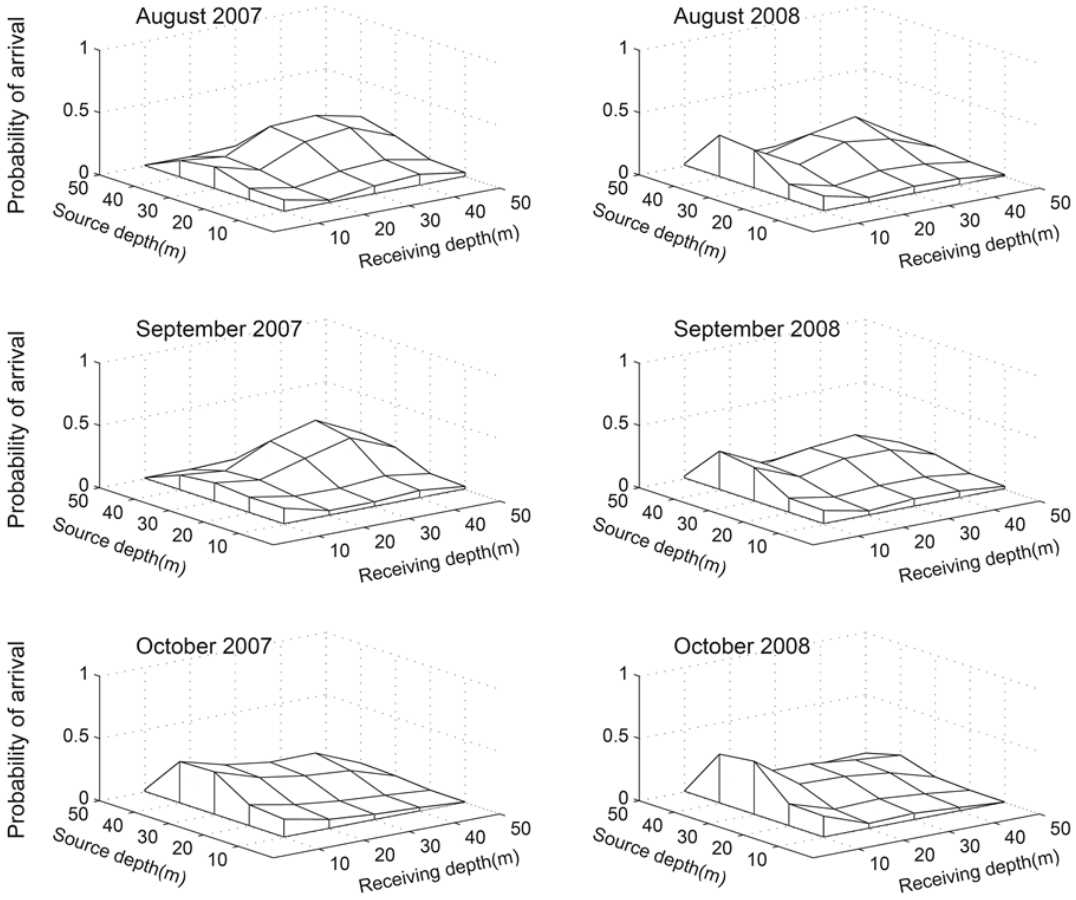

A.03 *M. faveolata* – $\breve{M}_T$ – passive scenario

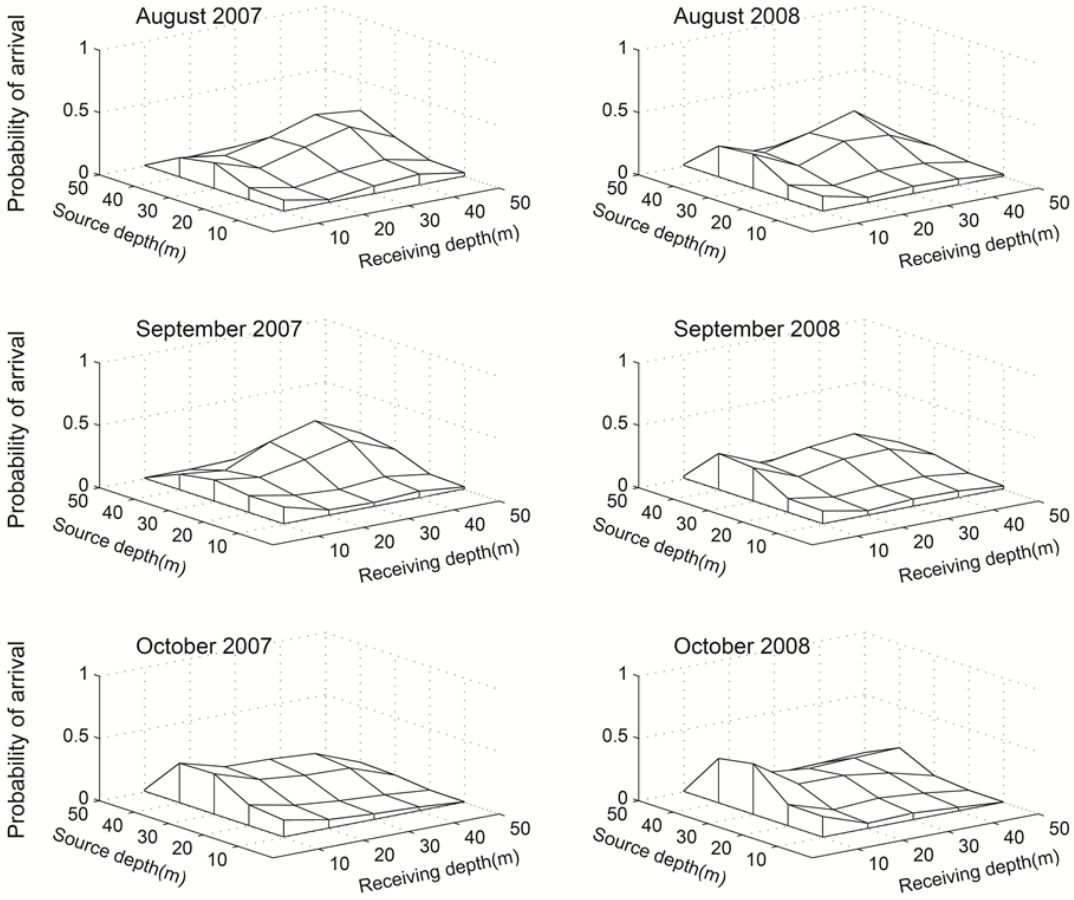

A.04 *M. faveolata* – $\breve{M}_T$ – active scenario

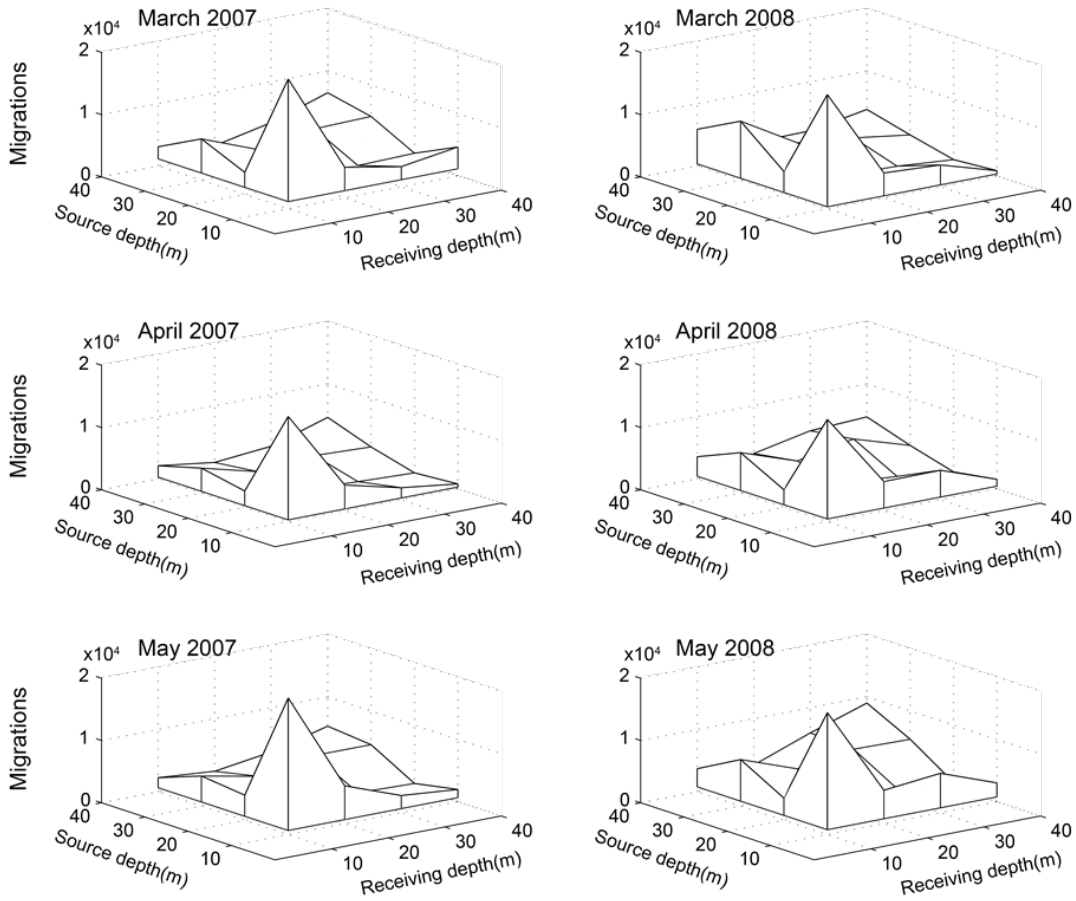

A.05 *P. astreoides* – M_T – passive scenario – March-May

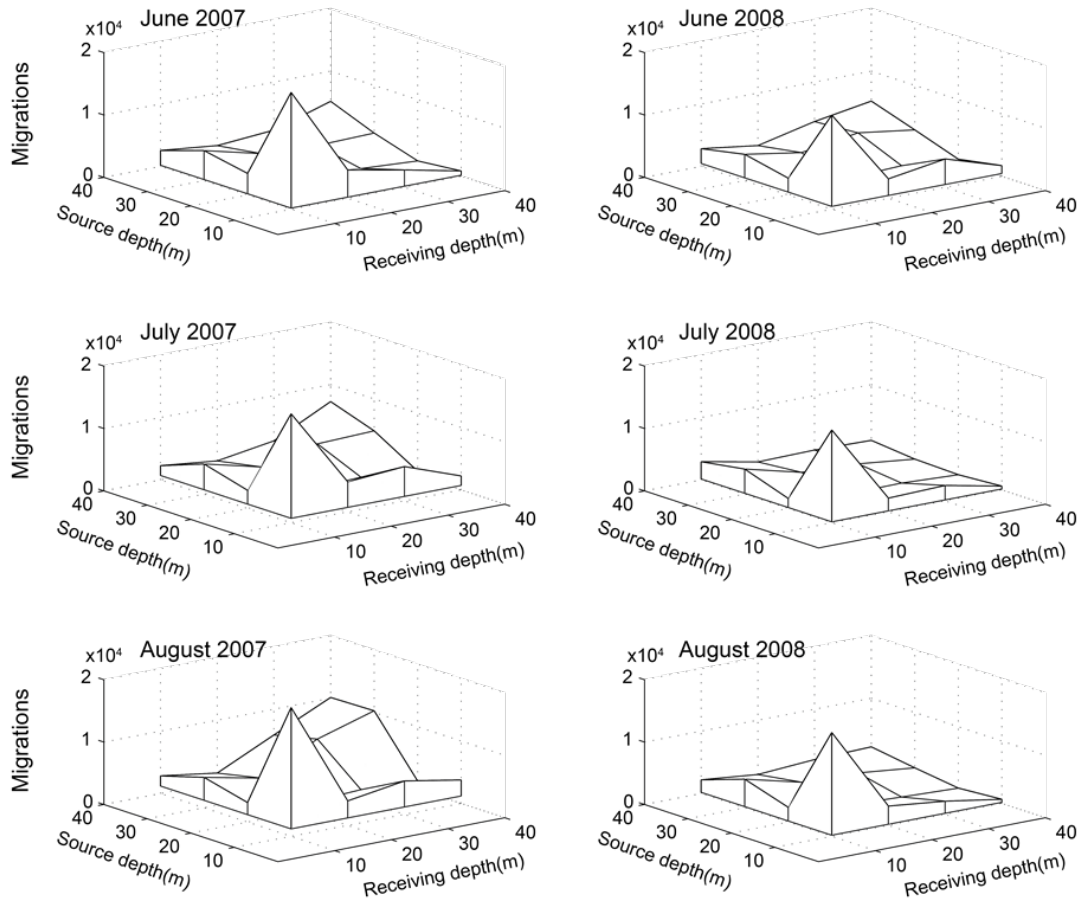

A.06 *P. astreoides* – M_T – passive scenario – June-August

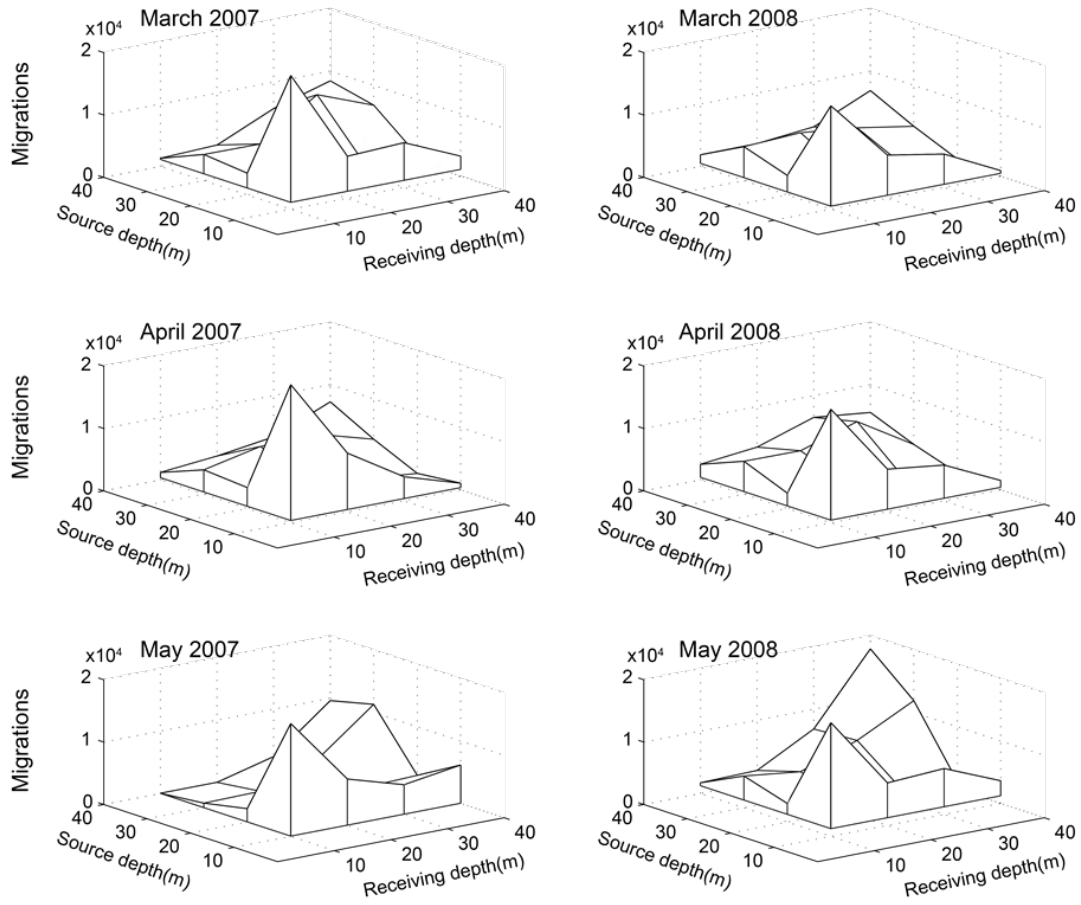

A.07 *P. astreoides* – M_T – active scenario – March-May

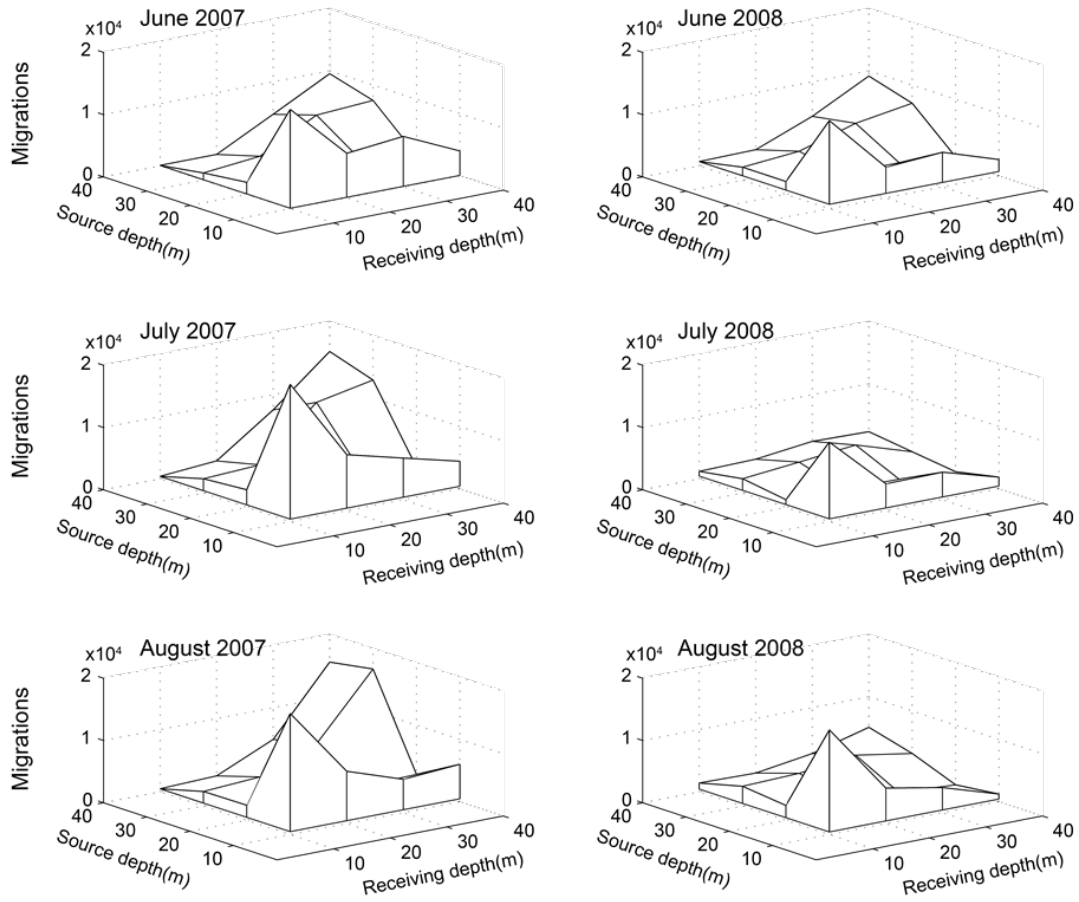

A.08 *P. astreoides* – M_T – active scenario – June-August

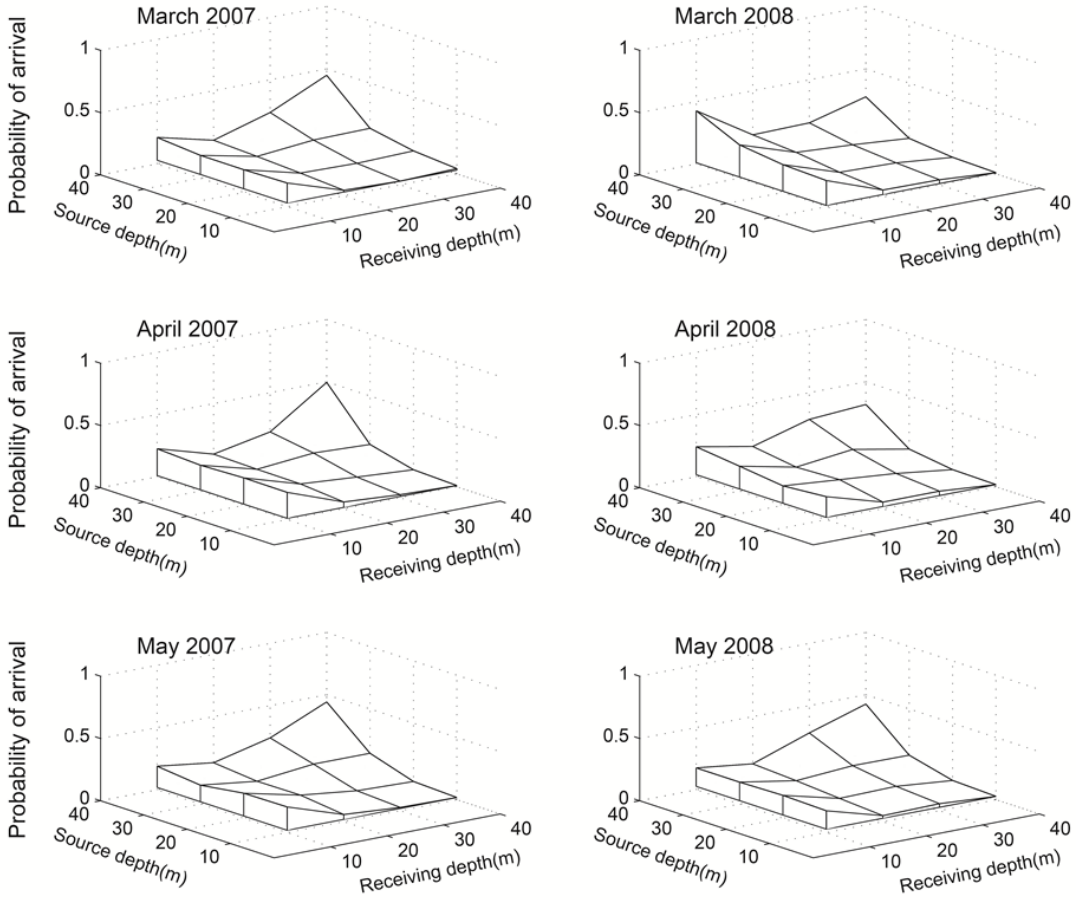

A.09 *P. astreoides* – $\breve{M}_T$ – passive scenario – March-May

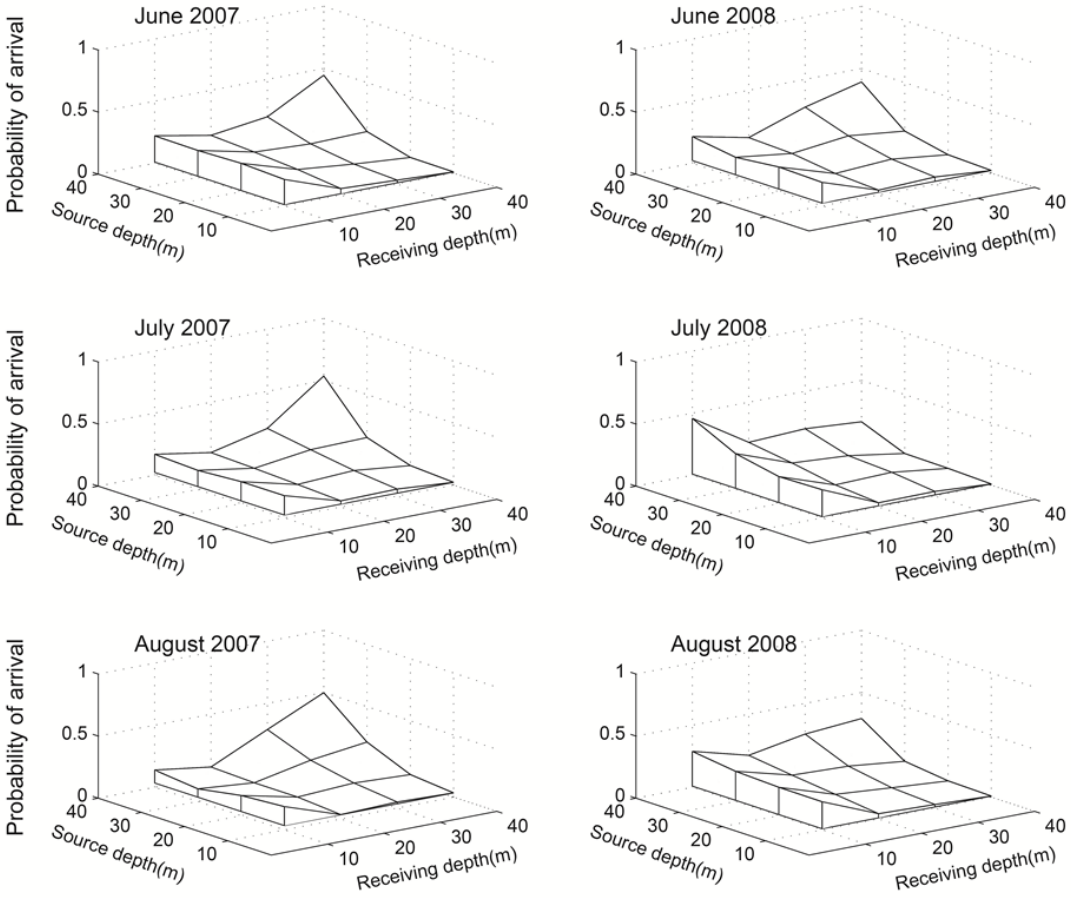

A.10 *P. astreoides* – $\widetilde{M}_T$ – passive scenario – June-August

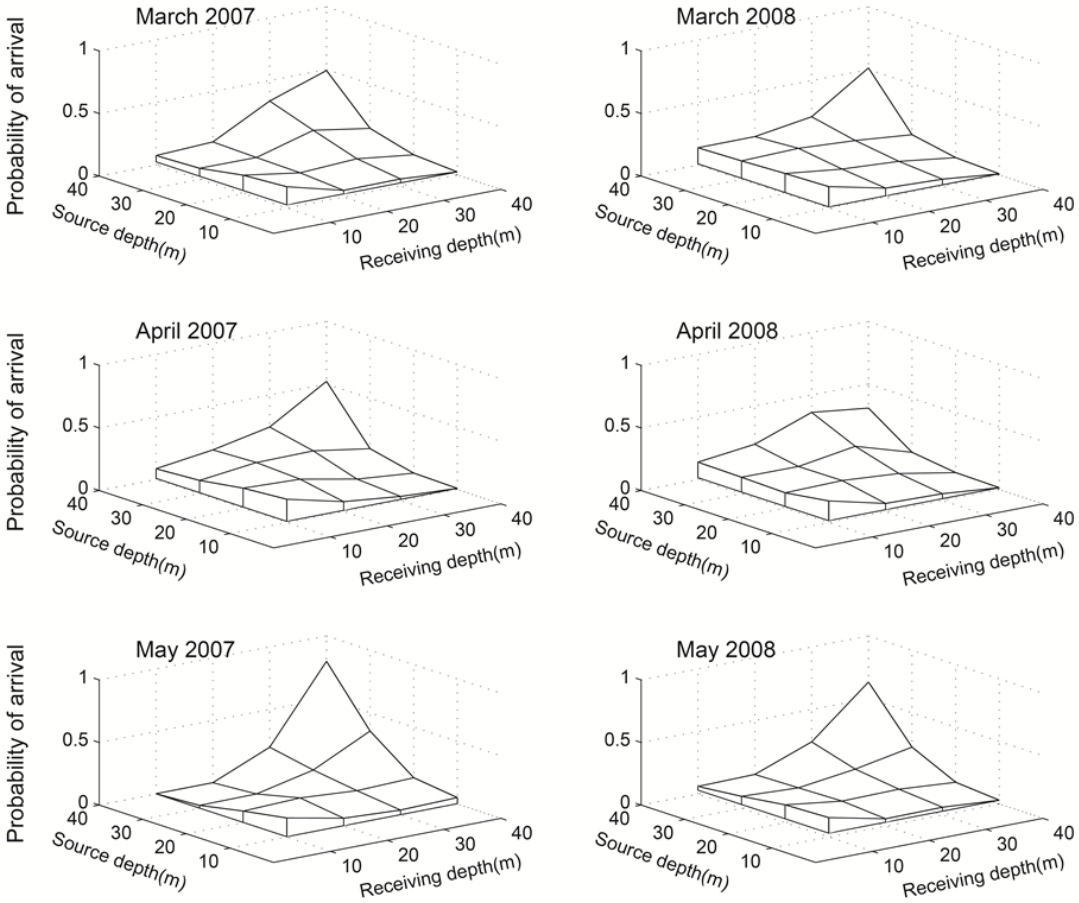

A.11 *P. astreoides* – $\breve{M}_T$ – active scenario – March-May

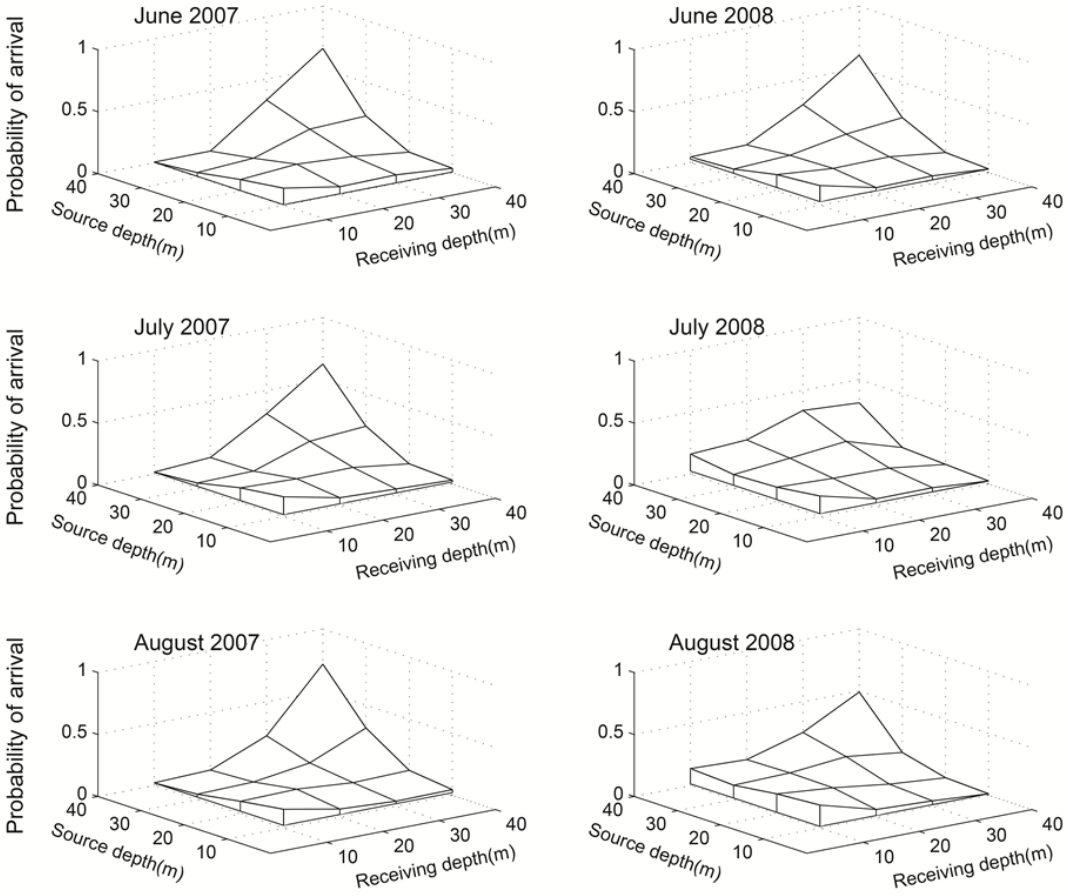

A.12 *P. astreoides* – $\breve{M}_T$ – active scenario – June-August

Appendix B. This appendix contains the strata module, code written for the CMS specifically for this study that allows for fine-resolution modeling of vertical connectivity, and examples of necessary input files. Further information on the CMS code and sub-modules can be found in Paris et al. (2013). Additional updates were made to other modules of the CMS in order to integrate this strata module, including loop.f90, input.f90, mod_reef.f90, def_particle.f90, def_globalvariables.f90, and output.f90. All code was written in Fortran 90 language.

The intention of the module is to assign a strata, or depth, to every habitat (larval production/settlement) polygon, and an initial strata to each particle based on the depth its origin. Strata are defined by the user in a strataFile input (see below), and can be at any depth, in equal or unequal increments. The particle carries information regarding its strata of origin with it throughout the model duration. Additionally, at each model time step particles check their depth and determine their strata. If a particle is competent and within the horizontal extent of settlement habitat, a settlement condition exists that requires a particle and settlement habitat to be within the same strata.

B.01 Particles and settlement habitat must be in the same strata in order for settlement to occur. Particles query their depth at each time step during larval competence.

B.02. The strata module.

```
!*****************************************************************************
!* System: Connectivity Modeling System (CMS)                                *
!* File : mod_strata.f90                                                     *
!* Last Modified: 2013-05-22                                                 *
!* Code contributors: Ana Vaz, Daniel Holstein, Claire B. Paris, Judith Helgers *
!*                                                                           *
!*                                                                           *
!* Copyright (C) 2011, University of Miami                                   *
!*                                                                           *
!* This program is free software: you can redistribute it and/or modify      *
!* it under the terms of the GNU Lesser General Public License as published *
!* by the Free Software Foundation, either version 3 of the License, or      *
!*(at your option) any later version.                                        *
!*                                                                           *
!* This program is distributed in the hope that it will be useful,           *
!* but WITHOUT ANY WARRANTY; without even the implied warranty of            *
!* MERCHANTABILITY or FITNESS FOR A PARTICULAR PURPOSE.
*
!* See the Lesser GNU General Public License for more details.               *
!*                                                                           *
!* You should have received a copy of the GNU Lesser General                 *
!* Public License along with this program.                                   *
!* If not, see <http://www.gnu.org/licenses/>.                               *
!*****************************************************************************

MODULE mod_strata

 USE mod_kinds
 USE constants
 USE mod_iounits

 IMPLICIT NONE

 real (kind = real_kind), allocatable, save  :: depthStrata(:)
 integer (kind=int_kind), save               :: numStrata

 CONTAINS

!*****************************************************************************
!load strata data
SUBROUTINE load_strata (StrataFilename)
!On mod_ibio.f90
```

```
 character(len = *), intent(in) :: StrataFilename
 integer (kind=int_kind) :: i,j, iunit
 real (kind = real_kind) :: cum
 logical (kind=log_kind) :: file_exists

!open file
 call get_unit(iunit)
 INQUIRE(FILE=trim(StrataFilename), EXIST=file_exists)
 IF (file_exists) THEN
  OPEN(UNIT=iunit,FILE=trim(StrataFilename),STATUS="old")
 ELSE
  print *, "Error: File ", trim(StrataFilename)," does not exist"
  stop
 ENDIF

!read file
 read(iunit, *) numStrata
! numStrata is the number of layers to be used
! depthStrata(1,:) are the initial depth of the layers
! depthStrata(2,:) are the final depth of the layers

 allocate(depthStrata(numStrata))
 read(iunit,*) (depthStrata(j), j=1, numStrata)

!close file
call release_unit(iunit)

!print *, "Finished loading vertical matrix"
 END SUBROUTINE load_strata


!*********************************************************************
****
!adds initial strata to particle
SUBROUTINE assign_strata_start(startdepth,stratastart)

real (kind = real_kind), intent(in)    :: startdepth
integer (kind = int_kind), intent(out) :: stratastart
integer (kind = int_kind)              :: y

!assign strata to particle

IF (startdepth .gt. depthStrata(numStrata)) THEN
  print *, "Depth in release file is greater than depths in strata matrix", startdepth
ELSE
```

```
!Assign a strata to a particle's depth
! loop over all strata
! checks what strata each particle is, by checking if the particle depth is between the
initial and final depth ! of each strata, given on vertStrata
  strata_loop: DO y=1, numStrata

  IF (startdepth .le. depthStrata(y)) THEN
   stratastart= y
   exit strata_loop

  ENDIF
 ENDDO strata_loop
ENDIF

END SUBROUTINE assign_strata_start


!*********************************************************************
****
!checks the strata of the particle
SUBROUTINE check_strata(pdepth,strataFlag)

real (kind = real_kind), intent(in)    :: pdepth
integer (kind = int_kind), intent(out) :: strataFlag
integer (kind = int_kind)                    :: y

!assign strata to particle

IF (pdepth .le. depthStrata(numStrata)) THEN
!Assign a strata to a particle's depth
! loop over all strata
! checks what strata each particle is, by checking if the particle depth is between the
initial and final depth ! of each strata, given on vertStrata
  strata_loop: DO y=1, numStrata
  IF (pdepth .le. depthStrata(y)) THEN
   strataFlag = y
   exit strata_loop
  ENDIF
 ENDDO strata_loop
 ELSE
   strataFlag=-1
ENDIF

END SUBROUTINE check_strata
```

```
!*****************************************************************
*********
!adds initial strata to polygon
SUBROUTINE poly_strata(pDepth,pStrata)

real (kind = real_kind), intent(in)    :: pDepth
integer (kind = int_kind), intent(out) :: pStrata
integer (kind = int_kind)              :: y


IF (pDepth .gt. depthStrata(numStrata)) THEN
   print *, "Depth in xyz file is greater than depths in strata matrix", pDepth
  ELSE

!    Assign a strata to a polygon's depth
   strata_loop: DO y=1, numStrata
    IF (pDepth .le. depthStrata(y)) THEN
     pStrata = y
     exit strata_loop
    ENDIF
   ENDDO strata_loop
  ENDIF

END SUBROUTINE poly_strata

!*****************************************************************
****
END module mod_strata
```

B.03. ibm.list including user input commands for the use of the strata module.

```
&ibm
!=========================================================================
=====!
!Adding buoyancy
buoyancy              = .false.
dens_particle         = 842.5         !in kg/m3
diam_particle         = 0.00025       !in meters
!=========================================================================
=====!
!Adding marine habitats
polygon               = .true.
polyFilename          = "USVIRUN_01vert.xyz"
settlementStart       = 6           !in days
!=========================================================================
=====!
!Adding probability matrix to move particle up and down
ibio                  = .false.
ibioFilename          = "vertmat"
ibioTimeStep          = 3600        !in seconds
!=========================================================================
=====!
!Adding mortality rate
mort                  = .false.
halflife              = 720000        !in seconds
!=========================================================================
=====!
!Adding different attributes to each particle
diffpart              = .false.
diffpartFilename      = "diffpart_matrix"
!=========================================================================
=====!
!Adding two ways  to move the particles up and down
massSpawning          = .false.
larvaStart            = 7             !in days
!=========================================================================
=====!
!Adding tidal stream movement
tidalmovement         = .false.
tstStart              = 14            !in days
!=========================================================================
=====!
```

```
!Adding strata
strata                  = .true.
strataFilename          = "strataFile"
!=============================================================================!
$end
```

B.04. An example of the necessary strataFile input. The first line defines the number of strata, and the second line defines the deeper limit to each strata in meters. Strata can be equal or unequal in size.

```
5
10 20 30 40 50
```